

Copyright  
by  
Ashley Elizabeth Smith  
2019

**The Dissertation Committee for Ashley Elizabeth Smith Certifies that this is  
the approved version of the following dissertation:**

**Integration of Homeostatic and Hedonic Brain Centers in the  
Regulation of Feeding Behaviors**

**Committee:**

---

Jonathan D. Hommel, Ph.D., Supervisor

---

Noelle C. Anastasio, Ph.D.

---

Mark R. Emmett, Ph.D.

---

Gracie Vargas, Ph.D.

---

Ralph DiLeone, Ph.D.

---

**Integration of Homeostatic and Hedonic Brain Centers in the  
Regulation of Feeding Behaviors**

**by**

**Ashley Elizabeth Smith, B.S.**

**Dissertation**

Presented to the Faculty of the Graduate School of  
The University of Texas Medical Branch  
in Partial Fulfillment  
of the Requirements  
for the Degree of

**Doctor of Philosophy**

**The University of Texas Medical Branch  
December, 2019**

## **Acknowledgements**

I want to express my gratitude to my mentor, Jonathan Hommel, for fostering my independence as a scientist and for allowing me to follow the data. Over the past four years, Jonathan provided me with the tools I needed to succeed in my graduate education and beyond, and I am forever indebted to him. I would also like to thank Jim Kasper for all of his help and support through long hours of surgery, behavior, and writing. I'm so very appreciative for his mentorship and his friendship. I would like to thank other members of the Hommel Laboratory for their support and encouragement (and silliness) over the years- especially Catherine Sampson and Hong Sun. I want to extend thanks to my dissertation committee for their wealth of knowledge and helpful suggestions. I also want to acknowledge other students, post-docs and members of the Center for Addiction Research for their willingness to listen, insightful conversations, and thoughtful ideas. Personally, I would like to thank my parents, Cindy and Ed Smith, who truly made my scientific career possible- throughout my life they graciously provided me with an environment that allowed me to relentlessly pursue my goals. I want to express my gratitude to Scott, who has supported me and been by my side through the ups and the downs of this journey. I also want to thank the friends who have inspired and empowered me over thousands of miles spent together- Heidi Walker and

Sarah Ryan (and many others) consistently push me and remind me to strive to be the best version of myself. There were many times (too many to count) where I wanted to give up- whether it was giving up on an experiment, giving up on writing, or giving up on an idea. When I started graduate school in 2015, I was in awe of all the opportunities ahead of me and this perspective helped me persist. When I officially joined Jonathan's lab in 2016, I found the research that I am profoundly passionate about in life- understanding how and why our brains drive pathological overconsumption of food. Too many people that I care about (and too many people that I have never met) have experienced too much suffering because of disordered eating. It is because of this suffering that I will continue to persist in academic research, with the promise that I won't stop until I find an answer.

# **The Integration of Homeostatic and Hedonic Brain Centers in the Regulation of Feeding Behaviors**

Publication No. \_\_\_\_\_

Ashley Elizabeth Smith, Ph.D.

The University of Texas Medical Branch, 2019

Supervisor: Jonathan D. Hommel

Binge-eating disorder (BED) and obesity are major public health problems that are associated with psychosocial distress, impairments in daily function, and life-threatening co-morbidities. Both diseases are driven by maladaptive feeding behaviors, namely pathological overconsumption of high-fat food. Pathological overconsumption of high-fat food is potentiated by aberrant homeostatic feeding behavior (i.e. titration of caloric intake), which typically associates with hypothalamic brain nuclei, specifically the paraventricular nucleus of the hypothalamus (PVN) which controls food intake to maintain body weight. Additionally, pathological overconsumption of high-fat food is exacerbated by the reinforcing properties of high-fat food that drive hedonic feeding, which is mediated by the nucleus accumbens (NAc) and the ventral tegmental area (VTA). Furthermore, dysfunction of homeostatic (PVN) and hedonic (NAc, VTA) feeding circuitry is hypothesized to underlie pathological overconsumption of high-fat food. This dissertation aimed to elucidate the interconnected mechanisms of

homeostatic and hedonic signaling that may underlie pathological overconsumption of high-fat food, and identified the neuropeptide receptor NMUR2 and the neurotransmitter glutamate as novel regulators of binge-type eating, intake of high-fat food, and motivation for high-fat food.

# TABLE OF CONTENTS

List of Figures .....	xii
List of Abbreviations .....	xv
Chapter 1 Introduction .....	16
Obesity Epidemic in the United States .....	16
Pathological Overconsumption of High-Fat Food Drives Obesity .....	17
Motivation for High-Fat Food.....	19
Neurobiological Underpinnings of Feeding Behaviors .....	20
Homeostatic Feeding is Driven by the Paraventricular Nucleus .....	20
Hedonic Feeding is Driven by the Nucleus Accumbens .....	21
Integration of Homeostatic and Hedonic Circuitry: PVN→NAc .....	23
Glutamate is an Important Regulator of Feeding Behaviors .....	24
Specific Aims .....	24
Chapter 2 General Materials and Methods .....	26
Animals .....	26
Viral Vector Administration .....	26
Guide Cannula Implantation.....	27
Perfusion and Euthanasia.....	28
Immunohistochemistry .....	28
Microdialysis.....	29
Behavioral Assays .....	30
Food Intake .....	30
Operant Conditioning.....	30
Fixed Ratio Schedule of Reinforcement.....	31
Progressive Ratio Schedule of Reinforcement .....	31
Locomotor Activity.....	32
Data Analysis .....	32



Chapter 3 Binge-Type Eating in Rats is Facilitated by Neuromedin U Receptor 2 in the Nucleus Accumbens and Ventral Tegmental Area ...	33
Introduction .....	33
BED and Obesity Share Overlapping Neural Phenotypes ....	34
Rodent Models of Pathological Overconsumption Behavior .	35
Neuromedin U Receptor 2 .....	36
Specific Methods .....	37
Animals .....	37
NMUR2 Immunoreactivity in the NAc and VTA.....	37
Binge-Type Eating Paradigm .....	38
NAc and VTA Protein Extraction .....	39
NMUR2 Protein Quantification via Capillary Electrophoresis .....	40
Data Analysis .....	41
Results .....	42
NMUR2 is Expressed Pre-synaptically in the NAc and the VTA .....	42
Fat Content is Critical for Binge-type Eating.....	44
Higher NAc NMUR2 Synaptosomal Protein Expression Potentiates Binge-type Eating of “Lower Fat” Food .....	46
Lower VTA NMUR2 Synaptosomal Protein Expression Halts Binge-type Eating of Extreme High-Fat Food.....	48
Discussion .....	50
Chapter 4 Neuroanatomical and Neurochemical Properties of PVN→NAc Projections.....	53
Introduction .....	53
Specific Methods .....	54
Animals .....	54
Surgeries .....	55
GFP Immunoreactivity in the PVN.....	56
Presynaptic Glutamate Immunoreactivity in the NAc.....	57
Nac Microdialysis .....	58
Phospho-cFos Immunoreactivity in the PVN and the NAc....	59

Data Analysis .....	60
Results .....	60
PVN→NAc Cell Bodies are Localized to Parvocellular Compartments of the PVN.....	61
PVN→NAc Synapses Co-Localize with VGLUT1, but not GAD <sub>67</sub> , TH, or TPH .....	63
hM3d-Induced Stimulation of PVN→NAc Increases Extracellular Glutamate in the Synapse .....	66
hM3d-Induced Stimulation of PVN→NAc Alters Neuronal Excitability in the NAc, but not the PVN .....	70
Discussion .....	76
Chapter 5 Glutamate Release from PVNNAc Projections Regulates Intake of High-Fat Food and Motivation for High-Fat Food .....	79
Introduction .....	79
Specific Methods .....	81
Animals .....	81
Surgeries: CTRL and hM3d.....	81
Surgeries: DIO CTRL and DIO hM3d .....	82
hM3d: Food Intake and Intra-NAc CNO Administration.....	82
hM3d: Operant Conditioning and Intra-NAc CNO Administration .....	83
hM3d: Locomotor Activity .....	84
hM3d: Euthanasia and Targeting .....	85
hM3d: Food Intake and Central CNO Administration.....	85
DIO hM3d: Operant Conditioning and Central CNO Administration .....	85
DIO hM3d: Locomotor Activity .....	86
DIO hM3d: Euthanasia and Targeting .....	87
Data Analysis .....	87
Results .....	89
hM3d-Induced Stimulation of PVN→NAc Decreases Intake of High-Fat Food.....	89
hM3d-Induced Stimulation of PVN→NAc Does not Alter Operant Responding For High-Fat Food.....	93

hM3d-Induced Stimulation of PVN→NAc Does not Alter Locomotor Activity.....	98
hM3d-Induced Stimulation of PVN→NAc with a DIO Viral Vector Approach Increases Intake of High-Fat Food....	100
hM3d-Induced Stimulation of PVN→NAc with a DIO Viral Vector Approach Decreases Operant Responding for High-Fat Food.....	103
hM3d-Induced Stimulation of PVNNAc with a DIO Viral Vector Approach Does not Alter Locomotor Activity .....	108
Discussion .....	110
General Discussion.....	110
Viral Promoter Specificity.....	113
Glutamate Dynamics .....	114
hM3d-Mediated Presynaptic Release vs. DIO hM3d-Mediated Action Potential .....	116
Dual Transmission Neurons .....	119
Chapter 6 Summary and Conclusions .....	121
General Conclusions .....	121
Chapter 3 Conclusions.....	127
Chapter 4 Conclusions.....	129
Chapter 5 Conclusions.....	129
Summary and Future Directions .....	131
References .....	136

Vita 162

## List of Figures

<b>Figure 3.1: NMUR2 immuno-reactivity in the NAc and the VTA. ....</b>	<b>43</b>
<b>Figure 3.2: Fat content is critical for binge-type eating.....</b>	<b>45</b>
<b>Figure 3.3: Higher NAc NMUR2 synaptosomal protein expression potentiates binge-type eating of “lower” fat food.....</b>	<b>47</b>
<b>Figure 3.4: Lower VTA NMUR2 synaptosomal protein expression halts binge-type eating of extreme high-fat food. ....</b>	<b>49</b>
<b>Figure 4.1: PVNNAc cell bodies are localized to parvocellular compartments of the PVN. ....</b>	<b>62</b>
<b>Figure 4.2: PVN→NAc terminals co-localize with VGLUT1.....</b>	<b>64</b>
<b>Figure 4.3: PVN→NAc terminals do not co-localize with GAD<sub>67</sub>, TH, or TPH. ....</b>	<b>65</b>
<b>Figure 4.4: Experimental timeline for microdialysis.....</b>	<b>67</b>
<b>Figure 4.5: hM3d-induced stimulation of PVN→NAc increases extracellular glutamate.....</b>	<b>69</b>
<b>Figure 4.6: Experimental timeline for phospho-cFos.....</b>	<b>71</b>
<b>Figure 4.7: hM3d-induced stimulation of PVN→NAc alters neuronal excitability in the NAc, but not the PVN. ....</b>	<b>73</b>
<b>Figure 4.8: Microdialysis targeting.....</b>	<b>75</b>



<b>Figure 5.12: Proposed mechanisms of hM3d DREADD approaches.....</b>	<b>118</b>
<b>Figure 6.1: Integration of homeostatic and hedonic brain centers in the regulation of feeding behaviors.....</b>	<b>122</b>

## List of Abbreviations

<b>AAV2</b>	adeno-associated virus 2
<b>AAV6</b>	adeno-associated virus 6
<b>aCSF</b>	artificial cerebrospinal fluid
<b>AMPA</b>	$\alpha$ -amino-3-hydroxy-5-methyl-4-isoxazolepropionic acid
<b>AMPA</b>	$\alpha$ -amino-3-hydroxy-5-methyl-4-isoxazolepropionic acid receptor
<b>ANOVA</b>	analysis of variance
<b>A/P</b>	anterior/posterior
<b>AUC</b>	area under the curve
<b>BED</b>	Binge-eating Disorder
<b>CAMKII</b>	Ca <sup>2+</sup> /calmodulin-dependent protein kinase II
<b>CNO</b>	clozapine-n-oxide
<b>DAMGO</b>	D-Ala <sup>2</sup> , N-MePhe <sup>4</sup> , Gly-ol
<b>DIO</b>	double-floxed inverse open reading frame
<b>DREADD</b>	Designer Receptor Exclusively Activated by a Designer Drug
<b>DTT</b>	dithiothreitol
<b>D/V</b>	dorsal/ventral
<b>FR</b>	fixed ratio
<b>GABA</b>	gamma aminobutyric acid
<b>GAD<sub>67</sub></b>	glutamic acid decarboxylase 67
<b>GFP</b>	green fluorescent protein
<b>GPCR</b>	G protein-coupled receptor
<b>hSyn</b>	human synapsin
<b>IP</b>	intraperitoneal
<b>IRES</b>	internal ribosome entry site
<b>mGluR</b>	metabotropic glutamate receptor
<b>M/L</b>	medial/lateral
<b>NAc</b>	nucleus accumbens
<b>NMDAR</b>	N-methyl-D-aspartate receptor
<b>NMUR2</b>	Neuromedin u receptor 2
<b>PBS</b>	phosphate buffered saline
<b>PFA</b>	paraformaldehyde
<b>phospho-cFos</b>	phosphorylated cFos
<b>PR</b>	progressive ratio
<b>PVN</b>	paraventricular nucleus of the hypothalamus
<b>SSRI</b>	selective serotonin reuptake inhibitor
<b>TH</b>	tyrosine hydroxylase
<b>TPH</b>	tryptophan hydroxylase
<b>VTA</b>	ventral tegmental area
<b>vGLUT</b>	vesicular glutamate transporter

# **Chapter 1 Introduction**

## **OBESITY EPIDEMIC IN THE UNITED STATES**

Obesity is an alarming chronic health crisis that affects almost 40% of the adult population in the United States (Hales et al., 2017). Obese individuals present a challenging public health problem because they are at increased risk for several life-threatening and costly co-morbidities including diabetes, metabolic syndrome, cardiovascular disease, and cancer (2013). Additionally, obesity is strongly linked to mental illness, including anxiety and depression, as well as neurodegenerative diseases that ultimately lead to cognitive decline (Freeman et al., 2014).

The medical costs associated with obesity and its comorbidities were estimated at \$147 billion dollars in 2008 (Finkelstein et al., 2009). Because the financial and health burdens of obesity are so pernicious, a more mechanistic appreciation of the maladaptive feeding behavior(s) that contribute to obesity is critical to understanding the etiology of this disease and for identifying druggable targets (Finkelstein et al., 2009). Several pharmacotherapies have been developed to treat obesity. However, current therapeutics offer limited efficacy, and have side effects that often result in noncompliance. For example, the anti-obesity drug orlistat blocks fat absorption in the gut through inhibition of gastrointestinal lipases, but causes severe diarrhea (Zhi et al., 1994). Liraglutide, another anti-obesity drug, stimulates insulin release from the pancreas to control blood sugar, but is hypothesized to alter feeding through central mechanisms (Pi-Sunyer et al.,



2015). While weight loss has been reported with liraglutide treatment, side effects can include pancreatitis and cancer (Pi-Sunyer et al., 2015). Overall, the efficacy of these pharmacotherapies is limited because they target the metabolic complications resulting from obesity, as opposed to targeting the maladaptive feeding behaviors that play a part in the pathology of obesity.

### **PATHOLOGICAL OVERCONSUMPTION OF HIGH-FAT FOOD DRIVES OBESITY**

One maladaptive feeding behavior that contributes to obesity is pathological overconsumption of highly palatable food. Highly palatable food, including high-fat food, is extremely reinforcing in both humans and rodents alike (Drewnowski, 1997; Drewnowski and Almiron-Roig, 2010; Drewnowski and Greenwood, 1983; Drewnowski et al., 1982). Reinforcement is defined in humans as an experience that produces a pleasurable effect and shapes future behavior (White, 2011). Humans frequently seek out naturally reinforcing stimuli, including social contact, sex, and food (Kelley and Berridge, 2002).

The reinforcement value attributed to food is determined by sensory responses to food that generate feelings of “liking” and “wanting” (Kelley and Berridge, 2002). Sensory responses to food include taste, macronutrient profile, and total caloric value. The taste and texture of fat create a combination that is extremely palatable, and fat is the most energy dense macronutrient (Drewnowski, 1997; Drewnowski and Almiron-Roig, 2010; Drewnowski and Greenwood, 1983; Drewnowski et al., 1982). Accordingly, the high palatability and reinforcement value associated with high-fat food drive overconsumption, irrespective of caloric state (Drewnowski, 1997; Drewnowski and Almiron-Roig, 2010; Drewnowski and

Greenwood, 1983; Drewnowski et al., 1982). Overconsumption has been primarily studied in the context of physiological and hormonal control of energy balance. However, overconsumption of high-fat food, even in the presence of positive energy balance, may be due to activation of reward neurocircuitry and overconsumption of high-fat food resembles drug-taking behavior observed in substance use disorder, and has been concisely described as the addictive dimensionality of obesity (Volkow et al., 2013a, b; Volkow and Wise, 2005).

The reinforcing properties of highly palatable food can perpetuate maladaptive feeding behaviors that mirror substance use disorder where repeated drug taking drives complex neuroadaptations in plasticity. These alterations eventually lead to an elevated reward threshold which promotes escalation behavior- accelerated and increased drug taking is required to achieve reinforcement value (Berthoud et al., 2011). Likewise, pathological overconsumption of high-fat food causes neurobiological changes leading to hyperphagia and craving, which may perpetuate obesity (Berthoud et al., 2011).

Moreover, the obese state also alters the reinforcing properties of highly palatable food. The obese state is partly characterized by dysregulated metabolic function, particularly decreased leptin signaling, increased ghrelin signaling, insulin resistance, and inflammation, all of which can potentiate maladaptive feeding (Kasper et al., 2017). Pathological overconsumption of a high-fat diet produces a pro-inflammatory environment in the brain, and endoplasmic reticulum stress (De Souza et al., 2005), which leads to neurotoxicity and cell death (Ozcan et al.,

2009). This may result in further dysregulation of energy balance and reinforcement governing brain structures.

### **MOTIVATION FOR HIGH-FAT FOOD**

The reinforcement value of food drives future intake, even in the absence of a caloric deficit. Perceived reinforcement value is intimately tied to reinforcement efficacy, or the amount of effort expended in order to obtain a reinforcer (Swanson, 1989). Generally speaking, motivation is described as the amount of effort an individual is willing to expend in order to obtain a specific goal (Swanson, 1989). A motivated individual will work towards obtaining a goal even though it may require complex activity and time (Swanson, 1989). Often, motivated behavior is initiated by a stimulus (external or internal), and is voluntary.

In rodents, operant conditioning is used to quantify reinforcement efficacy. During operant conditioning, rodents learn to associate lever pressing with the delivery of a reinforcer, such as a high-fat food pellet. Motivation underlies this reinforced behavior (Dayan and Balleine, 2002), and requires coordinated recruitment of complex brain circuitry, including the nucleus accumbens (NAc) (Sharma et al., 2013).

Motivation is quantified with operant conditioning where rodents learn to perform a behavior (lever press) in response to a cue (light) that the animal associates with a specific reinforcement, such as a high-fat food pellet. Specifically, motivation is association of the cue with the reinforcement (Dayan and Balleine, 2002), and requires coordinated recruitment of reward circuitry in the

brain (Sharma et al., 2013). In Chapter 5, we investigated motivation for a high-fat food pellet reinforcer via operant conditioning.

## **NEUROBIOLOGICAL UNDERPINNINGS OF FEEDING BEHAVIORS**

Feeding behavior is a complex process that is orchestrated through a web of neural circuitry and a multitude of central and peripheral signals which serve to either promote or inhibit food intake (Ferrario et al., 2016; Rossi and Stuber, 2018). Food intake is driven by both homeostatic nutritional requirements and also by the reinforcing properties of food. The paraventricular nucleus of the hypothalamus (PVN) is one brain region that plays a critical role in the management of food intake and body weight. On the other hand, the NAc controls the reinforcing properties of food to control hedonic feeding. The remainder of this section is focused on describing both the PVN and the NAc and how they regulate feeding behavior.

### ***HOMEOSTATIC FEEDING IS DRIVEN BY THE PARAVENTRICULAR NUCLEUS***

Food intake is partially driven by metabolic energy demand, which is regulated by the hypothalamus. The PVN is one nucleus within the hypothalamus that is described as a “relay switch” that integrates a multitude of central and peripheral signals to regulate food intake and energy balance. The hypothalamus is characterized by glutamatergic connectivity between sub-nuclei, including the PVN, which has been shown to express markers of glutamatergic neurons (Ziegler et al., 2002). Several afferents innervate the PVN to control appetite, food intake, and energy homeostasis through appetite-modifying neurotransmission (Elmquist et al., 1999; Williams et al., 2001). The PVN also integrates signals from peripheral

circulation, including the hormones insulin, leptin and ghrelin (Mimee et al., 2013). Once current metabolic status is established, the PVN relays signals to either drive food intake or suppress food intake. Lesioning of the PVN increases food intake and obesity in rats (Leibowitz et al., 1981). Lesions restricted to the PVN result in a 104% increase in food intake and a 207% increase in body weight, while lesions made to surrounding tissue had no effect (Leibowitz et al., 1981). Overall, the PVN regulates food intake at the level of physiological energy requirements, and facilitates homeostatic feeding behavior.

### ***HEDONIC FEEDING IS DRIVEN BY THE NUCLEUS ACCUMBENS***

Food intake is also driven by the hedonic value of food, which is regulated by the NAc (Berridge, 1996). The NAc is well-characterized as a regulator of reinforcement and goal-directed behaviors, and receives input from feeding-related circuitry. These afferents originate from other striatal structures, cortical structures, thalamic and hypothalamic structures and facilitate communication from feeding circuitry that regulates taste perception and energy homeostasis to the NAc (Kelley et al., 2005; Swanson, 2000).

Within the NAc, several neuromodulatory systems have been implicated in feeding behavior, including gamma aminobutyric acid (GABA), dopamine, and endogenous opioids (Evans and Vaccarino, 1986; Mucha and Iversen, 1986; Zhang et al., 2003). The NAc and its sub-regions are densely populated by GABA medium spiny neurons (Meredith et al., 1993). Pharmacological stimulation of GABA receptors in the NAc markedly increases intake of all macronutrient types—sucrose, carbohydrate and fat, but does not alter salt or water intake (Basso and

Kelley, 1999; Stratford et al., 1999; Zhang et al., 2003). However, similar studies investigating the effects of intra-NAc infusion of the GABA receptor agonist muscimol on motivation for food determined that stimulation of GABA receptors in the NAc does not affect motivation for food (Zhang et al., 2003).

Within the NAc, dopamine neurons are also implicated in regulating food intake, however the literature on dopamine feeding effects is mixed (Baldo et al., 2002; Carlezon and Thomas, 2009; Trojnar et al., 2007; Zhu et al., 2016). Lesions to NAc dopamine D1 receptor expressing neurons demonstrate decreased food intake (Baldo et al., 2002; Heffner et al., 1977; Salamone et al., 1990). Pharmacological manipulations of NAc dopamine, including intra-NAc infusion of dopamine agonists and antagonists, does not induce robust feeding effects (Zhang et al., 2003). In fasted animals, however, intra-NAc administration of amphetamine decreases food intake and motivation for food (Baldo et al., 2002).

Studies investigating opioids and feeding behavior have demonstrated that efficacy of opioid agonists and antagonists on feeding is intimately tied to palatability (Zhang et al., 2003). Arguably, high-fat food is the most palatable macronutrient due to the taste, texture, and its caloric density (Drewnowski, 1997). Robinson and Berridge developed a model to describe some of these aspects of palatability, and hypothesized that the neural circuitry that underlies motivated behavior can be disentangled into a “wanting” system and a “liking” system (Berridge, 1996; Berridge and Robinson, 1998). “Liking” is mediated by endogenous opioids, such as enkephalin, which is expressed throughout several

striatal regions, including the NAc (Pickel et al., 1980). The NAc is also densely populated with mu, delta and kappa opioid receptors (Le Merrer et al., 2009). Pharmacological agonism of the mu opioid receptor via intra-NAc infusion of DAMGO potently and selectively increases intake of high-fat food, while antagonism of the mu opioid receptor decreases feeding (Kelley et al., 1996; Zhang et al., 1998; Zhang and Kelley, 2000). Furthermore, intra-NAc infusion of DAMGO increases motivation for food, underscoring the importance of the opioid system in regulating feeding behaviors (Zhang et al., 2003).

#### **INTEGRATION OF HOMEOSTATIC AND HEDONIC CIRCUITRY: PVN→NAc**

PVN projections to the NAc (PVN→NAc) were first identified via retrograde labeling in the NAc by Dolen and colleagues (Dölen et al., 2013). The PVN→NAc neural pathway expresses oxytocin receptor, both pre and post-synaptically, and mediates social reinforcement via an oxytocin-dependent manner (Dölen et al., 2013). Both the PVN and the NAc have been implicated in the control of feeding behaviors, but the direct interplay of these regions, including functional mechanisms of PVN→NAc signaling, in regulating feeding behavior is unknown (Anastasio et al., 2019; Baldo and Kelley, 2007; Benzon et al., 2014; Corwin et al., 2011; Maldonado-Irizarry et al., 1995; McCue et al., 2017; Sharma et al., 2013; Smith et al., 2019). We show for the first time that PVN→NAc is a novel regulator of intake of highly palatable food. Specifically, we show that PVN→NAc neurons are localized to parvocellular PVN, equipped with vesicular glutamate transporter 1, and that stimulation of PVN→NAc neurons increases presynaptic glutamate in the NAc. Furthermore, stimulation of PVN→NAc decreases intake of highly

palatable food in rats. Overall, our data provide both neuroanatomical and functional evidence of an integrated neural circuit between homeostatic and hedonic brain regions that underlies feeding behavior.

### **GLUTAMATE IS AN IMPORTANT REGULATOR OF FEEDING BEHAVIORS**

Glutamate signaling is a critical regulator of feeding behaviors in both the PVN and in the NAc. The PVN is densely populated by glutamatergic neurons that express vesicular glutamate transporter 1 (VGLUT) (Ziegler et al., 2002). The presence of these VGLUT1 positive neurons in the PVN would suggest that glutamate signaling plays a role in homeostatic control of feeding. In the NAc, pharmacological blockade of presynaptic glutamate receptors is extremely relevant to feeding behavior. Specifically, infusion of non N-methyl-D-aspartate receptor (NMDAR) glutamate antagonists into the medial NAcSh have been shown to evoke an immediate and sustained increase in food intake (Maldonado-Irizarry et al., 1995; Stratford et al., 1998). Additionally, infusion of  $\alpha$ -amino-3-hydroxy-5-methyl-4-isoxazolepropionic acid (AMPA) directly into the NAc decreases food intake in food restricted rats (Stratford et al., 1998). We suspect that this observed increase in food intake might be mediated by postsynaptic  $\alpha$ -amino-3-hydroxy-5-methyl-4-isoxazolepropionic receptors (AMPA) in the NAc.

### **SPECIFIC AIMS**

PVN→NAc has been described as oxytocinergic in nature, however the neuroanatomical properties and functional mechanism of PVN→NAc signaling are not known. Therefore, the goal of Specific Aim 1 was to identify the



neuroanatomical and neurochemical properties of PVN→NAc. To accomplish Specific Aim 1, we utilized viral tracing techniques to label PVN→NAc, and then immunohistochemistry to further characterize neuronal cell bodies in the PVN and synapses in the NAc. To determine the functional mechanism of PVN→NAc signaling, we employed hM3d, the excitatory designer receptor exclusively activated by a designer drug (DREADD), to stimulate presynaptic release of neurotransmitters from PVN→NAc. Neurotransmitters were identified and quantified in real-time via microdialysis.

Although PVN→NAc has been implicated in social reinforcement, the pathway has not been investigated in the context of feeding behavior. Both the PVN and the NAc have been implicated in the control of feeding behaviors, but the direct interplay of these regions, including functional mechanisms of PVN→NAc signaling, in regulating feeding behavior is unknown (Anastasio et al., 2019; Baldo and Kelley, 2007; Benzon et al., 2014; Corwin et al., 2011; Maldonado-Irizarry et al., 1995; McCue et al., 2017; Sharma et al., 2013; Smith et al., 2019).

Specific Aim 2 was designed to identify the role of PVN→NAc in regulating intake of highly palatable food. We employed the excitatory hM3d to facilitate neurotransmitter release from PVN→NAc, and quantified intake of high-fat food and motivation for high-fat food.

Based on the existing literature about the role of glutamate in the regulation of feeding behaviors in both the PVN and the NAc, we hypothesized that PVN→NAc regulates feeding behaviors in a glutamate-dependent manner.

## Chapter 2 General Materials and Methods

### ANIMALS

Male Sprague-Dawley rats (Harlan, Houston, TX) weighing 225-250g were used in all experiments. Animals were housed individually in a temperature- (21-23°C) and humidity- (40-50%) controlled environment with a standard 12h light-dark cycle (lights on between 0600 and 1800 hours). All animals were given *ad libitum* access to normal chow (17% fat by kcal; Teklad LM-485 Mouse/Rat Sterilizable Diet; Teklad Diets, Madison, WI) and water in their home cages. Upon arrival, animals were allowed to acclimate to the room for seven days prior to handling and experimental procedures. All experiments were conducted in accordance with the *NIH Guide for Use and Care of Laboratory Animals* (2011), and with approval from the Institutional Animal Use and Care Committee at the University of Texas Medical Branch.

### VIRAL VECTOR ADMINISTRATION

Rats were deeply anesthetized with 1-5% isoflurane (VetEquip, Pleasanton, CA) and secured in a stereotaxic apparatus (Kopf Instruments, Tujunga, CA). A small incision was made along the midline and the skull exposed. Flat head placement was ensured by comparing the D/V coordinates of bregma and lambda (<0.03mm difference). Bilateral holes were drilled through the skull at the indicated A/P and M/L coordinates.

5ul syringes with 26 gauge blunt-tipped needles (Hamilton, Reno, NV) containing purified virus were inserted bilaterally and lowered to the D/V

coordinates (Benzon et al., 2014; Kasper et al., 2016; McCue et al., 2017). Viruses were delivered at 0.2ul/30 seconds for 5 minutes. Syringes remained in place for 2 minutes subsequent the injection. Incisions were closed using surgical staples. Rats received injections of 0.1mg bupivacaine (63323-464-37, Fresenius Kabi USA, Lake Zurich, IL), 0.3mg penicillin (0049-0520-84, Pfizer, New York, NY) in addition to topical lidocaine and topical neomycin at the incision site. Rats recovered for 7 days post-surgery before training and at least 14 days post-surgery before experiments to allow for optimal viral expression. All surgeries were performed during the light cycle (0600-1800).

#### **GUIDE CANNULA IMPLANTATION**

Rats were deeply anesthetized with 1-5% isoflurane (VetEquip, Pleasanton, CA) and secured in a stereotaxic apparatus (Kopf Instruments, Tujunga, CA). A small incision was made along the midline and the skull exposed. Flat head placement was ensured by comparing the D/V coordinates of bregma and lambda (<0.03mm difference). Bilateral holes were drilled through the skull at the indicated A/P and M/L coordinates. Guide cannula (PlasticsOne, Roanoke, VA) were inserted bilaterally and lowered to the D/V coordinates (Kasper et al., 2016; McCue et al., 2017).

Guide cannula were secured with dental cement and two stainless-steel bone screws. Incisions were closed using surgical staples. Rats received injections of 0.1mg bupivacaine (63323-464-37, Fresenius Kabi USA, Lake Zurich, IL), 0.3mg penicillin (0049-0520-84, Pfizer, New York, NY) in addition to topical lidocaine and topical neomycin at the incision site. Rats recovered for 7 days post-

surgery before training and at least 14 days post-surgery before experiments to allow for optimal viral expression. All surgeries were performed during the light cycle (0600-1800). In surgeries requiring viral vector administration and guide cannula implantation, viral vectors were administered before guide cannula implantation.

#### **PERFUSION AND EUTHANASIA**

Rats were anesthetized with 5% isoflurane and perfused intracardially with 1X PBS for 5 minutes, then with 4% paraformaldehyde (PFA) for 15 minutes. Heads were removed using a guillotine and brains extracted manually. Brains were post-fixed in 4% PFA at 4°C overnight. The following day, brains were moved to 1X PBS and 20% glycerol and stored at 4°C until immunohistochemical analysis.

#### **IMMUNOHISTOCHEMISTRY**

Brains were sliced into 40um sections using a cryostat (SM2010R, Leica, Buffalo Grove, IL). Sections were washed twice in 1X PBS, and then in 1% SDS for 5 minutes for antigen unmasking. Next, sections were blocked in donkey serum for 1-hour and incubated in primary antibody for 24-hours or overnight at room temperature.

The following day, sections were washed 3 times in 1X PBS, then incubated with secondary antibody for 2 hours. Sections were washed 3 times in 1X PBS, then mounted on glass slides (12-550-15, Fisher Scientific, Waltham, MA). Slides were allowed to dry for a minimum of 4-hours prior to rehydration.

For rehydration, slides were incubated in 1X PBS for 20 minutes, followed by a series of ethanol washes (80%, 90% and 100%) for 10 seconds each. Lastly, slides were incubated two times in Citrisolv Hybrid solution (1601H, Decon Labs Inc., King of Prussia, PA) for 3 minutes each (6 minutes total). DPX Mounting Medium (13510, Electron Microscopy Sciences, Hatfield, PA) was used to secure coverslips to slides. Slides were visualized via confocal microscopy once dry (usually overnight).

### **MICRODIALYSIS**

Neurotransmitter data was collected via microdialysis and quantified by capillary electrophoresis with laser-induced fluorescence (Bowser and Kennedy, 2001; Kasper et al., 2015; Li et al., 2008). A standard curve (7 concentrations of glutamate, aspartate, ornithine, GABA, taurine, glutamine, serine, and glycine ranging from 0 to 20  $\mu\text{M}$ ) was generated using a microdialysis probe prior to beginning the experiment. The elution time of these neurotransmitters had been validated and characterized previously (Bowser and Kennedy, 2001). After calibration, the probe was implanted in a non-anesthetized and freely moving rat via the guide cannula. A baseline for each animal was collected for 2 hours prior to the experiment (average glutamate 6.20  $\mu\text{M}$ , GABA 0.37  $\mu\text{M}$ ).

For the experiment, 2 $\mu\text{L}$  of 1 $\mu\text{M}$  clozapine-N-oxide (CNO) (6329, Tocris Biosciences, Minneapolis, MN) was administered via the guide cannula at a rate of 0.5 $\mu\text{L}/\text{min}$ . Microdialysis probe placement and cannula placement were verified and all misses were eliminated prior to data analysis.

## **BEHAVIORAL ASSAYS**

### ***FOOD INTAKE***

Rats were maintained in their home cages with *ad libitum* access to normal chow (17% fat by kcal; Teklad LM-485 Mouse/Rat Sterilizable Diet; Teklad Diets, Madison, WI) and water during food intake studies, which began at the onset of the dark cycle. At 1800 hours, labeled food hoppers containing high-fat chow (45% fat by kcal, D12451, Research Diets, New Brunswick, NJ) were placed in home cages and rats were given *ad libitum* access for 24-hours. Food hopper weights were recorded at 2-hours (2000 hours), 4-hours (2200 hours) and 24-hours (1800 hours on the next day). Differences in food hopper weights were quantified and interpreted as grams consumed.

### ***OPERANT CONDITIONING***

Rats were placed in standard rat operant chambers (Med Associates, Georgia, VT) between 0800 and 1000 housed in ventilated and noise-cancelling boxes with fans (Med Associates, Georgia, VT). Each chamber contained a delivery receptacle for food pellets centered between two response levers with a house light on the opposite side of the chamber. Levers were assigned as either “active” or “inactive” via Med Associates Software. Responses on the active lever resulted in delivery of a high-fat food pellet (45% fat by kcal, 45mg, F06162, Bioserv, Frenchtown, NJ), while responses on the inactive lever yielded no outcome. Operant chambers were randomized such that some chambers had an active lever on the right/inactive lever on the left or an inactive lever on the right/active lever on the left. Rats were placed in the same chamber throughout

and active/inactive designations were consistent throughout training and experimental days.

#### ***FIXED RATIO SCHEDULE OF REINFORCEMENT***

Operant chambers were used to train rats to self-administer high-fat food pellets. Rats trained daily for 30 minute sessions, and were promptly returned to their home cages at the conclusion of the program. Initially, rats trained on a fixed ratio (FR) 1 schedule, where one correct response on the active lever results in the delivery of the high-fat food pellet. Rats were advanced to an FR3 schedule once the percentage of responses on the active lever exceeded 85% for three consecutive days, where 3 correct responses are required for delivery of the high-fat food pellet. Accordingly, when rats met criteria on FR3, they were advanced to FR5 (5 correct responses). Rats unable to maintain at least 20 responses on the active lever during a 30-minute session were eliminated from the study.

#### ***PROGRESSIVE RATIO SCHEDULE OF REINFORCEMENT***

Once rats achieved criteria on FR5, they advanced to a progressive ratio (PR) schedule, where earning each successive high-fat food pellet within the session requires a greater number of responses (1,2,3,6,9,12,15,20,25,32,40,50,62,77,95). During the 30-minute experimental session, responses on the active lever, inactive lever, reinforcements delivered, and latency were recorded and used in data analysis.

### ***LOCOMOTOR ACTIVITY***

Locomotor activity was quantified in all rats included in behavioral assays to identify any potential motor effects. Rats were placed in a Photobeam Activity System-Home Cage (PAS-HC, San Diego Instruments, San Diego, CA) that consisted of a 4x8 photobeam mounting frame enclosed with clear plexi-glass. The Photobeam Activity System utilizes software that records all beam interruptions, including central peripheral activity and rearing. One to two inches of corncob bedding was placed in the bottom of each chamber. Rats were placed in chambers between 0800-1000. Central beam breaks, peripheral beam breaks, and elevated beam breaks (rearing) were quantified during a 30-minute session.

### **DATA ANALYSIS**

All statistical analyses were performed in GraphPad Prism 7.0a (GraphPad Software Inc., La Jolla, CA) with an experiment wise error rate of  $\alpha=0.05$ . For surgeries, viruses were administered in an interleaved fashion to avoid an effect of surgeon. For behavioral assays, each rat received aCSF/CNO or vehicle/CNO on different experimental days to control for nonspecific effects.



# **Chapter 3 Binge-Type Eating in Rats is Facilitated by Neuromedin U Receptor 2 in the Nucleus Accumbens and Ventral Tegmental Area<sup>1</sup>**

## **INTRODUCTION**

Binge-eating disorder (BED) is an under-recognized public health problem that is prevalent worldwide (Guerdjikova et al., 2017; Kessler et al., 2013). In the US, BED affects 3.5% of adult women and 2% of adult men, with a combined lifetime prevalence of 1.4% (Guerdjikova et al., 2017; Kessler et al., 2013). Although BED is the most common eating disorder, it remains both under-diagnosed and understudied (Guerdjikova et al., 2017). Therefore, a more mechanistic appreciation of feeding behaviors that contribute to BED is critical to understanding disease etiology and for identifying potential pharmacotherapeutic targets.

BED is characterized by binge episodes when an individual overconsumes high-fat food in a discrete period of time ( $\leq 2$  hours) (2017; Association, 2013a, b). The frequency of these binge episodes are a hallmark of BED and are used to determine disease severity (2017; Association, 2013a, b). BED is partially attributed to increased availability of highly-palatable food, and also shares physiological, psychological, and epidemiological overlaps with obesity (2017;

---

<sup>1</sup> Smith, A.E., Kasper, J.M., Ara 13, Anastasio, N.C., Hommel, J.D. (2019, February). Binge-Type Eating in Rats is Facilitated by Neuromedin U Receptor 2 in the Nucleus Accumbens and Ventral Tegmental Area. *Nutrients*. 11(2):327. PMID: 30717427; PMCID: PMC6412951

Berridge, 2009; Berridge et al., 2010; de Zwaan, 2001; Kessler et al., 2013; Rancourt and McCullough, 2015; Volkow et al., 2013b).

Obesity is an alarming health crisis that affects 39.8% of adults within the US alone (Hales et al., 2017). Obese individuals present a challenging public health problem due to increased risk for life-threatening co-morbidities (2013). Thus, the health burden of obesity is immense and demands an improved understanding of the feeding behaviors that contribute to obesity. Similar to BED, one of the feeding behaviors that contributes to obesity is pathological overconsumption of high-fat food.

#### ***BED AND OBESITY SHARE OVERLAPPING NEURAL PHENOTYPES***

Highly-palatable food, including high-fat food, is both energy dense and highly reinforcing in humans and rodents (Drewnowski and Almiron-Roig, 2010). These reinforcing properties promote overconsumption behavior that is potentiated by dysregulation in portion control (Carstairs et al., 2018; Lyons et al., 2018; Reale et al., 2018; Rippin et al., 2018). In fact, individuals with BED ascribe higher reinforcement value to high-fat food than individuals without BED (Price et al., 2018a; Schebendach et al., 2013). The reinforcing properties of food are largely encoded by brain regions within the mesolimbic “reward” pathway, which includes the nucleus accumbens (NAc) and the ventral tegmental area (VTA) (Volkow et al., 2013a; Volkow and Wise, 2005). Both the NAc and the VTA have been implicated in BED and obesity (Corwin et al., 2016; Davis and Carter, 2009; Dichter et al., 2012; Guerdjikova et al., 2017; Satta et al., 2018; Volkow et al., 2013a, b; Volkow and Wise, 2005; Witt and Lowe, 2014). Reinforcement value is

mediated by the NAc, a key neuroanatomical region that regulates hedonic feeding, or food intake in the absence of a caloric deficit (Volkow et al., 2013a, b; Volkow and Wise, 2005). The VTA, also linked to reinforcement value, affects obesogenic diet consumption (Hommel et al., 2006).

### ***RODENT MODELS OF PATHOLOGICAL OVERCONSUMPTION BEHAVIOR***

Overall, BED and obesity share multifaceted feeding behaviors involving multiple brain circuits that regulate a complex interplay of emotions, food intake, and food reinforcement. These feeding behaviors can be probed using animal models designed for quantifying specific aspects of these diseases. Models of binge-type eating have been validated in rodents, demonstrating success in studying the overconsumption behavior characteristic of both BED and obesity (Babbs et al., 2012; Benzon et al., 2014; Corwin et al., 2011; Corwin and Babbs, 2012; Corwin and Wojnicki, 2006; Kasper et al., 2014; Price et al., 2018b; Price et al., 2018c; Wojnicki et al., 2010). The intermittent access model provides *ad libitum* access to regular chow and water, with limited presentation of a highly palatable food, which simulates a binge episode, similar to that observed in BED and obesity (Benzon et al., 2014; Corwin et al., 2011; Corwin and Babbs, 2012; Corwin and Wojnicki, 2006; Kasper et al., 2014; Price et al., 2018c). While this model can recreate and quantify food intake during a binge episode, it does not replicate the psychological aspects of BED, such as feelings of loss of control and feelings of shame and guilt (2017; Association, 2013a, b; Guerdjikova et al., 2017). Nonetheless, this model is helpful in understanding neural mechanisms underlying

binge-type consumption and identifying potential regulators of this specific maladaptive feeding behavior.

### ***NEUROMEDIN U RECEPTOR 2***

Here, we investigate a novel mediator of binge-type eating, the neuropeptide receptor neuromedin U receptor 2 (NMUR2). NMUR2 is a G protein-coupled receptor predominantly expressed throughout the mammalian central nervous system. This receptor is known to regulate food intake and body weight (Brighton et al., 2004; Hosoya et al., 2000; Howard et al., 2000; Raddatz et al., 2000; Shan et al., 2000). For example, NMUR2-knockout mice are hyperphagic and demonstrate increased food intake patterns (Egecioglu et al., 2009). Additionally, deletion of hypothalamic NMUR2 via viral-mediated RNAi resulted in increased motivation for high-fat food and potentiated binge-type eating (Benzon et al., 2014; McCue et al., 2017). These studies indicate that NMUR2 regulates food intake, a process dysregulated in BED and obesity. Interestingly, the role of NMUR2 in reinforcement brain centers such as the NAc and VTA in binge-type eating has not been explored.

Importantly, endogenous expression of NMUR2 is highly variable among individuals and among various brain regions (Egecioglu et al., 2009; Gartlon et al., 2004; Kasper et al., 2018). Neuroanatomical variability and individual differences in NMUR2 expression may underlie aspects of individual differences observed in BED and obesity (Zander and De Young, 2014). The purpose of the current study is to explore relationships between synaptosomal NMUR2 expression in the NAc and the VTA—key brain regions associated with reinforcement—in a rodent model

of binge-type eating across a spectrum of dietary fat contents. Our findings revealed a strong positive correlation between intake of “lower” fat food and synaptosomal NMUR2 protein expression in the NAc and a strong negative correlation between intake of “extreme” high-fat food and synaptosomal NMUR2 protein expression in the VTA.

## **SPECIFIC METHODS**

### **ANIMALS**

Male Sprague-Dawley rats (Harlan, Houston, TX) weighing 225-250g were used in all experiments. Animals were housed individually in a temperature- (21-23°C) and humidity- (40-50%) controlled environment with a standard 12h light-dark cycle (lights on between 0600 and 1800 hours). All animals were given *ad libitum* access to normal chow (17% fat by kcal; Teklad LM-485 Mouse/Rat Sterilizable Diet; Teklad Diets, Madison, WI) and water in their home cages, including during binge sessions. Upon arrival, animals were allowed to acclimate to the room for seven days prior to handling and experimental procedures. All experiments were conducted in accordance with the *NIH Guide for Use and Care of Laboratory Animals* (2011), and with approval from the Institutional Animal Use and Care Committee at the University of Texas Medical Branch.

### **NMUR2 IMMUNOREACTIVITY IN THE NAC AND VTA**

Naïve rats (n=4) were anesthetized with 1-5% isoflurane, perfused with 1X PBS for 5 minutes, followed by 4% paraformaldehyde (PFA) for 15 minutes. Brains were removed and sliced into 40um sections using a cryostat. NAc and VTA

sections were stained as described in previous studies (Benzon et al., 2014; Kasper et al., 2016; McCue et al., 2017). Briefly, sections were washed twice in 1X PBS, and then antigen-unmasked with 1% SDS for 5 minutes. Next, sections were blocked in donkey serum and incubated in 1:150 primary antibody rabbit  $\alpha$ NMUR2 (Novus Biologicals, NBP1-02351) overnight. The following day, sections were washed 3 times in 1X PBS, then incubated with 1:200 donkey  $\alpha$ rabbit IgG Alexa Fluor 568 (Invitrogen, A10042). Images were acquired using Leica True Confocal Scanner SPE with 63X objective in confocal mode and Leica Application Suite X software (Leica Microsystems, Wetzlar, Germany).

### ***BINGE-TYPE EATING PARADIGM***

Our binge-type eating protocol is based on models published previously (Benzon et al., 2014; Corwin et al., 2011; Corwin and Wojnicki, 2006; Kasper et al., 2014; Price et al., 2018c). Briefly, male Sprague-Dawley rats (n=10) were maintained on a diet of normal chow (17% fat by kcal) and water. Rats were not food restricted prior to the binge period, and had *ad libitum* access to normal chow and water throughout the study, including during the binge period. Two days prior to experiments, animals were exposed to a mixture of 60% fat by kcal and 40% carbohydrate by kcal to minimize food neophobia. Fat mixtures were prepared and weighed immediately before the binge period. Vegetable shortening (Crisco, Orrville, OH) comprised of 100% fat by energy was mixed with marshmallow creme (Kraft, Chicago, IL), containing 100% carbohydrate by energy, to create combinations of 20% fat (80% carbohydrate, 0% protein), 40% fat (60% carbohydrate, 0% protein), 60% fat (40% carbohydrate, 0% protein), 80% fat (20%

carbohydrate, 0% protein), and 100% fat (0% carbohydrate, 0% protein) by energy. One limitation is that the marshmallow creme does contain some flavoring. However, the consistency and texture of the marshmallow cream were required to promote homogeneity among the mixtures.

Rats were randomized into five groups using a Latin square design, with each animal receiving all mixtures of fat in a randomized order. Each group was presented with mixtures of 20% fat, 40% fat, 60% fat, 80% fat, and 100% fat, for a period of 5 days. Exposure to fat mixtures occurred during the binge 1 at the first 2-hours of the dark cycle (1800-2000) and binge 2 at 2-hours near the end of the light cycle (1400-1600). For all exposures, fat mixtures were weighed prior to presentation and then immediately after the 2-hour binge period. Differences in food weight were interpreted as total grams consumed or total calories consumed during the binge period.

#### ***NAC AND VTA PROTEIN EXTRACTION***

After the completion of binge studies, rats (n=10) were anesthetized with 1-5% isoflurane, and brains were removed. Both NAc and VTA were microdissected from each rat, using guidance from a rat brain atlas (Hommel et al., 2006; Kasper et al., 2018; Paxinos and Watson, 2007), then stored at -80C until protein extraction. The crude synaptosomal protein fraction was isolated as previously published to identify long-term changes in protein expression (Anastasio et al., 2015). NAc and VTA tissue were homogenized in ice-cold Krebs-sucrose buffer containing protease inhibitors (P8340, Millipore Sigma, St. Louis, MO), and phosphatase inhibitors (P5726, P0044 Millipore Sigma, St. Louis, MO). The crude

synaptosomal protein fractionation protocol enriches samples for pre- and postsynaptic proteins (i.e. presynaptic terminals, postsynaptic membranes, etc.) (Breukel et al., 1997). Samples were centrifuged for 10 minutes at 1000g at 4C to pellet the nuclear protein fraction. The supernatant was centrifuged for 20 minutes at 16000g at 4C to separate the crude synaptosomal protein fraction (pellet). The NAc and VTA synaptosomal protein fractions were used for all further analyses. After extraction, total protein concentration was determined using a Pierce BCA Protein Assay Kit (23225, Thermo Fisher, Waltham, MA).

#### ***NMUR2 PROTEIN QUANTIFICATION VIA CAPILLARY ELECTROPHORESIS***

NAc (n=10) and VTA (n=10) samples were assayed for NMUR2 protein expression using the Wes™ (ProteinSimple, San Jose, CA) automated western blotting system. Wes™ is a capillary electrophoresis-based immunoblotting instrument, and was optimized for receptor quantification in brain tissues (Anastasio et al., 2015; Fink et al., 2015). Wes™ reagents (biotinylated molecular weight marker, streptavidin-HRP fluorescent standards, luminol-S, hydrogen peroxide, sample buffer, DTT, stacking matrix, separation matrix, running buffer, wash buffer, matrix removal buffer, secondary antibodies, antibody diluent, and capillaries) were obtained from the manufacturer (ProteinSimple) and used according to the manufacturer's specifications with minor modifications. NMUR2 polyclonal antibody (NBP1-02351, Novus Biologicals, Littleton, CO) was diluted 1:50 in antibody diluent.

Samples were prepared and subjected to capillary electrophoresis-based immunoblotting as described previously (Anastasio et al., 2015). Briefly, 2ug of



protein was denatured in 0.1X sample buffer and 5X master mix at 95°C for 5 minutes. Then, samples and primary antibody were dispensed into a prefilled microplate (ProteinSimple). Capillary electrophoresis (375 V, 25 min, 25°C) and immunodetection were completed using the following settings: separation matrix load: 200s, stacking matrix load: 15s, sample load: 9s, antibody diluent: 30 min, primary antibody incubation: 60 min, secondary antibody incubation: 30 min, and chemiluminescent signal exposure for 15s, 30s, 120s, 240s, and 480s. Data were analyzed using Compass Software (ProteinSimple). The Western blot analyses signal is defined as the area under the curve (AUC) for the NMUR2 peak at 48kDa and representative “virtual blot” electrophoretic images for NMUR2 were automatically generated by the Compass Software (ProteinSimple).

#### **DATA ANALYSIS**

All statistical analyses were performed in GraphPad Prism 7.0a (GraphPad Software Inc., La Jolla, CA) with an experiment wise error rate of  $\alpha=0.05$ . For the binge-type eating curve, intake of 40%, 60%, 80% and 100% fat mixtures were compared to intake of a 20% fat mixture using two-way ANOVA with Bonferroni's multiple comparisons ( $n=10$ ,  $*p<0.05$  and  $**p<0.01$ ).

Relationships between intake of 20%, 40%, 60%, 80% and 100% fat mixtures and synaptosomal NMUR2 protein expression in the NAc were determined via linear regression ( $n=10$ ,  $*p<0.05$ ,  $**p<0.01$ ). Relationships between intake of 20%, 40%, 60%, 80% and 100% fat mixtures and synaptosomal NMUR2 protein expression in the VTA were determined via linear regression ( $n=10$ ,  $*p<0.05$ ,  $**p<0.01$ ).

## RESULTS

### ***NMUR2 IS EXPRESSED PRE-SYNAPTICALLY IN THE NAc AND THE VTA***

Previous work in our lab demonstrated that NMUR2 is expressed post-synaptically in the paraventricular nucleus of the hypothalamus (PVN) and pre-synaptically in the NAc (Benzon et al., 2014; Kasper et al., 2016). We confirmed NAc and VTA localization of NMUR2 with immunohistochemistry. We observed a “beads on a string” staining pattern indicative of presynaptic NMUR2 expression in the NAc (**Figure 3.1a**), as well as in the VTA (**Figure 3.1b**). Interestingly, we also observed staining of cell bodies in the VTA, suggesting that NMUR2 is also expressed post-synaptically in the VTA.

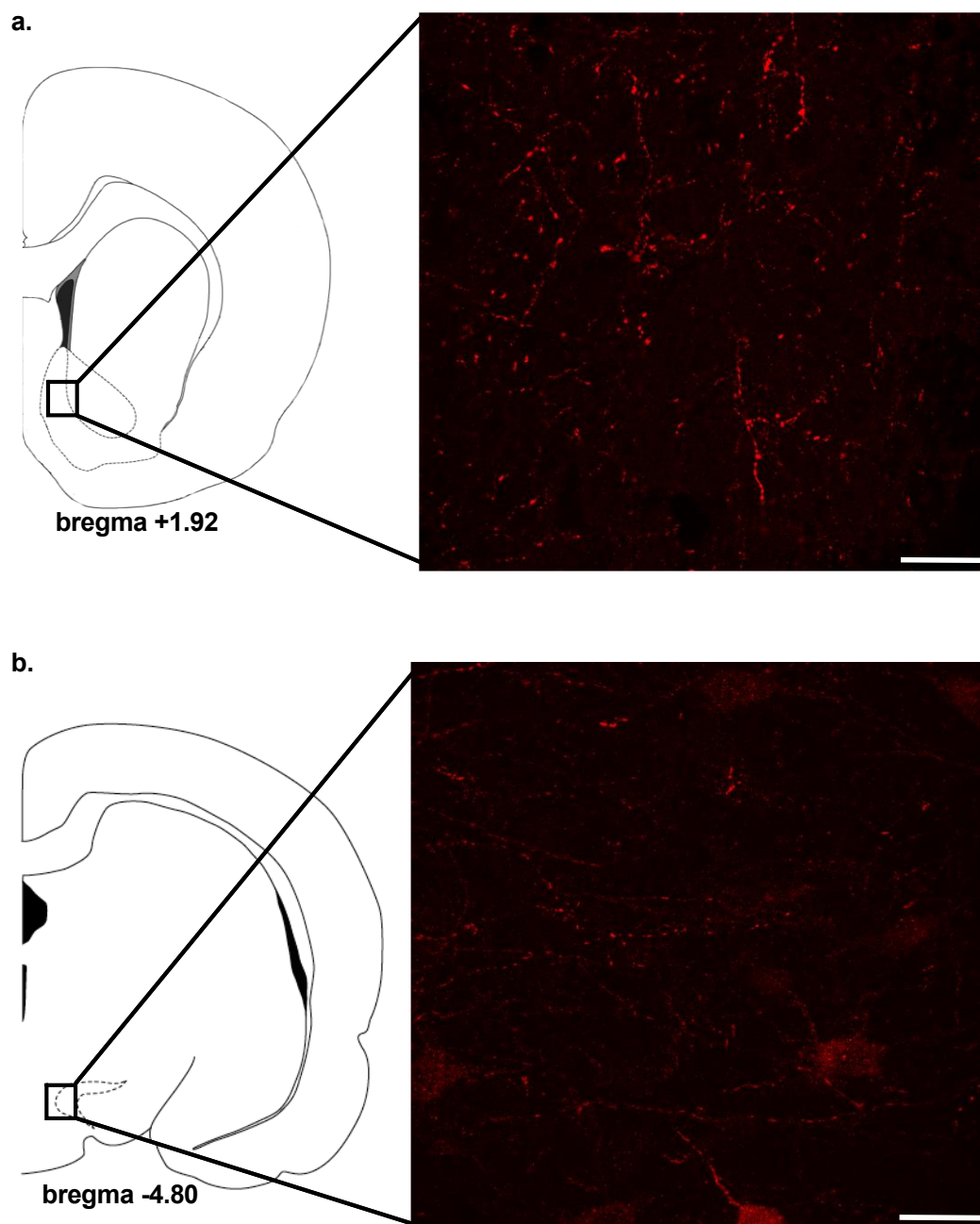


**Figure 3.1: NMUR2 immuno-reactivity in the NAc and the VTA.**

a. representative image of NMUR2 immunostaining in the NAc (bregma +1.92); b. representative image of NMUR2 immunostaining in the VTA (bregma -4.80). Images were acquired from the regions indicated at 63X oil in confocal mode with scale bar = 25 $\mu$ m.

### ***FAT CONTENT IS CRITICAL FOR BINGE-TYPE EATING***

Using our binge-type eating paradigm, we quantified how much rats would consume during a 2-hour binge period (**Figure 3.2**). **Figure 3.2** illustrates intake across a spectrum of fat contents during two different binge sessions- binge 1 and binge 2. Statistical comparisons were made within each binge to intake of a 20% fat mixture. In binge 1, rats consumed significantly less grams of 100% fat mixture ( $p=0.0003$ ) compared to a 20% fat mixture (**Figure 3.2**). In binge 2, rats consumed significantly more grams of a 60% fat mixture ( $p=0.010$ ) compared to a 20% fat mixture (**Figure 3.2**). Notably, common western diet foods contain percentages of fat that fall at the peak of the curve, including French fries (42% fat), potato chips (56% fat), cheesecake (63% fat), and peanut butter (78% fat), which gives context for the percentages of fat used in our rodent studies.

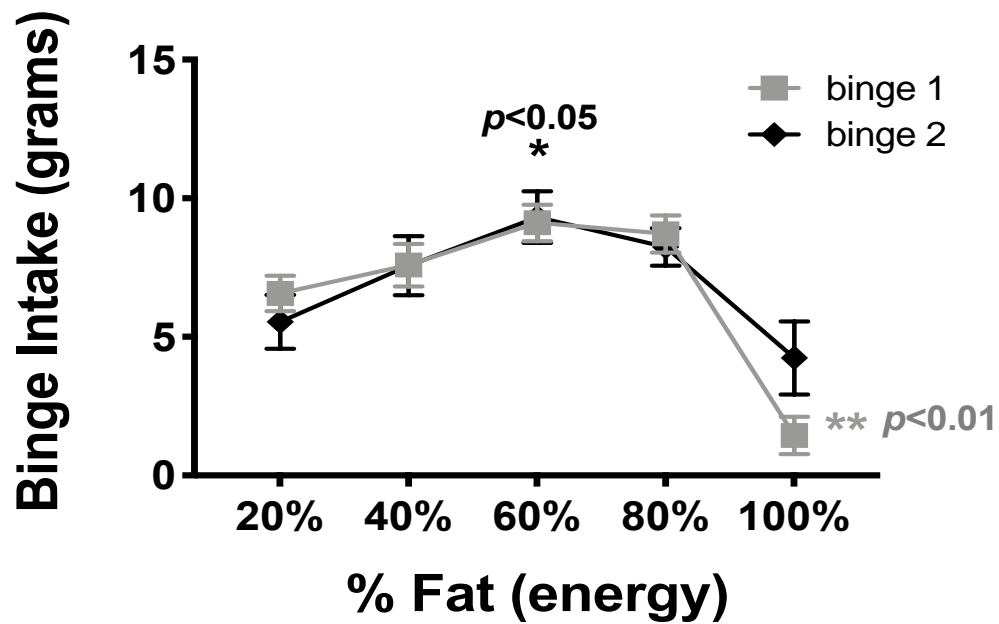


**Figure 3.2: Fat content is critical for binge-type eating.**

Rat binge-type eating across a spectrum of fat contents. Binge-type eating in rats is highest at 60% fat and lowest at 80% fat compared to 20% fat;  $n=10$ ,  $*p<0.05$  and  $**p<0.01$  by two-way ANOVA with Bonferroni's multiple comparisons.

**HIGHER NAc NMUR2 SYNAPTOSOMAL PROTEIN EXPRESSION POTENTIATES BINGE-TYPE EATING OF “LOWER FAT” FOOD**

To determine the relationship between binge-type intake and NMUR2 expression in the NAc, we quantified NAc NMUR2 synaptosomal protein (48kDa) (**Figure 3.3a**), and correlated it to fat intake during the binge period (**Figure 3.3b-f**). Interestingly, NAc NMUR2 expression demonstrated a strong positive correlation with binge intake of a “lower” fat mixture, specifically 20% fat ( $p=0.047$ ) and 40% fat ( $p<0.001$ ) (**Figure 3.3b-c**). As fat content is increased, the relationship diminishes. However, no significant correlation was observed when the data are correlated as total calories consumed to compensate for energy density. In addition, we found no significant correlation between NAc NMUR2 and binge intake of a 60% ( $p=0.86$ ), 80% ( $p=0.084$ ), or 100% ( $p=0.86$ ) fat mixture (**Figure 3.3d-f**).

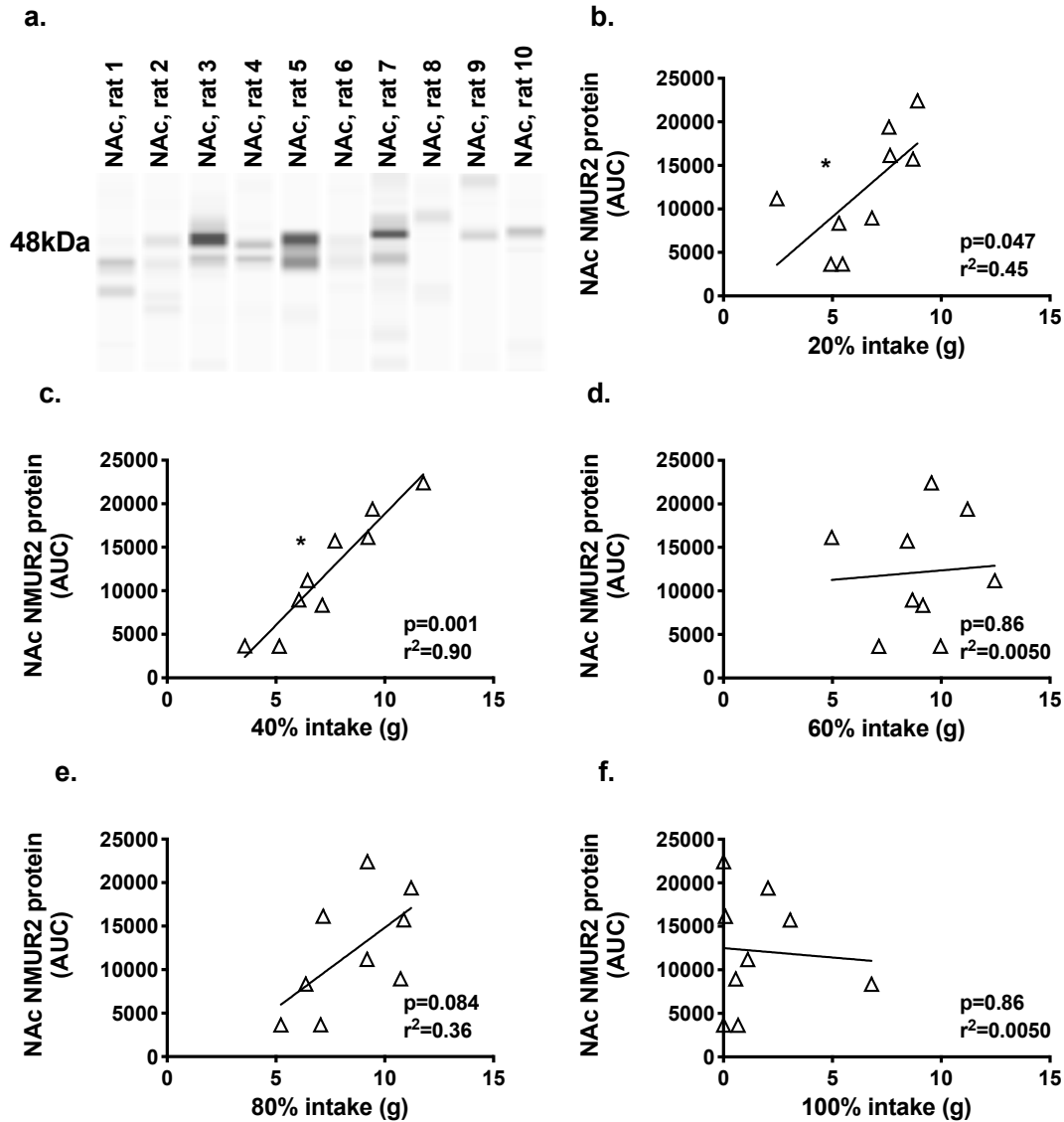


**Figure 3.3: Higher NAc NMUR2 synaptosomal protein expression potentiates binge-type eating of "lower" fat food.**

a. representative Western blot image for NMUR2 synaptosomal protein from NAc samples; b. NAc NMUR2 expression is positively correlated with intake of a 20% fat mixture; c. NAc NMUR2 expression is positively correlated with intake of 40% fat mixture; d. NAc NMUR2 expression is not correlated with intake of a 60% fat mixture; e. NAc NMUR2 expression is not correlated with intake of an 80% fat mixture; f. NAc NMUR2 protein expression is not correlated with intake of a 100% fat mixture;  $n=10$ ,  $*p<0.05$ ,  $**p<0.01$  by linear regression.

***LOWER VTA NMUR2 SYNAPTOSOMAL PROTEIN EXPRESSION HALTS BINGE-TYPE EATING OF EXTREME HIGH-FAT FOOD***

Next, we quantified VTA NMUR2 synaptosomal protein (48kDa) (Figure 3.4a). We correlated VTA NMUR2 synaptosomal protein to fat intake during the binge period (Figure 3.4b-f). No significant correlation was observed between VTA NMUR2 and binge intake of a 20% ( $p=0.11$ ), 40% ( $p=0.37$ ), 60% ( $p=0.95$ ), or 80% ( $p=0.26$ ) fat mixture (Figure 3.4b-e). VTA NMUR2 demonstrated a strong negative correlation with binge intake of an “extreme” high-fat mixture of 100% fat ( $p=0.034$ ) (Figure 3.4f). Interestingly, the slope of the trend line transitions from a positive slope value for the lower fat mixtures to a negative slope for the higher fat mixtures.



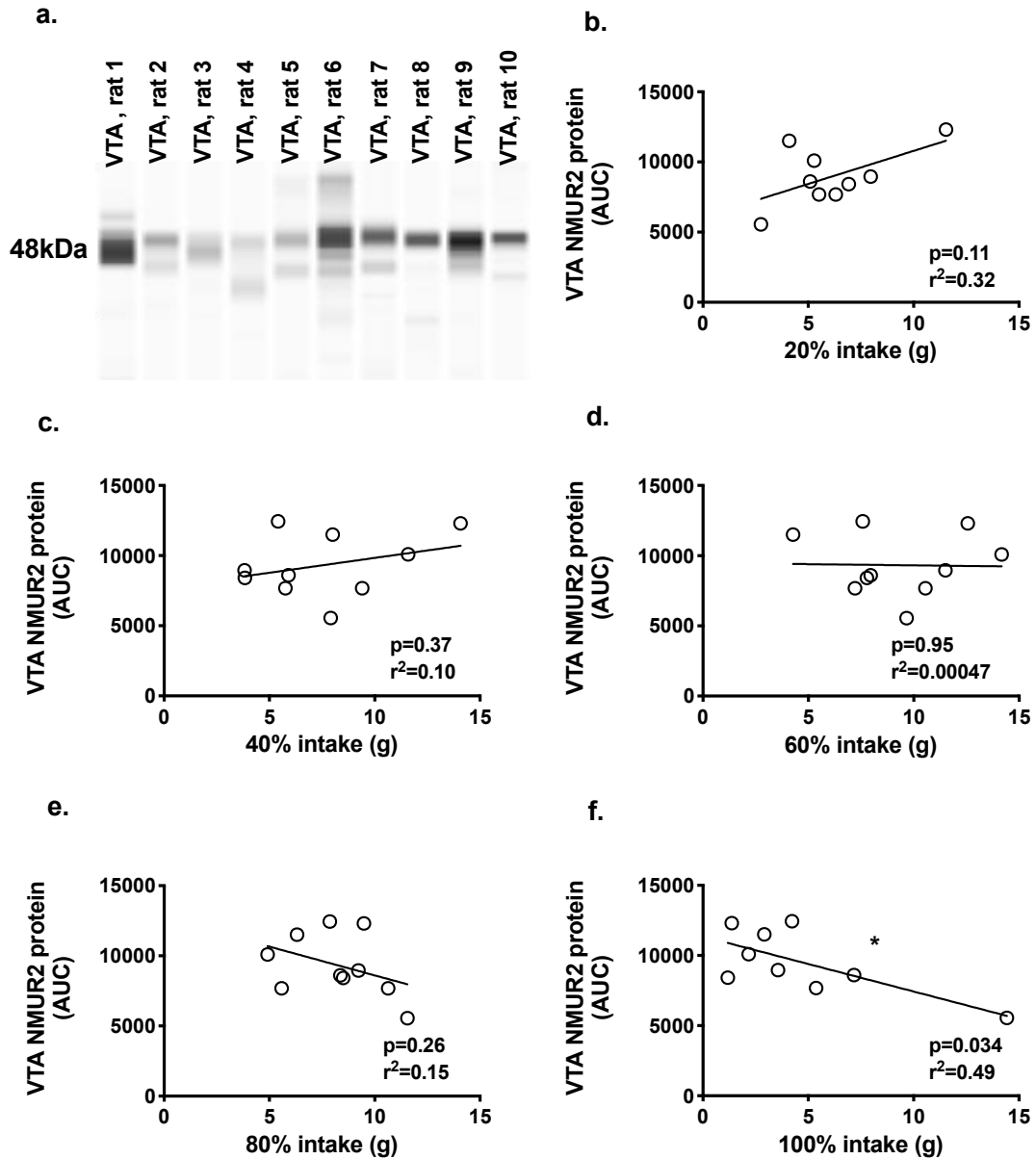


**Figure 3.4: Lower VTA NMUR2 synaptosomal protein expression halts binge-type eating of extreme high-fat food.**

a. representative Western blot image for NMUR2 synaptosomal protein from VTA samples; b. VTA NMUR2 expression is not correlated with intake of a 20% fat mixture; c. VTA NMUR2 expression is not correlated with intake of a 40% fat mixture; d. VTA NMUR2 expression is not correlated with intake of a 60% fat mixture; e. VTA NMUR2 expression is not correlated with intake of an 80% fat mixture; f. VTA NMUR2 expression is negatively correlated with intake of a 100% fat mixture;  $n=10$ , \* $p<0.05$ , \*\* $p<0.01$  by linear regression.

## DISCUSSION

In the present study, we assessed synaptic localization of NMUR2 in the NAc and the VTA. Our results support previous studies indicating synaptic NMUR2 expression in the NAc. Additionally, these results extend our knowledge by demonstrating western blot staining of NMUR2 in synaptosomal VTA fractions, and by visualizing punctate staining patterns for NMUR2 in the VTA consistent with synaptic localization (Kasper et al., 2016). Our NMUR2 antibody has previously been shown to stain NMUR2 expressing cell bodies in the PVN, suggesting that the staining pattern is not an antibody limitation (Benzon et al., 2014). In the NAc, NMUR2 is localized to synapses that express a neuronal marker of GABAergic signaling, which suggests a potential role for NMUR2 in inhibitory signaling (Kasper et al., 2016). As such, more studies are needed to determine the functional role of NMUR2 in the mesoaccumbens circuit, including its effects on BED and obesity.

Next, we used an animal model of binge-type eating to quantify binge intake in rats. This model only simulated a binge episode, similar to that observed in BED and obesity (Benzon et al., 2014; Corwin et al., 2011; Corwin and Babbs, 2012; Corwin and Wojnicki, 2006; Kasper et al., 2014; Price et al., 2018c). One of the major limitations of our study is the inability of our model to replicate all clinical aspects of BED. While our model can quantify food intake during a binge episode, it does not replicate the psychological aspects of BED, such as feelings of loss of control and feelings of shame and guilt (2017; Association, 2013a, b; Guerdjikova et al., 2017). Nonetheless, this model is helpful in understanding neural

mechanisms underlying binge-type consumption and identifying potential regulators of this specific overconsumption behavior. During our studies animals were maintained on their normal chow consisting of 17% fat by kcal. Fat mixtures were designed to contain higher fat concentrations that are preferred by rats and have translational relevance in humans (Drewnowski, 1997; Drewnowski and Almiron-Roig, 2010; Drewnowski and Greenwood, 1983; Drewnowski et al., 1982; Kasper et al., 2014).

Using our model of binge-type eating, we quantified binge-type consumption across a spectrum of fat mixtures and correlated it to synaptosomal NMUR2 protein expression in the NAc and the VTA in rats. To our knowledge, we are the first to quantify synaptosomal NMUR2 protein in the NAc and VTA and the first to explore relationships between NMUR2 expression and binge intake.

Our results demonstrated a strong positive correlation between synaptosomal NMUR2 protein expression in the NAc and binge intake of “lower” fat contents of 20% fat and 40% fat. This region-specific effect of NAc NMUR2 facilitated binge-type intake of “lower” fat food, especially food around 40% fat, which is commonly overconsumed in humans (Drewnowski, 1997; Drewnowski and Almiron-Roig, 2010; Drewnowski and Greenwood, 1983; Drewnowski et al., 1982; Yanovski et al., 1992). This finding supports a role of increased NAc NMUR2 as a “behavioral accelerator” on binge intake of “lower” fat food.

Synaptosomal VTA NMUR2 protein expression demonstrated a strong negative correlation with binge intake of an “extreme” high fat mixture, particularly 100% fat. Contrary to NAc NMUR2, this finding implicates VTA NMUR2 as an

inhibitor of binge intake of “extreme” high-fat food. Thus, VTA NMUR2 may act as a “behavioral brake” on binge intake of high-fat food. While these findings are strong, statistically sound relationships, the small sample size is one limitation of our study.

Overall, our findings demonstrate key relationships brain region specific differences in synaptosomal NMUR2 protein expression, and establish NMUR2 as a regulator of binge-type intake in rats in the NAc and the VTA. Binge-type eating changes based on fat content and NMUR2 expression varies not only across animals, but across brain regions. Thus, endogenous NMUR2 may be a driver of individual differences in binge-type eating. Although the observed high degree of inter-animal variability and inter-brain region variability of NMUR2 can limit data interpretation based on averaged differences in NMUR2, it also suggests that NMUR2 protein may contribute to individual differences for binge-type food intake in humans.

The clinical implications of our findings establish NMUR2 as a novel regulator of binge-type eating and therefore as a potential druggable candidate for the overconsumption behavior observed in BED and obesity. Recently, we showed that small-molecule NMUR2 agonists successfully decrease high-fat food intake in rats, which supports NMUR2 as a viable drug target (Sampson et al., 2018). Future studies will continue to investigate the contribution of NMUR2 in the NAc and the VTA at molecular, neural, and pharmacological levels, including investigating the effects of these small-molecule NMUR2 agonists on binge-type eating.

## **Chapter 4 Neuroanatomical and Neurochemical Properties of PVN→NAc Projections**

### **INTRODUCTION**

Food intake is orchestrated by complex neural pathways that influence feeding behaviors through the integration of homeostatic nutritional requirements with natural hedonic reward (Berthoud, 2011; Ferrario et al., 2016; Rossi and Stuber, 2018; Saper et al., 2002). Homeostatic feeding behavior is typically associated with hypothalamic brain nuclei, specifically the paraventricular nucleus of the hypothalamus (PVN) which controls food intake to maintain body weight (Elmquist et al., 1999; Leibowitz et al., 1981; Morton et al., 2006; Williams et al., 2001). On the other hand, the nucleus accumbens (NAc) regulates reinforcement and goal-directed behavior and has been demonstrated to drive hedonic feeding (Berridge, 2009; Carlezon and Thomas, 2009). One manner in which the PVN may regulate reinforcement is through its direct inputs to the nucleus accumbens (NAc) (Dölen et al., 2013; Hajnal et al., 1997). Both the PVN and the NAc have been implicated in the control of feeding behaviors, but the direct interplay of these regions, including functional mechanisms of PVN→NAc signaling, in regulating feeding behavior is unknown (Anastasio et al., 2019; Baldo and Kelley, 2007; Benzon et al., 2014; Corwin et al., 2011; Maldonado-Irizarry et al., 1995; McCue et al., 2017; Sharma et al., 2013; Smith et al., 2019). To date, PVN→NAc projections are largely uncharacterized-it is established that these projections synthesize and release oxytocin, but little else is known (Dölen et al., 2013).

Therefore, we sought to define the neuroanatomical and the functional properties of PVN→NAc.

Through a combination of neuronal tracing techniques and immunohistochemistry, we described both pre- and post-synaptic characteristics of PVN→NAc projection neurons. To identify neurotransmitters released from PVN→NAc projection neurons, we employed microdialysis followed by capillary electrophoresis and laser-induced fluorescence (CE-LIF). We show for the first time that PVN→NAc neurons are localized to parvocellular PVN, equipped with vesicular glutamate transporter 1 (VGLUT1), and that stimulation of PVN→NAc neurons increases extracellular glutamate in the NAc.

## **SPECIFIC METHODS**

### **ANIMALS**

Male Sprague-Dawley rats (Harlan, Houston, TX) weighing 225-250g were used in all experiments. Animals were housed individually in a temperature- (21-23°C) and humidity- (40-50%) controlled environment with a standard 12h light-dark cycle (lights on between 0600 and 1800 hours). All animals were given *ad libitum* access to normal chow (17% fat by kcal; Teklad LM-485 Mouse/Rat Sterilizable Diet; Teklad Diets, Madison, WI) and water in their home cages. Upon arrival, animals were allowed to acclimate to the room for seven days prior to handling and experimental procedures. All experiments were conducted in accordance with the *NIH Guide for Use and Care of Laboratory Animals* (2011), and with approval from the Institutional Animal Use and Care Committee at the

University of Texas Medical Branch and the Institutional Animal Use and Care Committee at the University of Florida (microdialysis).

### ***SURGERIES***

For retrograde tracing of NAc inputs, rats (n=3) received bilateral injection of a retrograde AAV6-GFP into the NAc (**Figure 4.1a**). To label terminals in the NAc, rats (n=3) received bilateral injection of AAV2-CAMKIIa-EGFP (**Figure 4.2**). All stereotaxic injections (Kopf Instruments, Tujunga, CA) were performed under 2-5% isoflurane anesthesia (VetEquip, Pleasanton, CA) aimed at the PVN or NAc shell at a 10 degree angle at the following coordinates: PVN: A/P -0.18mm; M/L +0.20mm; D/V -0.82mm from bregma; NAc: A/P +0.14mm; M/L +0.20mm; D/V -0.68mm (Paxinos and Watson, 2007). We targeted the NAcSh for its known involvement in reinforcement and goal-directed behavior. Rats recovered for 2 weeks post-surgery to ensure optimal viral expression.

To determine the functional mechanism of PVN→NAc neurons, rats received bilateral injection of AAV2-CAMKIIa-EGFP (CTRL (plasmid 50469, Addgene) or AAV2-CAMKII-HA-hM3D(G<sub>q</sub>)-IRES-mCitrine (hM3D) (plasmid 50466, Addgene) into the PVN at A/P -0.18mm; M/L +0.20mm; D/V -0.82mm from bregma (Paxinos and Watson, 2007). Unilateral guide cannula for CNO micro-infusion (C315GA/SPC26GA, PlasticsOne, Roanoke, VA) cut 6mm below the pedestal were implanted at a 20 degree outside angle at the following coordinates: A/P +1.4mm; M/L +3.2mm; D/V -5.8mm from bregma and a unilateral guide cannula for microdialysis probe placement was implanted at a 0 degree outside angle at the following coordinates: A/P +1.4mm; M/L -0.18mm; D/V -5.3mm from

bregma (Kasper et al., 2016). Guide cannulae were secured with dental cement and stainless-steel screws. Microdialysis probes with 2 mm active length and 13,000 molecular weight cut off were constructed as previously described (Kasper et al., 2015). After calibration, probes were inserted in the guide cannula (see **Figure 4.7** for placement), connected to a dual channel swivel, and perfused with aCSF at 1  $\mu$ L/min. The swivel was mounted atop a modified home cage lid so that animals could move freely and have access to food and water during the experiment.

### ***GFP IMMUNOREACTIVITY IN THE PVN***

Rats were anesthetized with 5% isoflurane and perfused with 1X PBS for 5 minutes then 4% paraformaldehyde for 15 minutes. Whole brains were collected and immediately post-fixed in 4% PFA overnight. The following day, brains were moved to a solution of 1X PBS + 20% glycerol. Brain slices (40 $\mu$ m) containing the PVN and/or the NAc were collected and stored in 1X PBS + 0.05% sodium azide until immunohistochemistry was performed. Briefly, slices were washed, unmasked, blocked and incubated in primary antibody overnight. The next day, slices were washed in 1X PBS and incubated in secondary antibody for 2 hours. Slices were washed in 1X PBS and mounted. Images were acquired using Leica True Confocal Scanner SPE in confocal mode and Leica Application Suite x software (Leica Microsystems).

The following primary antibodies were used: Anti-chicken GFP (1020, 1:200, Aves Labs; Anti-mouse vesicular glutamate transporter 1 (VGLUT1) (ab135311, 1:200, Synaptic Systems); Anti-mouse glutamate decarboxylase 67



(GAD<sub>67</sub>) (ab26116, 1:200, Abcam); Anti-mouse tyrosine hydroxylase (TH) (T2928, 1:500, Sigma); Anti-mouse tryptophan hydroxylase (TPH) (T0678, 1:500, Sigma); Anti-rabbit phospho-cFos (5348, 1:200, Cell Signaling) The following secondary antibodies were used: Donkey anti-chicken 488 (703-545-155, 1:200, Jackson ImmunoResearch); Donkey anti-mouse AlexaFluor 488 (A21202, 1:200, Invitrogen); Donkey anti-mouse AlexaFluor 555 (A31570, 1:200, Invitrogen); Donkey anti-rabbit AlexaFluor 568 (A10042 1:200, Invitrogen).

Neurons of the PVN are defined by their location within structurally established parvocellular or magnocellular regions (Paxinos and Watson, 2007). These regions were superimposed on 10X tile scan images to outline a region of interest for quantification of GFP+ cell bodies projecting to the NAc. Researcher quantification was confirmed by an objective quantification via Fiji Is Just Image J (FIJI, Image J). Briefly, a region of interest was applied to all images, then background subtracted. Image threshold was adjusted and size and circularity parameters applied to each image.

#### ***PRESYNAPTIC GLUTAMATE IMMUNOREACTIVITY IN THE NAC***

Rats were anesthetized with 5% isoflurane and perfused with 1X PBS for 5 minutes then 4% paraformaldehyde for 15 minutes. Whole brains were collected and immediately post-fixed in 4% PFA overnight. The following day, brains were moved to a solution of 1X PBS + 20% glycerol. Brain slices (40um) containing the PVN and/or the NAc were collected and stored in 1X PBS + 0.05% sodium azide until immunohistochemistry was performed. Briefly, slices were washed, unmasked, blocked and incubated in primary antibody overnight. The next day,

slices were washed in 1X PBS and incubated in secondary antibody for 2 hours. Slices were washed in 1X PBS and mounted. Images were acquired using Leica True Confocal Scanner SPE in confocal mode and Leica Application Suite x software (Leica Microsystems).

The following primary antibodies were used: Anti-chicken GFP (1020, 1:200, Aves Labs; Anti-mouse vesicular glutamate transporter 1 (VGLUT1) (ab135311, 1:200, Synaptic Systems); Anti-mouse glutamate decarboxylase 67 (GAD<sub>67</sub>) (ab26116, 1:200, Abcam); Anti-mouse tyrosine hydroxylase (TH) (T2928, 1:500, Sigma); Anti-mouse tryptophan hydroxylase (TPH) (T0678, 1:500, Sigma); Anti-rabbit phospho-cFos (5348, 1:200, Cell Signaling) The following secondary antibodies were used: Donkey anti-chicken 488 (703-545-155, 1:200, Jackson ImmunoResearch); Donkey anti-mouse AlexaFluor 488 (A21202, 1:200, Invitrogen); Donkey anti-mouse AlexaFluor 555 (A31570, 1:200, Invitrogen); Donkey anti-rabbit AlexaFluor 568 (A10042 1:200, Invitrogen).

Images of synapses in the NAc that originate in the PVN were acquired at 63X (oil). Images were analyzed for co-localization using Leica Application Suite x software (Leica Microsystems). Synapses were identified by size ~1um and co-localization was quantified via overlap coefficient.

### ***NAc MICRODIALYSIS***

Neurotransmitter data was collected via microdialysis and quantified using with capillary electrophoresis with laser-induced fluorescence (Bowser and Kennedy, 2001; Kasper et al., 2015; Li et al., 2008). A standard curve (7 concentrations of glutamate, aspartate, ornithine, GABA, taurine, glutamine,

serine, and glycine ranging from 0 to 20  $\mu\text{M}$ ) was generated using a microdialysis probe prior to beginning the experiment. The elution time of these neurotransmitters have been validated and characterized previously (Bowser and Kennedy, 2001). After calibration, the probe was implanted in a non-anesthetized and freely moving rat via the guide cannula. A baseline for each animal was collected for 2 hours prior to the experiment (average glutamate 6.20  $\mu\text{M}$ , GABA 0.37  $\mu\text{M}$ ). For the experiment, 2 $\mu\text{L}$  of 1 $\mu\text{M}$  CNO (6329, Tocris Biosciences) was administered via the guide cannula at a rate of 0.5 $\mu\text{L}/\text{min}$  for 4 minutes (Stachniak et al., 2014). Microdialysis probe placement and cannula placement were verified and all misses were eliminated prior to data analysis.

#### ***PHOSPHO-cFos IMMUNOREACTIVITY IN THE PVN AND THE NAc***

Immunohistochemistry was conducted as previously described (Kasper et al., 2018; Kasper et al., 2016; McCue et al., 2017; Smith et al., 2019). Phospho-cFos was immuno-enhanced using anti-rabbit phospho-cFos (Ser 32) (Cell Signaling, 5348), then visualized in the PVN and in the NAc. Tile scans were acquired at 10X using Leica True Confocal Scanner SPE in camera mode and Leica Application Suite x software (Leica Microsystems). Images were analyzed for phospho-cFos expression using FIJI (Image J). A region of interest was created in FIJI and applied to all images. The following parameters were applied to all images for analysis: rolling ball radius: 20.0, threshold: 0-20, particle size: 50-infinity (pixel units), circularity: 0.00-1.00.

## **DATA ANALYSIS**

All statistical analyses were performed in GraphPad Prism 7.0a (GraphPad Software Inc., La Jolla, CA) with an experiment wise error rate of  $\alpha=0.05$ . GFP-positive PVN cell bodies that project to the NAc were counted throughout anterior to posterior PVN, in parvocellular and magnocellular regions. The number of GFP-positive PVN cell bodies in parvocellular vs. magnocellular regions were compared via unpaired T-test ( $n=3$ ,  $**p<0.01$ ) The number of GFP-positive PVN cell bodies that project to the NAc within anterior, medial and posterior PVN were compared by one-way ANOVA ( $n=3$ ,  $p>0.05$ ).

PVN→NAc co-localization with neurotransmitter markers were counted in the NAc. Quantification of PVN→NAc+ VGLUT1+ events were compared to PVN→NAc+GAD<sub>67</sub>+, TH+ and TPH+ events by one-way ANOVA ( $n=4$ ,  $*p<0.05$ ). Extracellular glutamate release was quantified in CTRL+CNO and hM3d+CNO rats and compared by two-way ANOVA (CTRL  $n=3$ , hM3d  $n=3$ ,  $*p<0.05$  and  $**p<0.01$ ). Extracellular GABA release was quantified in CTRL+CNO and hM3d+CNO rats and analyzed via two-way ANOVA (CTRL  $n=3$ , hM3d  $n=3$ ,  $p>0.05$ ).

Phospho-cFos positive events were quantified via FIJI in the PVN of CTRL+CNO and hM3d+CNO rats and analyzed via unpaired T-test (CTRL  $n=3$ , hM3d  $n=3$ ,  $p>0.05$ ). Phospho-cFos positive events were quantified in FIJI in the NAc of CTRL+CNO and hM3d+CNO rats and analyzed via unpaired T-test (CTRL  $n=3$ , hM3d  $n=3$ ,  $**p<0.01$ ).

## **RESULTS**

### ***PVN→NAc CELL BODIES ARE LOCALIZED TO PARVOCELLULAR COMPARTMENTS OF THE PVN***

To define the origin of PVN inputs to the NAc, we employed a retrograde tracer in the NAc and examined green fluorescent protein (GFP)-labeled PVN cell bodies distributed across magnocellular and parvocellular regions of the PVN (**Figure 4.1**). Quantification of GFP-positive cell bodies revealed that PVN→NAc cell bodies are highly localized to parvocellular regions of the PVN (**Figure 4.1b**), and are uniformly distributed throughout anterior, medial and posterior regions of the PVN (**Figure 4.1c**). Representative images of GFP-labeled cells bodies within parvocellular and magnocellular regions of the PVN are shown in **Figure 4d**. In the anterior PVN (bregma -1.08mm), GFP-labeled cell bodies are seen immediately adjacent to the third ventricle (3V). In the medial PVN (bregma -1.44mm), GFP-labeled cell bodies are also immediately adjacent to 3V, and thus are localized to the medial parvocellular compartment (PaMP). In the posterior PVN (bregma -1.80mm), GFP-labeled cell bodies are again surrounding 3V and localized to the parvocellular compartment.

The presence of GFP-positive cell bodies throughout parvocellular regions of the PVN is evidence of a pathway arising in the PVN and projecting directly to the NAc. A critical functional distinction exists between parvocellular and magnocellular regions of the PVN- the parvocellular region is known to drive intake of highly palatable food, whereas the magnocellular region is not (Jhanwar-Uniyal et al., 1993). The localization of PVN→NAc neurons to the parvocellular region provides neuroanatomical evidence that the PVN→NAc pathway may regulate feeding behavior (Jhanwar-Uniyal et al., 1993).

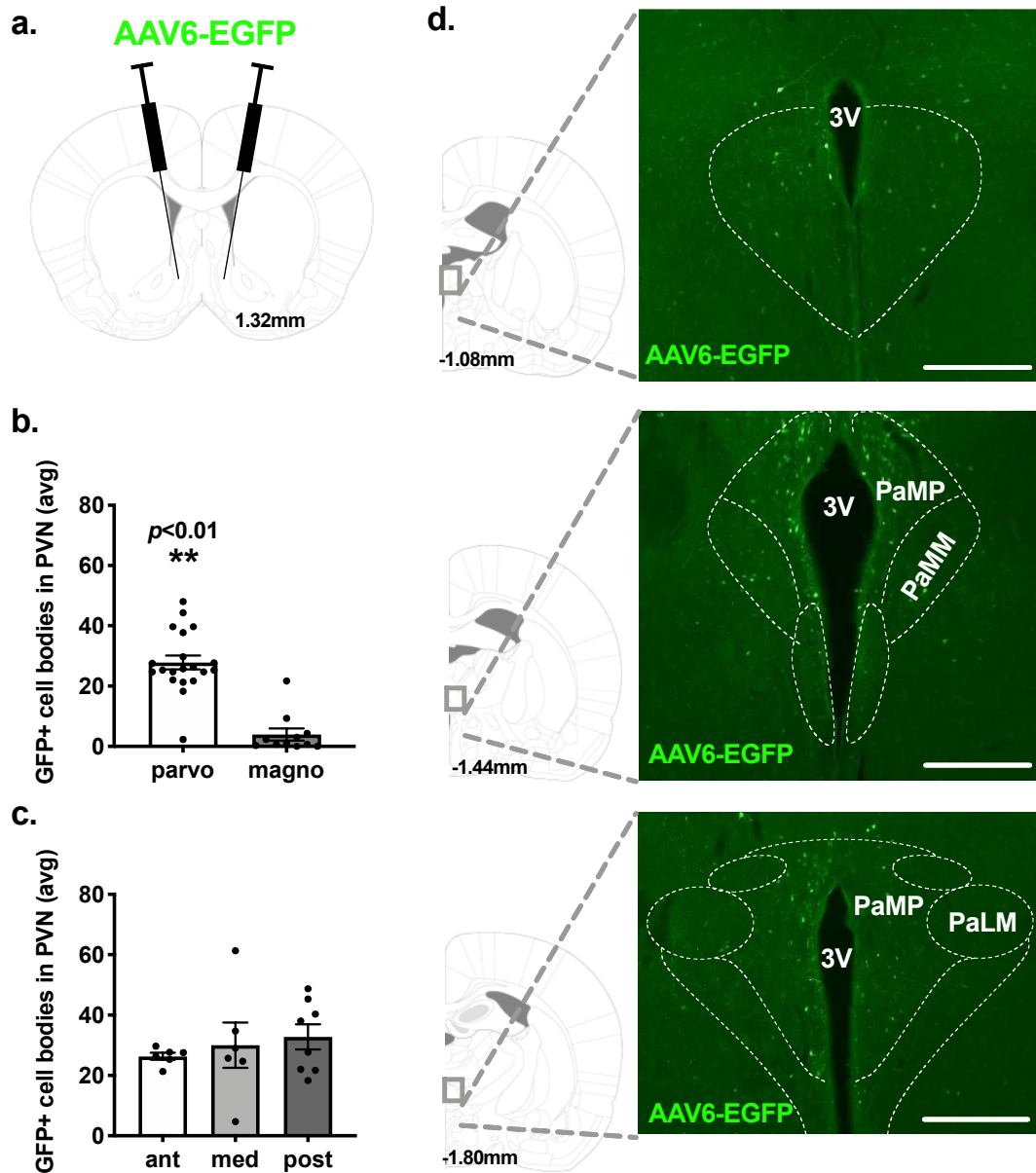


**Figure 4.1: PVN→Nac cell bodies are localized to parvocellular compartments of the PVN.**

a. viral targeting approach to label PVN→Nac cell bodies. b. PVN cell bodies that project to the NAc are localized to parvocellular regions of the PVN.  $n=3$  per region,  $**p < 0.01$  by unpaired T-test. c. PVN cell bodies that project to the NAc are uniformly localized in anterior, medial and posterior PVN.  $n=3$  per region,  $p > 0.05$  by one-way ANOVA. d. representative PVN images from  $n=3$  brains of anterior, medial and posterior PVN with outlined structures used in quantification.

### ***PVN→NAc SYNAPSES CO-LOCALIZE WITH VGLUT1, BUT NOT GAD<sub>67</sub>, TH, OR TPH***

We also profiled PVN→NAc using an anterograde tracer in the PVN to identify co-localization of GFP-labeled terminals in the NAc with specific neurotransmitter markers (**Figure 4.2a**). We investigated co-localization of PVN→NAc terminals with VGLUT1 (glutamate), GAD<sub>67</sub> (GABA), TH (dopamine), and TPH (serotonin). Our analysis revealed several co-localization events of PVN→NAc with VGLUT1 (**Figure 4.2b**). Interestingly, we identified that PVN→NAc terminals co-localize the most frequently with VGLUT1 (**Figure 4.2c**), compared to GAD<sub>67</sub>, TH, and TPH (**Figure 4.3**) and is consistent with VGLUT1 expression in the hypothalamus, and also converges with the role of glutamate afferents to the NAc altering feeding behavior (Baldo and Kelley, 2007; Liguz-Leczna and Skangiel-Kramska, 2007; Maldonado-Irizarry et al., 1995). This provides neuroanatomical evidence for glutamate as the major neurotransmitter involved in PVN→NAc signaling.

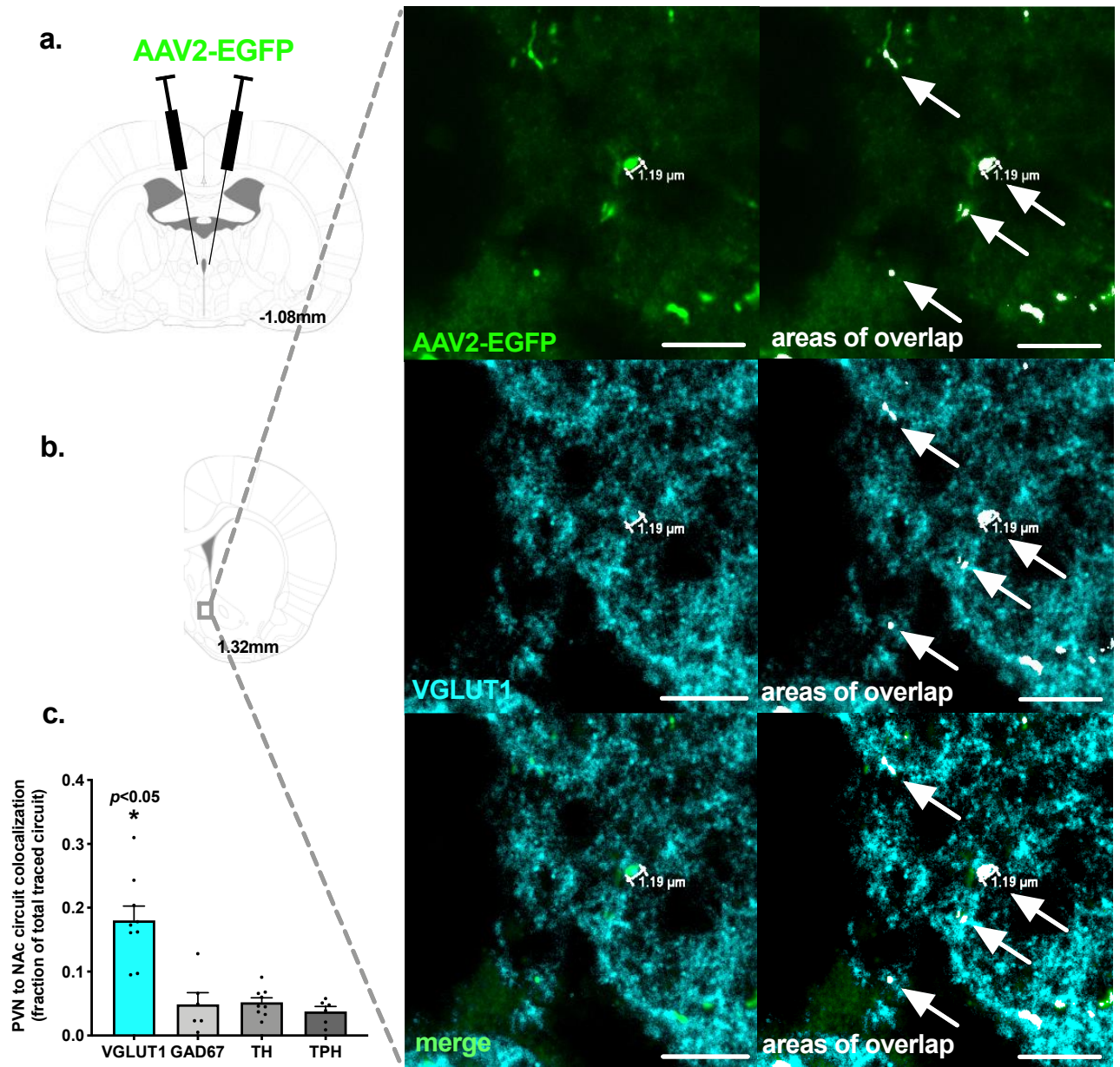


**Figure 4.2: PVN→NAc terminals co-localize with VGLUT1.**

a. viral targeting approach to label PVN→NAc terminals. b. representative NAc images from  $n=4$  brains illustrating PVN→NAc terminals overlap with VGLUT1. Images were taken at 63x with digital zoom factor 7 using Leica software. c. PVN→NAc terminals strongly localize with VGLUT1 compared to GAD<sub>67</sub>, TH and TPH.  $n=4$ ,  $*p < 0.05$  by one-way ANOVA.



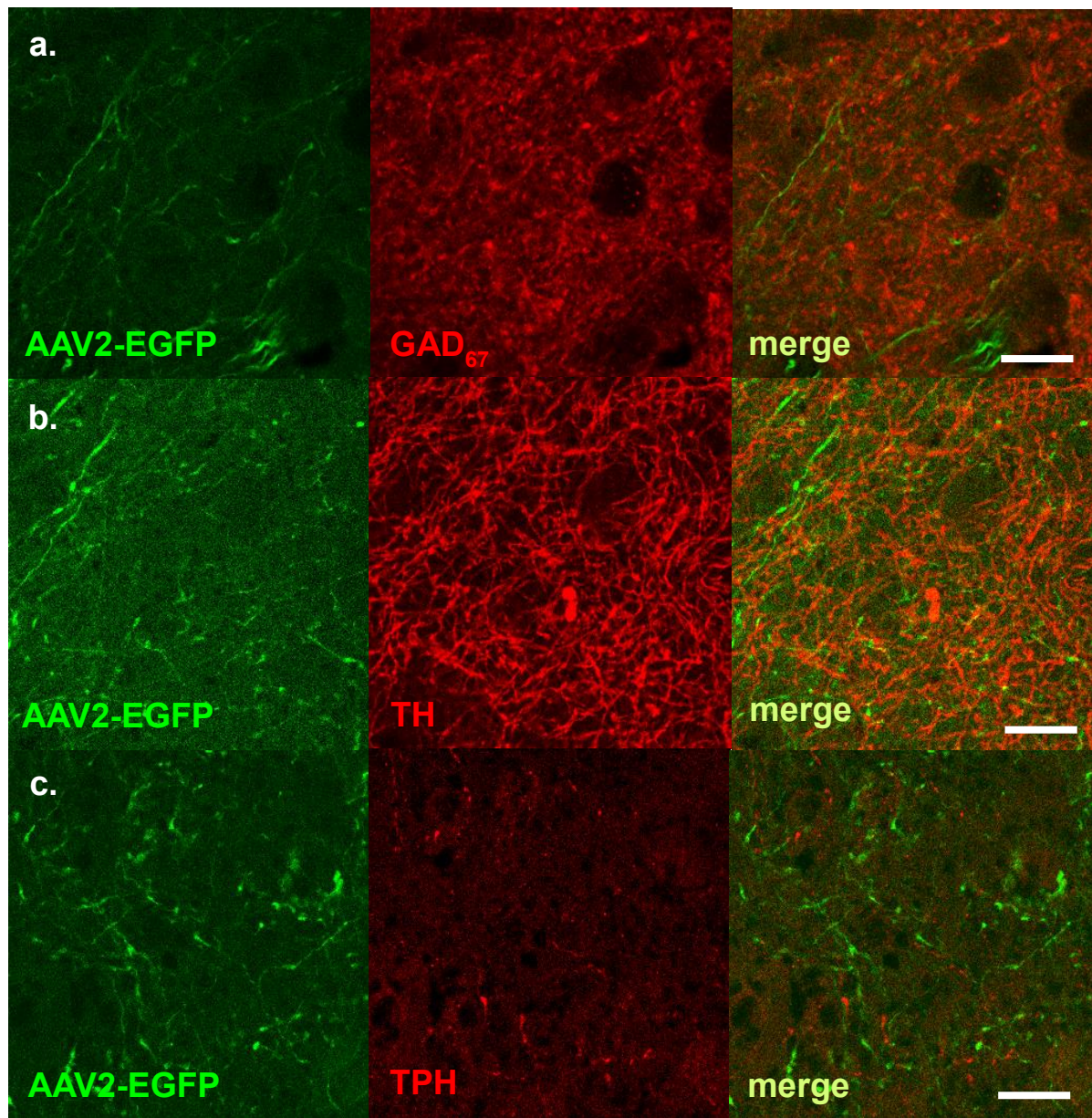


**Figure 4.3: PVN→NAc terminals do not co-localize with GAD<sub>67</sub>, TH, or TPH.**

a. representative NAc images from n=4 brains illustrating PVN→NAc terminals do not overlap with GAD<sub>67</sub>, a marker of GABAergic signaling. b. representative NAc images from n=4 brains illustrating PVN→NAc terminals do not overlap with TH, a marker of dopaminergic signaling. c. representative NAc images from n=4 brains illustrating PVN→NAc terminals do not overlap with TPH, a marker of serotonergic signaling. Images were taken at 63x.

***HM3D-INDUCED STIMULATION OF PVN→NAC INCREASES EXTRACELLULAR GLUTAMATE IN THE SYNAPSE***

To determine the functional mechanism of PVN→NAc signaling, we used a pharmacogenetic approach to stimulate neurotransmitter release from PVN→NAc projections. Neurotransmitters were identified and quantified in real time via capillary electrophoresis followed by laser-induced fluorescence (See Methods). Neurotransmitters were collected for 4 hours prior to CNO micro-infusion to establish a baseline for each animal (**Figure 4.4**).



**Figure 4.4: Experimental timeline for microdialysis.**

Rats expressing CTRL or hM3d virus recovered in their home cages for 14 days to allow for peak viral expression. For the experiment, individual rats were placed in a standard rat cage adapted for microdialysis. Baseline dialysate was collected for 4 hours. After 4 hours, test dialysate was collected. 12 minutes into the 4-hour test collection, 1uM CNO was administered intra-NAc.

We used AAV2 to transduce PVN→NAc neurons with the excitatory designer receptor exclusively activated by a designer drug (DREADD) hM3d or an empty vector (CTRL) into the PVN. This viral paradigm allows for the transport of hM3d to terminal regions of PVN efferents, including the NAc. To selectively stimulate the PVN→NAc pathway, clozapine-N-oxide (CNO) was micro-infused directly into the NAc via a guide cannula placed below the microdialysis probe, which is designed to trigger presynaptic release of neurotransmitters from the PVN into the NAc (**Figure 4.5b**) (Stachniak et al., 2014). Pharmacogenetic stimulation of PVN→NAc resulted in a robust, sustained increase in extracellular glutamate in the hM3d group compared to CTRL (**Figure 4.5b**). This effect was observed immediately upon CNO administration and endured for approximately 30 minutes (**Figure 4.5b**). No change in extracellular GABA from PVN→NAc projections was observed in either hM3d or CTRL groups (**Figure 4.5b**), indicating the glutamatergic nature of this pathway.

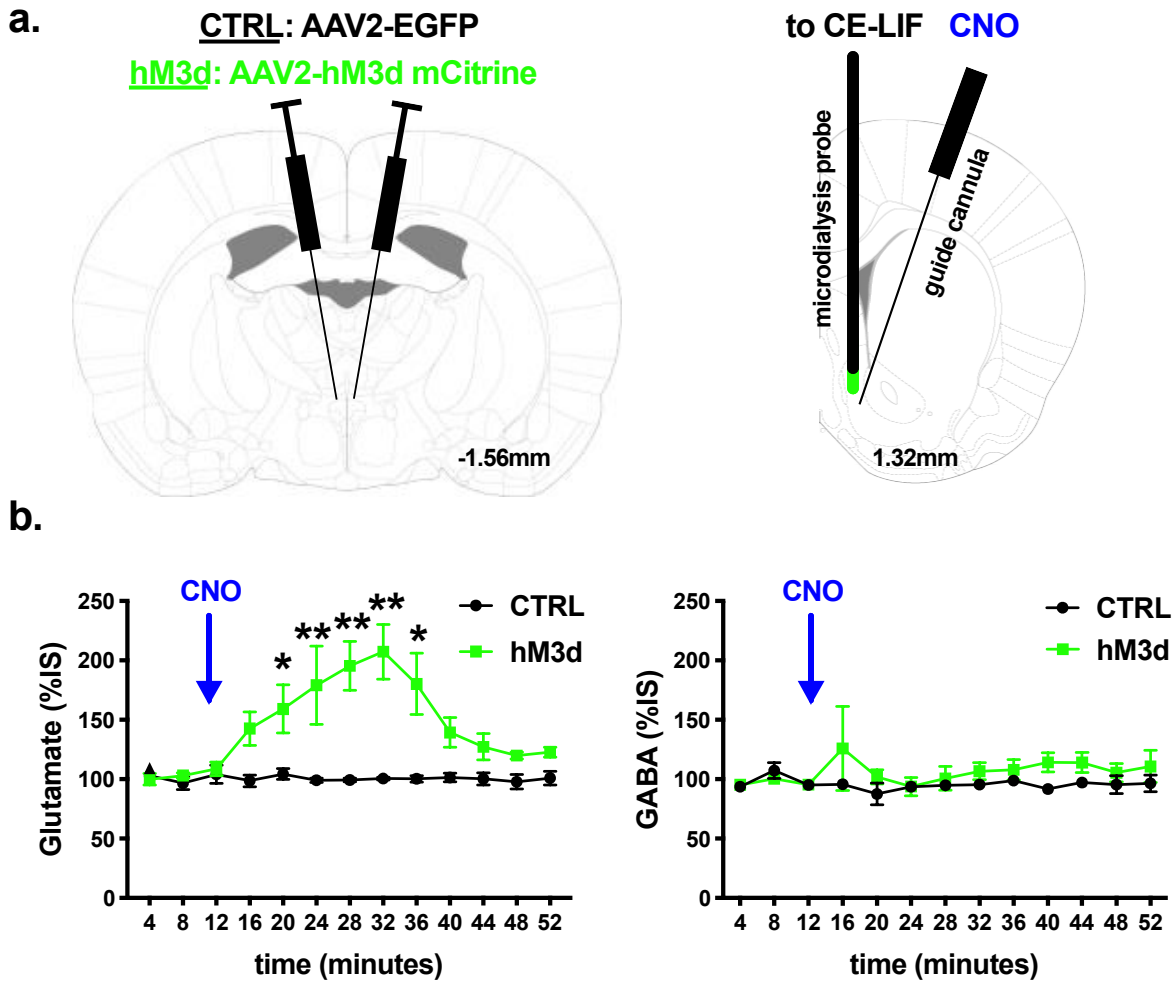


**Figure 4.5: hM3d-induced stimulation of PVN→NAc increases extracellular glutamate.**

a. PVN CTRL and hM3d targeting approach, NAc guide cannula placement, NAc microdialysis probe placement to achieve PVN→NAc specific neurotransmitter release. b. hM3d-induced stimulation of PVN→NAc neurons induced a robust, sustained increase in extracellular glutamate. CTRL n=3, hM3d n=3, \* $p<0.05$  and \*\* $p<0.01$  by 2-way ANOVA; hM3d-induced stimulation of PVN→NAc neurons did not increase extracellular GABA. CTRL n=3, hM3d n=3,  $p>0.05$  by two-way ANOVA.

***HM3D-INDUCED STIMULATION OF PVN→NAC ALTERS NEURONAL EXCITABILITY IN THE NAC, BUT NOT THE PVN***

To identify the immediate consequence of glutamate from PVN→NAC neurons, we quantified phosphorylated-cFos protein in the PVN and in the NAc following intra-NAc administration of CNO in hM3d and control groups (**Figure 4.6**) (Stachniak et al., 2014).

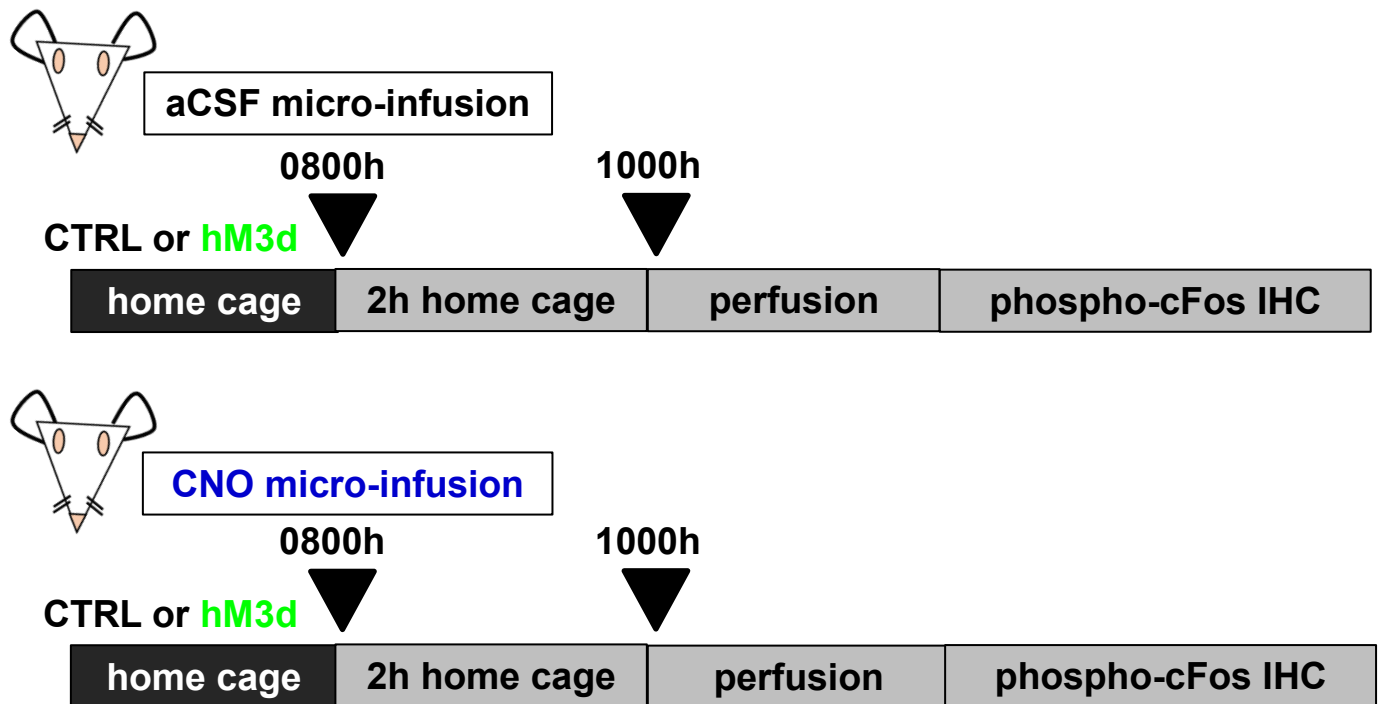


**Figure 4.6: Experimental timeline for phospho-cFos.**

Rats expressing CTRL or hM3d virus recovered in their home cages for 14 days to allow for peak viral expression. Beginning at 0800, rats expressing CTRL or hM3d virus were given an intra-NAc aCSF or 1uM CNO micro-infusion, then returned to their home cages for 2 hours. Beginning at 1000, rats were perfused with 1X PBS for 5 minutes, then 4% paraformaldehyde for 15 minutes. Brains were extracted and processed for phospho-cFos immunohistochemistry.

Phosphorylated-cFos was significantly elevated in the NAc of hM3d+CNO rats, supporting that pharmacogenetic stimulation of PVN→NAc induces glutamate release in the NAc and excites local NAc neurons (**Figure 4.7b**). Conversely, minimal phosphorylated-cFos was detected in the PVN of hM3d+CNO rats, evidence that our pharmacogenetic stimulation approach in which presynaptic DREADDs are directly stimulated by CNO does not alter excitability of PVN→NAc neurons themselves (**Figure 4.7a**). This data supports the conclusion that glutamate release from the PVN into the NAc increases the firing rate of NAc neurons downstream of PVN→NAc.



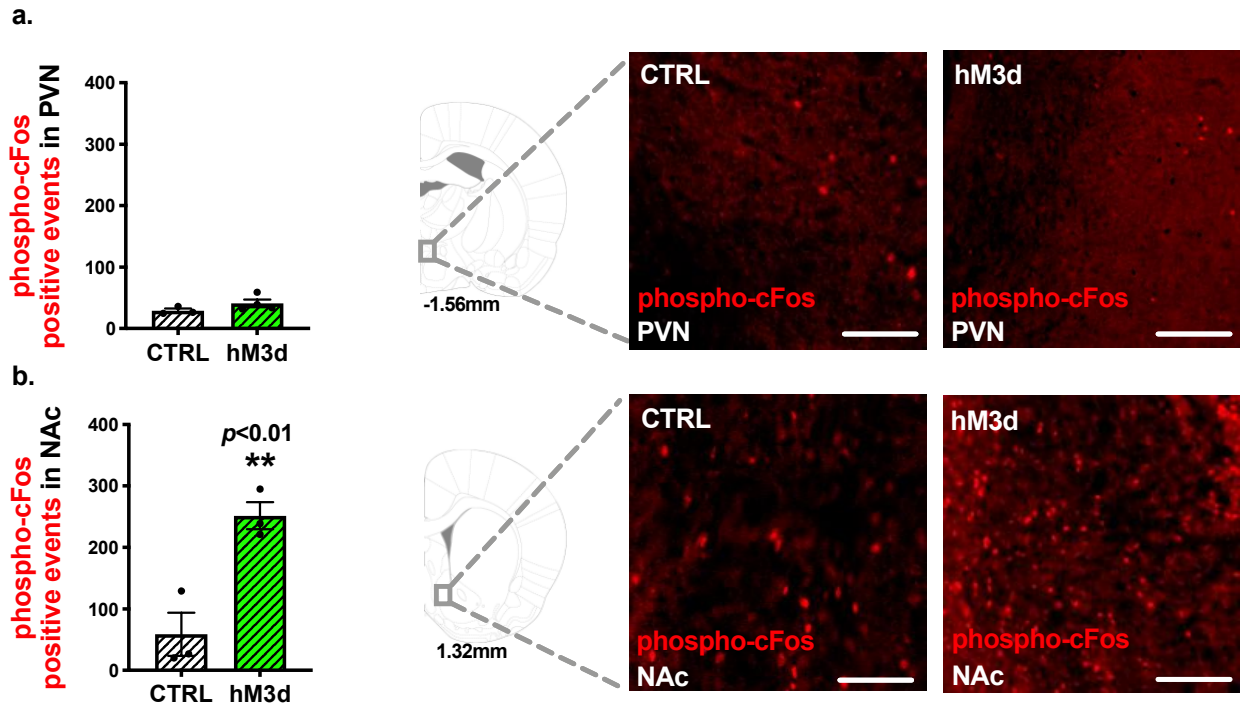


**Figure 4.7: hM3d-induced stimulation of PVN→NAc alters neuronal excitability in the NAc, but not the PVN.**

a. PVN CTRL and hM3d targeting approach, NAc guide cannula placement, NAc microdialysis probe placement to achieve PVN→NAc specific neurotransmitter release. b. hM3d-induced stimulation of PVN→NAc neurons induced a robust, sustained increase in extracellular glutamate. CTRL  $n=3$ , hM3d  $n=3$ , \* $p < 0.05$  and \*\* $p < 0.01$  by 2-way ANOVA; hM3d-induced stimulation of PVN→NAc neurons did not increase extracellular GABA. CTRL  $n=3$ , hM3d  $n=3$ ,  $p > 0.05$  by two-way ANOVA.

Placement of microdialysis probe and guide cannula were determined at the end of the study and are illustrated in **Figure 4.8**.

**a.**

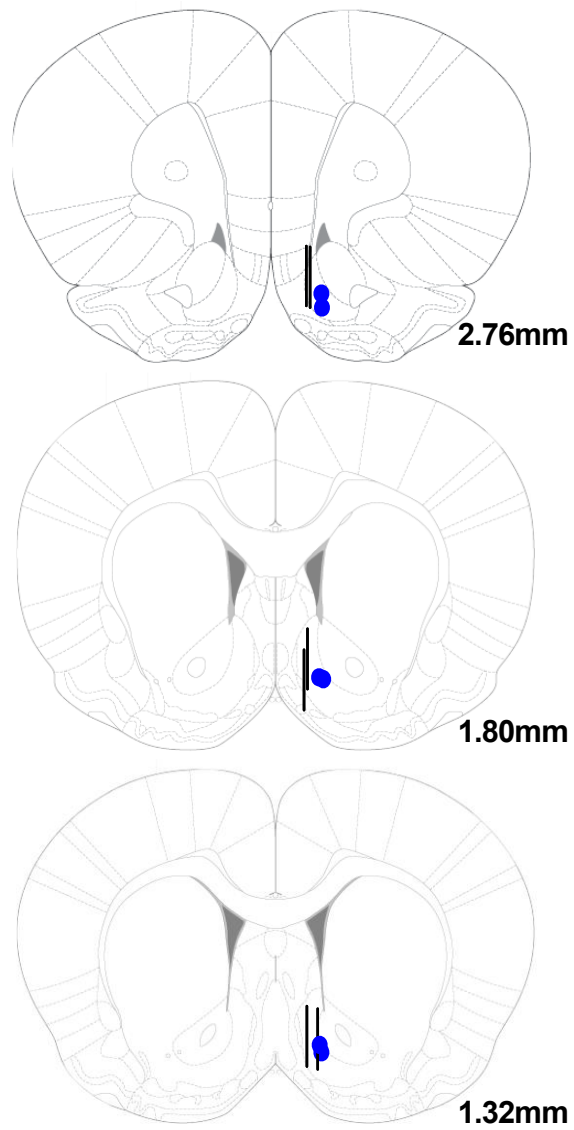


**Figure 4.8: Microdialysis targeting.**

a. Placement of microdialysis probe (black line) and placement of guide cannula for CNO administration (blue dot).

## DISCUSSION

PVN→NAc connectivity coordinates social reinforcement, but it is unclear whether the interplay of PVN→NAc regulates feeding behaviors (Dölen et al., 2013). While the PVN is a link between homeostatic and hedonic brain nuclei, it is uncertain whether PVN inputs to the NAc might modulate hedonic feeding. In this study, we define PVN→NAc as a novel source of glutamatergic input to the NAc. We also establish that PVN→NAc regulates intake of high-fat food in a glutamate-related manner.

Through viral tracing techniques, our results visually provide neuroanatomical evidence that the parvocellular compartment of the PVN directly interacts with the NAc. This finding corroborates an existing role for the parvocellular PVN in driving intake of high-fat food (Jhanwar-Uniyal et al., 1993). We observed co-localization of presynaptic VGLUT1 staining with PVN→NAc, indicating that PVN projections to the NAc are equipped for glutamate transport (Liguz-Lecznar and Skangiel-Kramska, 2007). Mice exposed to chronic high-fat diet demonstrate decreased expression of VGLUT1, which provides evidence for dysregulated glutamate signaling in pathological overconsumption of high-fat food (Lizarbe et al., 2018).

Because co-localization of PVN→NAc with VGLUT1 is not an indication of an exclusively glutamatergic pathway, we also characterized co-localization of PVN→NAc with other neurotransmitter markers. Our analysis revealed that PVN→NAc does not express markers associated with GABA, dopamine, or

serotonin synthesis. Taken together, our tracing studies support PVN→NAc as a large neural circuit that utilizes glutamate.

Selective pharmacogenetic stimulation of PVN→NAc neurons resulted in an increase in presynaptic extracellular glutamate in hM3d rats. This finding corroborates our immunohistochemical results that PVN→NAc is predominantly comprised of glutamatergic neurons. We did not identify any changes in presynaptic extracellular GABA, suggesting that the PVN→NAc pathway does not participate in co-release of glutamate and GABA. However, our microdialysis design was limited by an inability to detect uncharged neurotransmitters, such as acetylcholine, which has been implicated in feeding behaviors, especially in the NAc. Intra-NAc infusion of the muscarinic receptor antagonist scopolamine decreases intake of high-fat food (Perry et al., 2009). Additionally, chronic binge-intake is known to alter NAc acetylcholine levels and create an imbalance (Avena et al., 2008a). Based on this literature, we cannot rule out the possibility of glutamate and acetylcholine co-release from PVN→NAc neurons, which could be confirmed with immunohistochemical staining for VGLUT2 or VGLUT3 (El Mestikawy et al., 2011).

We were also limited by the size of the microdialysis probe, which permitted collection of molecules less than 6kDa, but not larger molecules such as neuropeptides (See Methods). Oxytocin is one neuropeptide that is released from PVN→NAc to regulate social reinforcement, and has been shown to decrease intake of high-fat food in humans and rodents (Dölen et al., 2013; Spetter et al., 2018). Previous work from our laboratory demonstrated that PVN→NAc co-

localizes with preproenkephalin, suggesting that PVN→NAc may utilize the neuropeptide enkephalin, which is known to encode the reinforcing aspects of high-fat food (Kelley et al., 2002; Kelley and Berridge, 2002; Zhang et al., 2003). Future studies should identify neuropeptides released from PVN→NAc neurons.

Presynaptic glutamate release from PVN→NAc neurons targets downstream cell bodies within the NAc. Post-CNO micro-infusion, we observed an increase in phosphorylated-cFos expression in the NAc of hM3d+CNO rats, suggesting that presynaptic glutamate release from PVN→NAc activates downstream neurons in the NAc. Potential downstream targets in the NAc include both dopamine receptor 1 medium spiny neurons (D1-MSNs) and dopamine receptor 2 medium spiny neurons (D2-MSNs). Zhu and colleagues investigated the effects of stimulation/inhibition of D1 and D2 neurons in the NAc on food intake in mice (Zhu et al., 2016). Their findings demonstrated that hM3d-induced stimulation of D1 neurons increases food intake in mice, while hM4d-induced inhibition of D1 neurons decreases food intake (Zhu et al., 2016). Interestingly, stimulation nor inhibition of D2 neurons had an effect on food intake (Zhu et al., 2016). Future studies should identify downstream targets of PVN→NAc, and interrogate their role in feeding behavior.

## **Chapter 5 Glutamate Release from PVN→NAc Projections Regulates Intake of High-Fat Food and Motivation for High-Fat Food**

### **INTRODUCTION**

In the previous chapter, we described the neuroanatomical and functional properties of PVN→NAc. We identified that PVN→NAc terminals co-localize with VGLUT1, and that PVN→NAc is localized to the parvocellular compartment of the PVN, providing evidence of glutamatergic pathway involved in feeding. Additionally, we utilized the excitatory hM3d DREADD to stimulate presynaptic release of neurotransmitters from PVN→NAc, which were then quantified via microdialysis. The microdialysis study corroborated our neuroanatomical findings, and demonstrated that PVN→NAc releases glutamate pre-synaptically in the NAc.

Glutamate in the NAc is a known regulator of intake of highly palatable food, and pharmacological manipulation of NAc glutamate alters feeding behavior. Infusion of non-N-methyl-D-aspartate receptor (non-NMDAR) glutamate antagonists into the medial NAc shell have been shown to evoke an immediate and sustained increase in food intake (Maldonado-Irizarry et al., 1995; Stratford et al., 1998). We suspect that this observed increase in food intake is mediated by postsynaptic  $\alpha$ -amino-3-hydroxy-5-methyl-4-isoxazolepropionic receptors (AMPA receptors) in the NAc. Additionally, infusion of AMPA directly into the NAc decreases food intake in food restricted rats (Stratford et al., 1998), underscoring the importance of glutamate release in the NAc as a modulator of feeding behavior.

To date, the PVN→NAc pathway has not been investigated for involvement in feeding behavior. Here, we propose that PVN→NAc regulates motivation for high-fat food through glutamate signaling. Although some PVN neurons are glutamatergic (Ziegler et al., 2002), the neurotransmitter(s) used in the PVN→NAc pathway was largely unknown until our microdialysis studies (Chapter 3) supporting that pharmacogenetic stimulation of PVN→NAc with the excitatory hM3d DREADD increases extracellular glutamate pre-synaptically in the NAc.

To directly probe the role of PVN→NAc glutamate release in driving feeding behaviors, we employed two different viral strategies utilizing the hM3d DREADD. Our first strategy directly mirrored the microdialysis approach- we administered an AAV2 containing hM3d in the PVN and implanted bilateral guide cannula in the NAc for aCSF/CNO micro-infusion. In this paradigm, hM3d is expressed in all PVN projection neurons, in addition to PVN→NAc projections. To achieve PVN→NAc specific glutamate release, aCSF/CNO are micro-infused directly into the NAc. Administration of CNO facilitates presynaptic glutamate release from glutamate-containing vesicles of PVN→NAc neurons, but an action potential is not generated.

Our second strategy utilized dual viral vectors- we administered an AAV2 containing hM3d flanked by *loxP* sites in the PVN, and an AAV6 containing Cre in the NAc. In this paradigm, only neurons that project from the PVN to the NAc express hM3d. Intraperitoneal (IP) administration of CNO depolarizes PVN→NAc neurons to generate an action potential, which releases glutamate in addition to other neurotransmitters, neuropeptides, etc.



While both paradigms achieve PVN→NAc specific glutamate release, one allows us to identify the effects of glutamate release on feeding behavior, while the other allows us to identify the effects of a PVN→NAc action potential on feeding behavior. Both methods will be compared and contrasted throughout this chapter.

## **SPECIFIC METHODS**

### **ANIMALS**

Male Sprague-Dawley rats (Harlan, Houston, TX) weighing 225-250g were used in all experiments. Animals were housed individually in a temperature- (21-23°C) and humidity- (40-50%) controlled environment with a standard 12h light-dark cycle (lights on between 0600 and 1800 hours). All animals were given *ad libitum* access to normal chow (17% fat by kcal; Teklad LM-485 Mouse/Rat Sterilizable Diet; Teklad Diets, Madison, WI) and water in their home cages. Upon arrival, animals were allowed to acclimate to the room for seven days prior to handling and experimental procedures. All experiments were conducted in accordance with the *NIH Guide for Use and Care of Laboratory Animals* (2011), and with approval from the Institutional Animal Use and Care Committee at the University of Texas Medical Branch.

### **SURGERIES: CTRL AND HM3D**

To determine the behavioral output of PVN→NAc neurons, rats (n=32) received bilateral injection of AAV2-CAMKIIa-EGFP (CTRL, n=16) (plasmid 50469, Addgene) or AAV2-CAMKII-HA-hM3d(Gq)-IRES-mCitrine (hM3d, n=16) (plasmid 50466, Addgene) into the PVN at A/P -0.18, M/L +0.15, D/V -0.82 from

bregma (Paxinos and Watson, 2007). Bilateral guide cannula (PlasticsOne) were implanted at 10-degree outside angle at the following coordinates: A/P +1.4; M/L +0.20; D/V -0.57 from bregma and secured with dental cement and stainless-steel screws (Paxinos and Watson, 2007). After surgery, animals recovered for 2 weeks to allow for optimal virus expression. Rats were habituated to cannula manipulation starting 1 week prior to aCSF/CNO administration.

#### ***SURGERIES: DIO CTRL AND DIO HM3D***

Rats received bilateral injection of AAV2-hSyn-DIO-hM3d(G<sub>q</sub>)-mCherry (DIO CTRL, n=8) (plasmid 44361, Addgene) into the PVN at A/P -0.18, M/L +0.20, D/V -0.82 from bregma (Paxinos and Watson, 2007).

Rats received bilateral injection of AAV2-hSyn-DIO-hM3d(G<sub>q</sub>)-mCherry into the PVN at A/P -0.18, M/L +0.15, D/V -0.82 from bregma (Paxinos and Watson, 2007) and bilateral injection of AAVrg-pmSyn1-EBFP-Cre (DIO hM3d, n=8) (plasmid 51507, Addgene) into the NAc at A/P +0.14, M/L +0.20, D/V -0.68 from bregma (Paxinos and Watson, 2007). After surgery, animals recovered for 2 weeks to allow for optimal virus expression. Virus placement was verified and all misses were eliminated prior to data analysis.

#### ***HM3D: FOOD INTAKE AND INTRA-NAC CNO ADMINISTRATION***

A visual representation of this experimental paradigm is available in **Figure 5.1**. On experimental day 1, rats (n=26) received intra-NAc micro-infusion of aCSF or 2uL of 1uM CNO at a rate of 0.5ul/minute for 4 minutes prior to onset of the dark cycle (1800) (Stachniak et al., 2014). Food hoppers containing 45% high fat chow

(D12451, Research Diets) were placed in home cages and rats were given *ad libitum* access for 24 hours. Food hopper weights were recorded at 2-hours, 4-hours and 24-hours post micro-infusion. This same paradigm was used to assess food intake on experimental day 2, where rats received aCSF (CNO on experimental day 1) or 1uM CNO (aCSF on experimental day 1) so that each rat served as its own control.

### ***hM3D: OPERANT CONDITIONING AND INTRA-NAC CNO ADMINISTRATION***

Rats were placed in standard rat operant chambers (Med Associates) between 0800 and 1000. Responding on the active lever associated with food delivery resulted in delivery of a high-fat food pellet (45% energy by kcal, 45mg, Bioserv F06162). Rats were trained for 30 minutes sessions on a fixed ratio 1 (FR1) schedule, where one correct response on the active lever results in the delivery of the high-fat food pellet. Rats were advanced to an FR3 schedule once the percentage of responses on the active lever exceeded 85% for three consecutive days, where 3 correct responses are required for delivery of the high-fat food pellet. Accordingly, when rats met criteria on FR3, they were advanced to FR5 (5 correct responses). Once rats achieved criteria on FR5, they advanced to a progressive ratio (PR) schedule, where earning each successive high-fat food pellet within the session requires a greater number of responses (1,2,3,6,9,12,15,20,25,32,40,50,62,77,95).

A visual representation of this experimental paradigm is available in **Figure 5.3**. On PR Test Day 1, rats expressing a control virus (CTRL, n=11) and rats expressing hM3d (hM3d, n=15) received an intra-NAc micro-infusion of artificial

cerebrospinal fluid (aCSF) or 2uL of 1uM CNO at a rate of 0.5ul/minute for 4 minutes (Stachniak et al., 2014). Immediately after micro-infusion, rats were placed in operant chambers and began a 30-minute PR session. Responses on the active, reinforced lever, number of infusions, and latency to press were quantified within the 30-minute session. The same paradigm was used on PR Test Day 2, where rats received aCSF (CNO on experimental day 1) or 1uM CNO (aCSF on experimental day 1).

### ***hM3D: LOCOMOTOR ACTIVITY***

In order to rule out any possible motor effects of micro-infusion of aCSF or CNO, locomotor activity was assessed in CTRL and hM3d rats. On Locomotor Test Day 1, rats expressing a control virus (CTRL, n=11) and rats expressing hM3d (hM3d, n=15) received an intra-NAc micro-infusion of artificial cerebrospinal fluid (aCSF) or 2uL of 1uM CNO at a rate of 0.5ul/minute for a total of 4 minutes (Stachniak et al., 2014). Immediately after micro-infusion, rats were placed in locomotor chambers and began a 30-minute locomotor activity session. Total beam breaks were quantified within the 30-minute session, and serve as a measure of central activity, peripheral activity, and rearing (vertical activity). The same paradigm was used on Locomotor Test Day 2, where rats received aCSF (CNO on Locomotor Test Day 1) or 1uM CNO (aCSF on Locomotor Test Day 1). Locomotor activity results are illustrated in **Figure 5.6**.

### ***HM3D: EUTHANASIA AND TARGETING***

Rats were perfused with 1X PBS for 5 minutes followed by 4% paraformaldehyde for 15 minutes. Brains were removed and post-fixed for 24 hours in 4% paraformaldehyde. Brains were stored in PBS glycerol sodium azide until slicing. Placement of guide cannula was identified during slicing and is illustrated in **Figure 5.6**.

### ***HM3D: FOOD INTAKE AND CENTRAL CNO ADMINISTRATION***

On experimental day 1, rats (n=8) received intraperitoneal injection of vehicle (saline) or 2mg/kg CNO prior to onset of the dark cycle (1800). Food hoppers containing 45% high fat chow (D12451, Research Diets) were placed in home cages and rats were given *ad libitum* access for 24-hours. Food hopper weights were recorded at 2-hours, 4-hours and 24-hours post-injection. This same paradigm was used to assess food intake on experimental day 2, where rats received vehicle (CNO on experimental day 1) or 2mg/kg CNO (vehicle on experimental day 1) so that each rat served as its own control.

### ***DIO HM3D: OPERANT CONDITIONING AND CENTRAL CNO ADMINISTRATION***

Rats were placed in standard rat operant chambers (Med Associates) between 0800 and 1000. Responding on the active lever associated with food delivery resulted in delivery of a high-fat food pellet (45% energy by kcal, 45mg, Bioserv F06162). Rats were trained for 30 minutes sessions on a fixed ratio 1 (FR1) schedule, where one correct response on the active lever results in the delivery of the high-fat food pellet. Rats were advanced to an FR3 schedule once

the percentage of responses on the active lever exceeded 85% for three consecutive days, where 3 correct responses are required for delivery of the high-fat food pellet. Accordingly, when rats met criteria on FR3, they were advanced to FR5 (5 correct responses). Once rats achieved criteria on FR5, they advanced to a progressive ratio (PR) schedule, where earning each successive high-fat food pellet within the session requires a greater number of responses (1,2,3,6,9,12,15,20,25,32,40,50,62,77,95).

On PR Test Day 1, rats expressing a control virus (CTRL, n=8) and rats expressing hM3d (hM3d, n=8) received an intraperitoneal injection of vehicle (saline) or 2mg/kg CNO. Immediately after injection, rats were placed in operant chambers and began a 30-minute PR session. Responses on the active, reinforced lever, number of infusions, and latency to press were quantified within the 30-minute session. The same paradigm was used on experimental day 2, where rats received vehicle (CNO on PR Test Day 1) or 1uM CNO (vehicle on PR Test Day 1).

### ***DIO hM3D: LOCOMOTOR ACTIVITY***

In order to rule out any possible motor effects of IP saline or CNO, locomotor activity was assessed in DIO CTRL and DIO hM3d rats. On Locomotor Test Day 1, rats expressing the DIO hM3d virus in the absence of Cre (DIO CTRL, n=8) and rats expressing the DIO hM3d virus in the presence of Cre (DIO hM3d, n=8) received IP administration of saline or 2mg/kg CNO. Immediately after injection, rats were placed in locomotor chambers and began a 30-minute locomotor activity session. Total beam breaks were quantified within the 30-minute session, and

serve as a measure of central activity, peripheral activity, and rearing (vertical activity). The same paradigm was used on Locomotor Test Day 2, where rats received saline (CNO on Locomotor Test Day 1) or 1uM CNO (saline on Locomotor Test Day 1).

### ***DIO HM3D: EUTHANASIA AND TARGETING***

Vehicle or CNO was administered 2 hours prior to euthanasia to quantify phospho-cFos in the PVN and the NAc. Rats were perfused with 1X PBS for 5 minutes followed by 4% paraformaldehyde for 15 minutes. Brains were removed and post-fixed for 24 hours in 4% paraformaldehyde. Brains were stored in PBS glycerol sodium azide until slicing.

### ***DATA ANALYSIS***

All statistical analyses were performed in GraphPad Prism 7.0a (GraphPad Software Inc., La Jolla, CA) with an experiment wise error rate of  $\alpha=0.05$ . In CTRL and hM3d rats, intake of high-fat food was quantified at 2-hours and 4-hours post aCSF/CNO micro-infusion. Intake of high-fat food in CTRL+aCSF and CTRL+CNO rats were compared and analyzed via two-way repeated measures ANOVA ( $n=11$ ,  $p>0.05$ ). Intake of high-fat food in hM3d+aCSF and hM3d+CNO rats were compared and analyzed via two-way repeated measures ANOVA ( $n=15$ , 2 hours:  $**p<0.01$ , 4 hours:  $*p<0.05$ ).

Active lever presses and reinforcers earned were quantified during a 30-minute operant session. Active lever presses in CTRL+aCSF and CTRL+CNO rats were compared and analyzed via paired T-test ( $n=11$ ). Active lever presses in

hM3d+aCSF and hM3d+CNO rats were compared and analyzed via paired T-test (n=15). Reinforcements in CTRL+aCSF and CTRL+CNO rats were compared and analyzed via paired T-test (n=11). Reinforcements in hM3d+aCSF and hM3d+CNO rats were compared and analyzed via paired T-test (n=15).

Locomotor activity was assessed in all groups. CTRL+aCSF and CTRL+CNO rats were compared and analyzed via paired T-test (n=11). hM3d+aCSF and hM3d+CNO rats were compared and analyzed via paired T-test (n=15).

In DIO CTRL and DIO hM3d rats, intake of high-fat food was quantified at 2-hours and 4-hours post saline/CNO injection. Intake of high-fat food in DIO CTRL+saline and DIO CTRL+CNO rats were compared and analyzed via two-way repeated measures ANOVA (n=8, 4 hours:  $*p>0.05$ ). Intake of high-fat food in DIO hM3d+saline and DIO hM3d+CNO rats were compared and analyzed via two-way repeated measures ANOVA (n=7).

Active lever presses and reinforcers earned were quantified during a 30-minute operant session. Active lever presses in DIO CTRL+saline and DIO CTRL+CNO rats were compared and analyzed via paired T-test (n=8). Active lever presses in DIO hM3d+saline and DIO hM3d+CNO rats were compared and analyzed via paired T-test (n=7,  $*p=0.02$ ). Reinforcements in DIO CTRL+saline and DIO CTRL+CNO rats were compared and analyzed via paired T-test (n=8). Reinforcements in DIO hM3d+aCSF and DIO hM3d+CNO rats were compared and analyzed via paired T-test (n=7).



Locomotor activity was assessed in all groups. DIO CTRL+saline and DIO CTRL+CNO rats were compared and analyzed via paired T-test (n=8). DIO hM3d+saline and DIO hM3d+CNO rats were compared and analyzed via paired T-test (n=7).

## RESULTS

### ***hM3D-INDUCED STIMULATION OF PVN→NAc DECREASES INTAKE OF HIGH-FAT FOOD***

Our microdialysis results from Chapter 4 demonstrated that hM3d-induced stimulation of PVN→NAc increases extracellular glutamate pre-synaptically in the NAc. Pharmacological blockade of glutamate in the NAc robustly increases food intake, as shown by the work of Ann Kelley and colleagues (Kelley et al., 2005; Kelley and Berridge, 2002; Maldonado-Irizarry and Kelley, 1995a, b; Maldonado-Irizarry et al., 1995). With these data in mind, we hypothesized that hM3d-induced stimulation of PVN→NAc would decrease intake of high-fat food and motivation for high-fat food.

To determine whether PVN→NAc glutamate release affects feeding behavior, we utilized the same viral paradigm as microdialysis to express hM3d or control in PVN→NAc neurons (**Figure 5.1, Figure 5.2**) and quantified intake of high-fat food (**Figure 5.1**). Artificial cerebrospinal fluid (aCSF) or CNO was micro-infused into the NAc immediately before rats were given *ad libitum* access to HPF (**Figure 5.1**) (Stachniak et al., 2014). In this paradigm, each rat received aCSF and CNO on different experimental days to control for potential CNO-related effects on intake of high-fat food.

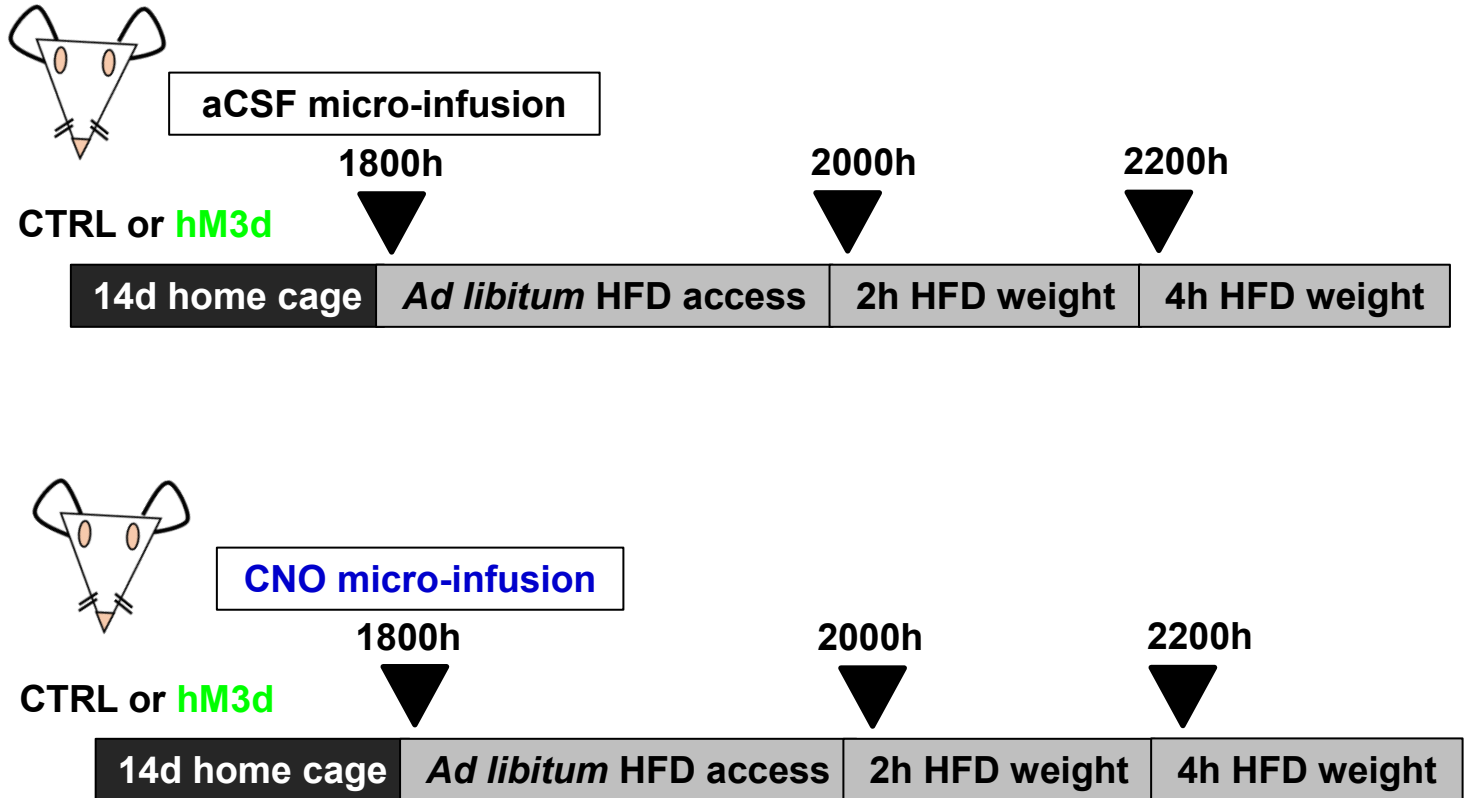


**Figure 5.1: Experimental timeline for high-fat food intake.**

Rats expressing CTRL or hM3d virus recovered in their home cages for 14 days to allow for peak viral expression. At 1800 on experimental day 1, CTRL and hM3d rats received micro-infusion of aCSF or 1uM CNO. Rats were returned to their home cages where they had *ad libitum* access to a high-fat diet (45% fat by kcal). High-fat diet food hoppers were weighed at 2000 (2 hours post micro-infusion) and 2200 (4 hours post micro-infusion). Differences in food hopper weight were interpreted as grams consumed.

At 2 hours and 4 hours, hM3d+CNO rats consumed significantly less high-fat food than hM3d+aCSF (**Figure 5.2c**), indicating that glutamate drive into the NAc decreases intake of high-fat food. Specifically, at 2 hours post-CNO micro-infusion, we observed a decrease in food intake in 5 out of 10 CTRL rats and an increase in food intake in 5 out of 10 rats. (**Figure 5.2b**). However, in rats with the hM3d excitatory DREADD, we observed a decrease of food intake in 10 out of 15 animals (**Figure 5.2c**).

A similar effect was observed at 4 hours post-CNO micro-infusion when 5 out of 10 CTRL rats responded through suppression of intake of high-fat food (**Figure 5.2b**), but that increased to 9 out of 15 responders in hM3d rats (**Figure 5.2c**). No significant change in intake of high-fat food was observed in CTRL+CNO and CTRL+aCSF (**Figure 5.2b**).

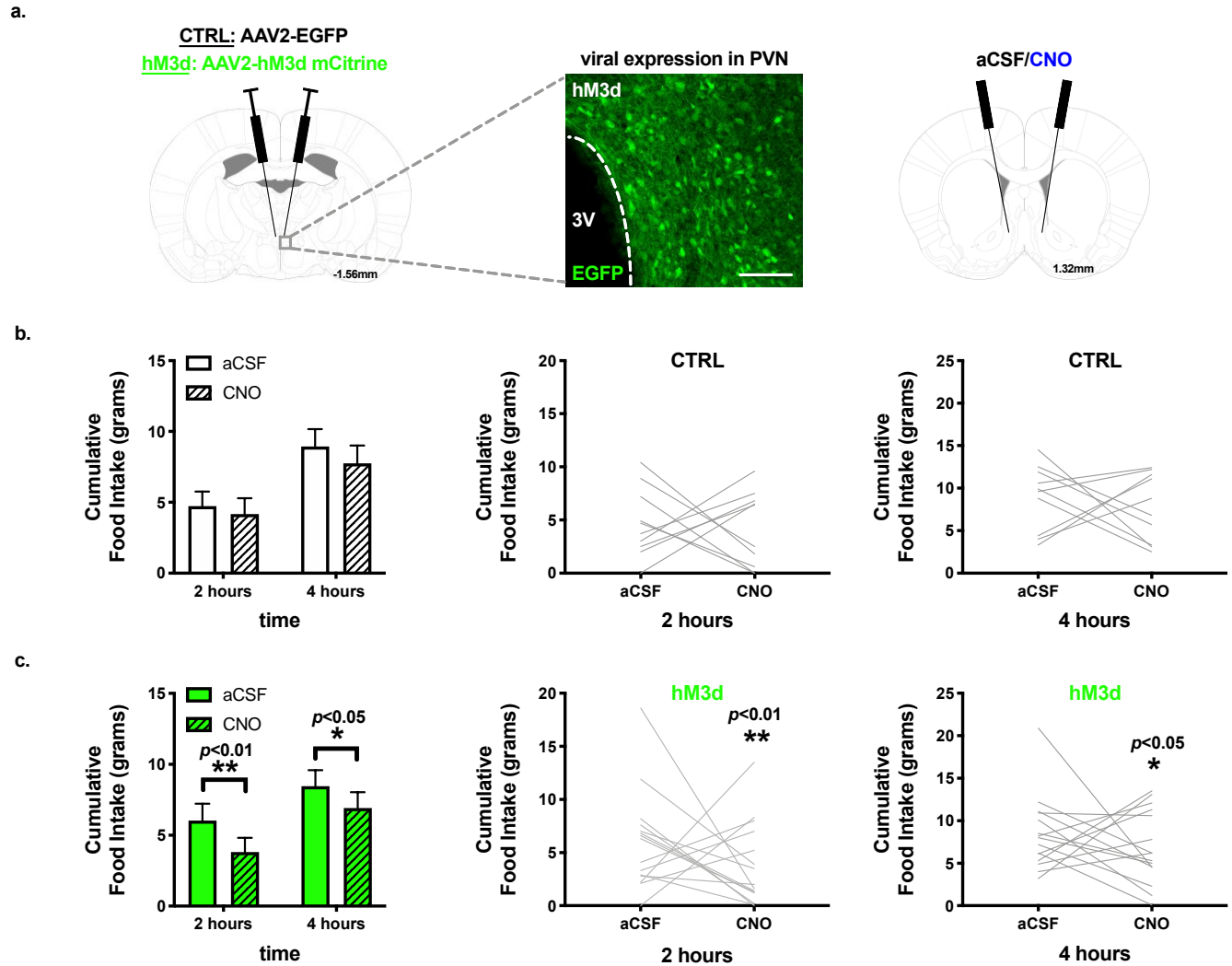


**Figure 5.2: PVN→NAc cell bodies are localized to parvocellular compartments of the PVN.**

a. PVN hM3d targeting approach with representative image of hM3d viral expression in the PVN, guide cannula placement in the NAc for aCSF/CNO administration. b. aCSF/CNO did not alter intake of HPF in CTRL rats.  $n=11$ ,  $p>0.05$  by two-way repeated measures ANOVA. c. CNO decreased intake of HPF hM3d rats at 2 hours and at 4 hours.  $n=15$ , 2 hours:  $**p<0.01$ , 4 hours:  $*p<0.05$  by two-way repeated measures ANOVA.

***hM3D-INDUCED STIMULATION OF PVN→NAc DOES NOT ALTER OPERANT RESPONDING FOR HIGH-FAT FOOD***

To determine whether PVN→NAc glutamate release affects motivated behavior for high-fat food, we utilized operant conditioning to train hM3d and CTRL rats to respond for a high-fat food pellet via lever presses (**Figure 5.3**). Both CTRL and hM3d rats acquired the task, demonstrating that the viral paradigm does not affect learning (**Figure 5.4**). However, at day 7 of training, the acquisition curves began to separate, with hM3d rats displaying lower active lever presses compared to CTRL rats. On training days 12-17 (PR), CTRL rats demonstrated higher basal active lever presses compared to hM3d rats. CTRL rats averaged approximately 50 active lever presses on training days 12-17 compared to hM3d rats which averaged approximately 30 active lever presses on training days 12-17. While this separation in the acquisition curves is not statistically significant, it does bring into question whether the excitatory hM3d DREADD exhibits endogenous activity (hM3d in the absence of CNO may alter glutamate tone in PVN→NAc neurons).

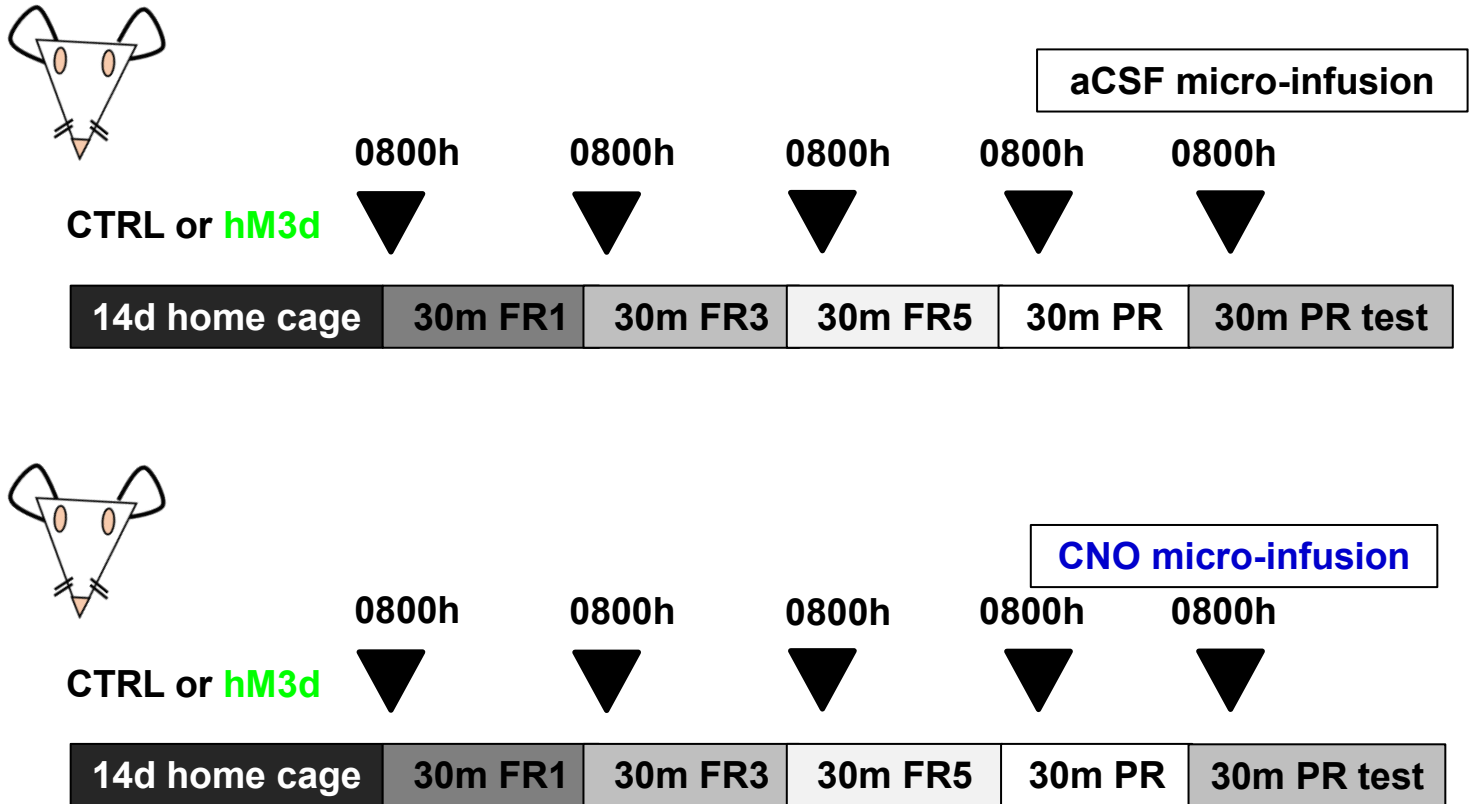


**Figure 5.3: Experimental timeline for operant conditioning: CTRL/hM3d cohort.**

Rats expressing CTRL or hM3d virus recovered in their home cages for 14 days to allow for peak viral expression. Rats underwent operant conditioning, beginning with a fixed ratio 1 (FR1) schedule for 30 minutes. Once rats reached stability, they were advanced to a fixed ratio 3 (FR3) schedule, then to a fixed ratio 5 (FR5) schedule, and finally to a progressive ratio (PR) schedule for 30 minutes. On experimental day 1, CTRL and hM3d rats received intra-NAc aCSF or 1 $\mu$ M CNO prior to a 30-minute PR session. On the experimental day 2, CTRL and hM3d rats received intra-NAc aCSF (CNO on experimental day 1) or CNO (aCSF on experimental day 2). Active lever presses and reinforcements were quantified.

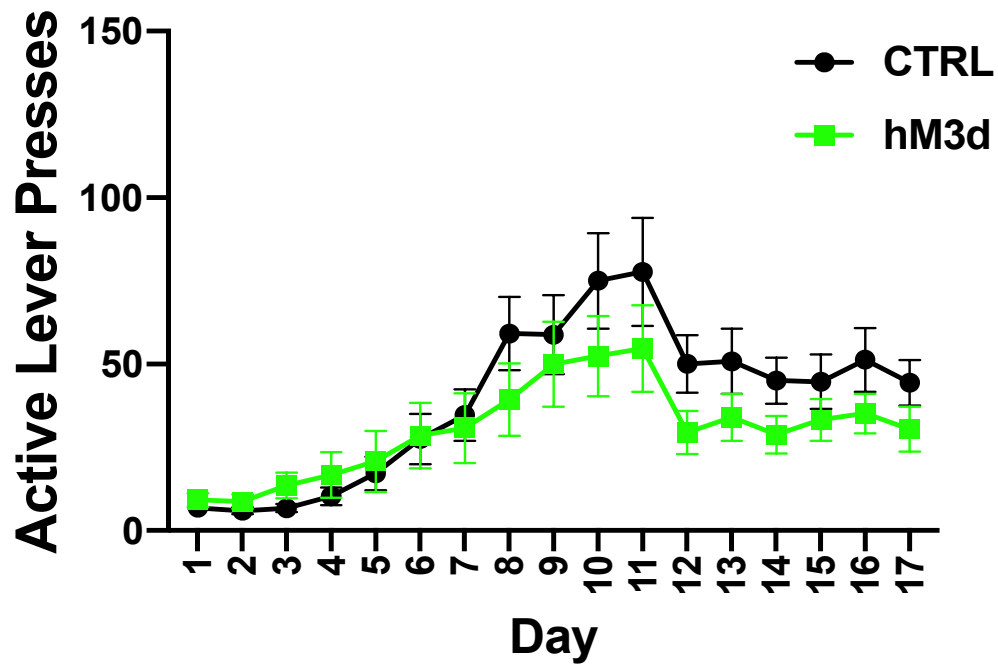


**Figure 5.4: Training acquisition for CTRL/hM3d cohort.**

Rats expressing CTRL or hM3d virus were trained to lever press for a 45% fat/kcal food pellet on a fixed ratio 1 schedule of reinforcement. Upon acquisition, rats were advanced to a fixed ratio 3 schedule, fixed ratio 5 schedule, then finally a progressive ratio schedule (Day 12-17) where earning each successive high-fat food pellet requires more effort.

Once CTRL and hM3d rats reached stability on PR responding, aCSF or CNO was micro-infused into the NAc immediately prior to a 30-minute PR session (**Figure 5.3**). Each rat received aCSF and CNO on different PR test days to control for potential CNO-related effects on active lever presses and reinforcers earned. No effect on active lever presses was observed in CTRL+aCSF rats or CTRL+CNO rats (**Figure 5.5a**). Both hM3d+aCSF rats and hM3d+CNO rats displayed lower basal active lever presses compared to CTRL rats: approximately 15 active lever presses for hM3d rats versus approximately 25 active lever presses for CTRL rats. A paired T-test revealed no difference in active lever presses between hM3d+aCSF and hM3d+CNO groups, suggesting that hM3d-induced stimulation of PVN→NAc does not alter operant responding for high-fat food (**Figure 5.5b**).

During the 30-minute PR test, we also quantified high-fat food pellets or reinforcers earned. Reinforcers earned is a proxy for reinforcement efficacy-or how effective the reinforcer is at generating a behavioral response. As seen with active lever presses, hM3d+aCSF rats and hM3d+CNO rats displayed lower reinforcers earned compared to CTRL rats: less than 4 high-fat food pellets for hM3d rats versus 5 high-fat food pellets for CTRL rats (**Figure 5.5c-d**). Again, a paired T-test revealed no difference in reinforcers earned between hM3d+aCSF and hM3d+CNO groups, suggesting that hM3d-induced stimulation of PVN→NAc does not alter the reinforcing effects of high-fat food.



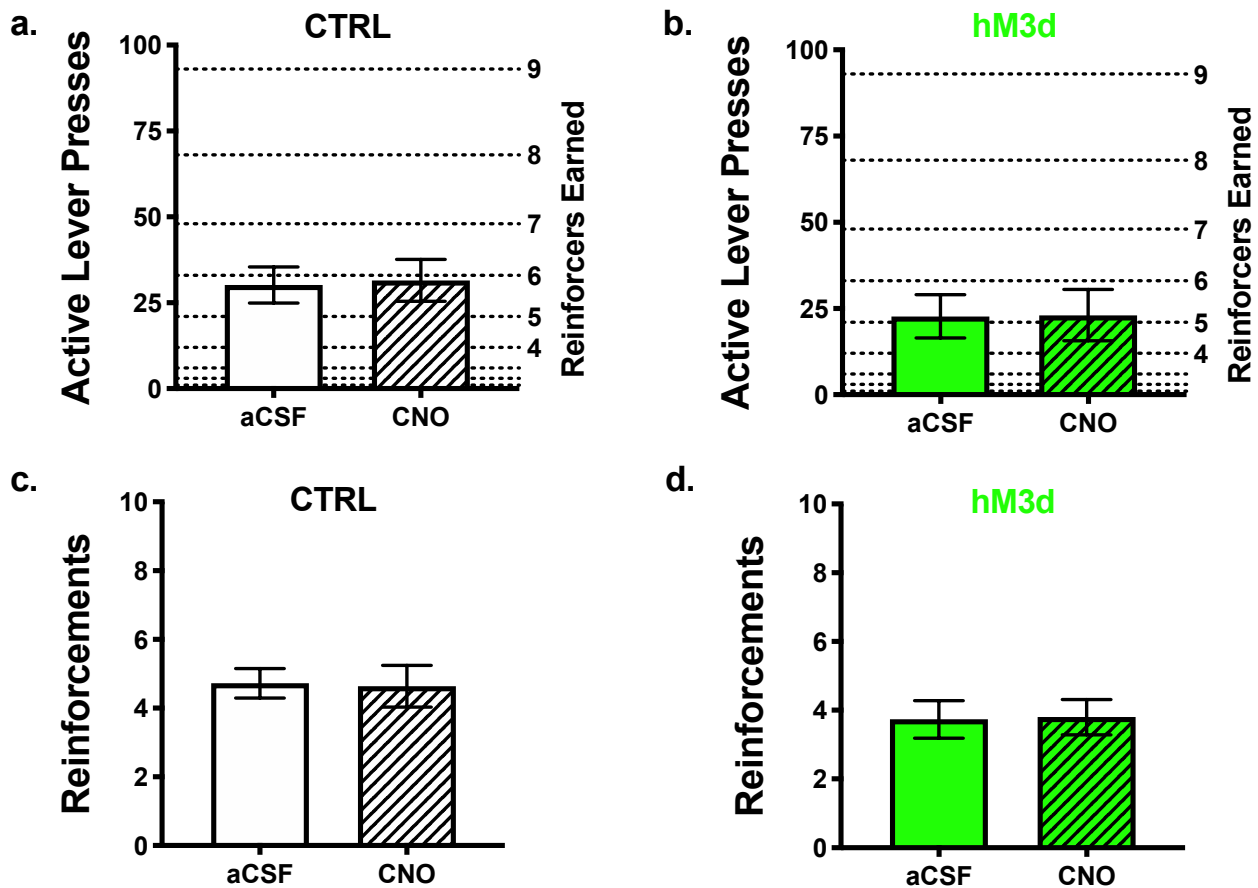


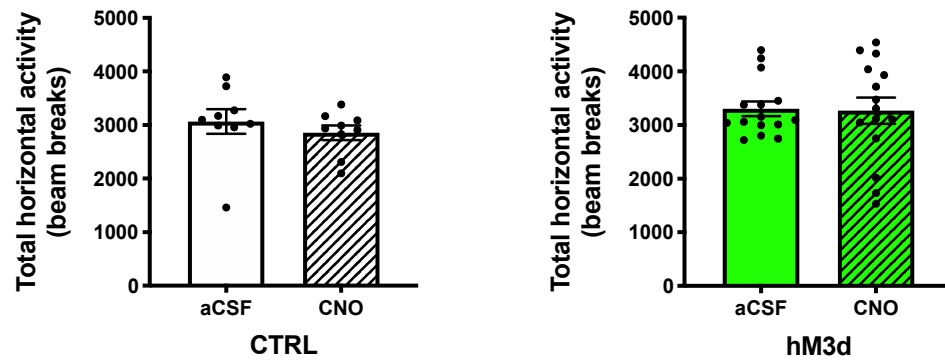
**Figure 5.5: hM3d-induced stimulation of PVN→NAC does not alter operant responding for high-fat food.**

a. Intra-NAC administration of aCSF or CNO to CTRL rats does not alter active lever presses for a high-fat food reinforcer.  $n=11$ . b. Intra-NAC administration of aCSF or CNO to hM3d rats does not alter active lever presses for a high-fat food reinforcer.  $n=15$ . c. Intra-NAC administration of aCSF or CNO does not alter high-fat reinforcements earned on a PR schedule of reinforcement in CTRL rats.  $n=11$ . d. Intra-NAC administration of aCSF or CNO does not alter high-fat reinforcements earned on a PR schedule of reinforcement in hM3d rats.  $n=15$ .

### ***HM3D-INDUCED STIMULATION OF PVN→NAC DOES NOT ALTER LOCOMOTOR ACTIVITY***

To identify any effects on locomotor activity, we quantified central, peripheral and vertical locomotor activity during a 30-minute test session. CTRL and hM3d rats received bilateral micro-infusion of aCSF or CNO on different test days to control for CNO-specific effects. No changes in total horizontal activity were observed in CTRL or hM3d groups (**Figure 5.6**). These findings show that any changes in food intake/active lever presses/reinforcers earned are not the result of changes in locomotor activity.

a.



b.

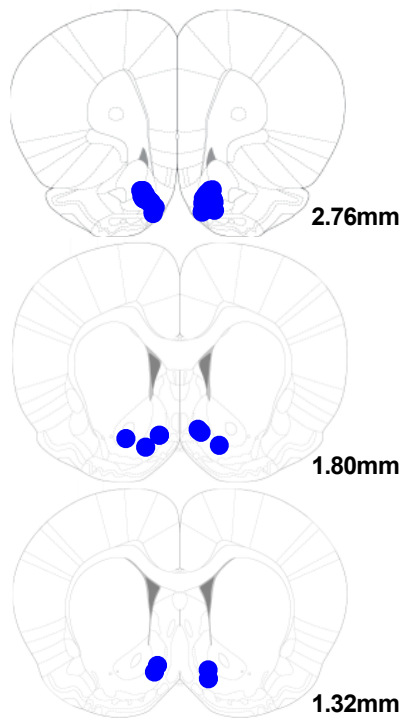


**Figure 5.6: hM3d-induced stimulation of PVN→NAc does not alter locomotor activity.**

a. aCSF or CNO administration does not alter locomotor activity in CTRL or hM3d rats.  
 b. placement of guide cannula for aCSF and CNO administration (blue dot).

### ***hM3D-INDUCED STIMULATION OF PVN→NAC WITH A DIO VIRAL VECTOR APPROACH INCREASES INTAKE OF HIGH-FAT FOOD***

We also utilized a dual viral vector approach to selectively stimulate PVN→NAC to mirror our single virus with intra-NAC cannula approach. In this paradigm, DIO CTRL (n=8) and DIO hM3d (n=7) rats received bilateral injection of an AAV2 virus expressing a Cre-dependent excitatory hM3d in the PVN (**Figure 5.7a**). DIO hM3d rats also received bilateral injection of a retrograde AAV expressing Cre in the NAc (**Figure 5.7a**). In DIO hM3d rats, hM3d is selectively expressed in PVN→NAC neurons only, and not in PVN projection neurons to other brain regions or collateral projections from PVN→NAC. In DIO CTRL rats, hM3d is not selectively expressed in PVN→NAC neurons because Cre is absent.

To determine whether selective stimulation of PVN→NAC neurons alters intake of high-fat food, we quantified intake of high-fat food in DIO CTRL and DIO hM3d rats. Rats received an I.P. injection of either saline or 2mg/kg CNO immediately prior to the onset of the dark cycle (1800), and were given *ad libitum* access to high-fat food (45% fat by kcal) in their home cages. Food hoppers containing high-fat food were weighed at 2-hours and 4-hours post injection. In this paradigm, each rat received saline and CNO on different experimental days to control for potential CNO-related effects on intake of high-fat food.

Intriguingly, at 2 hours and 4 hours, DIO hM3d+CNO rats consumed more high-fat food than DIO hM3d+saline (**Figure 5.7c**), suggesting that selective stimulation of PVN→NAC increases intake of high-fat food. Specifically, at 2 hours post-CNO injection, we observed a suppression in food intake in 6 out of 8 DIO

CTRL rats and a suppression of food intake in only 2 out of 7 DIO hM3d rats. **(Figure 5.7b).**

A similar effect was observed at 4 hours post-CNO injection when 6 out of 8 DIO CTRL rats responded through suppression of intake of high-fat food (**Figure 5.7b**), but that decreased to 2 out of 7 responders in DIO hM3d rats (**Figure 5.7c**). A significant change in intake of high-fat food was observed in DIO CTRL+saline and DIO CTRL+CNO rats (**Figure 5.7b**), while no significant change in intake of high-fat food was observed in DIO hM3d+saline and DIO hM3d+CNO rats.

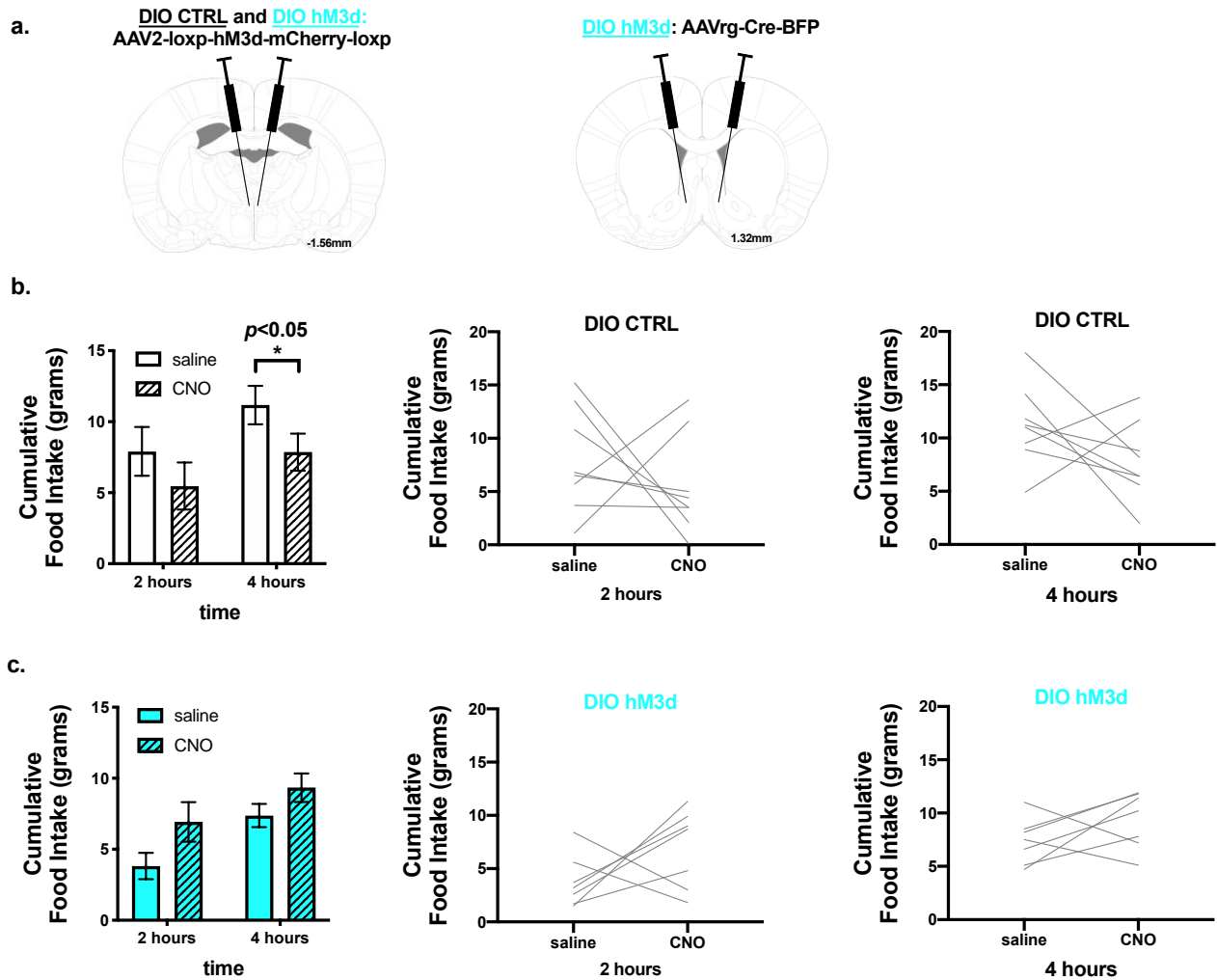


**Figure 5.7: hM3d-induced stimulation of PVN→NAc with a DIO viral vector approach increases intake of high-fat food in DIO hM3d rats.**

a. PVN hM3d targeting approach with NAc retrograde Cre targeting approach allows for expression of hM3d only in PVN→NAc projections infected with both viruses. b. DIO CTRL+CNO rats decreased intake of high-fat food at 4-hours post-injection.  $n=8$ ,  $*p > 0.05$  by two-way repeated measures ANOVA. c. DIO+hM3d rats receiving saline/CNO did not alter intake of high-fat food.  $n=7$ .

***HM3D-INDUCED STIMULATION OF PVN→NAC WITH A DIO VIRAL VECTOR APPROACH DECREASES OPERANT RESPONDING FOR HIGH-FAT FOOD***

To determine whether selective stimulation of PVN→NAc with a DIO viral vector approach affects motivated behavior for high-fat food, we utilized operant conditioning to train DIO CTRL rats and DIO hM3d rats to respond for a high-fat food pellet via lever presses (**Figure 5.8**). Both DIO CTRL and DIO hM3d rats acquired the task, indicating that the viral paradigm does not affect learning (**Figure 5.9**). On training days 12-17 (PR), DIO hM3d rats demonstrated higher basal active lever presses compared to DIO CTRL rats. DIO hM3d rats averaged approximately 60 active lever presses on training days 12-17 compared to DIO CTRL rats which averaged approximately 50 active lever presses on training days 12-17 (**Figure 5.9**). This separation in the acquisition curves is opposite of what was observed earlier in Chapter 5 with CTRL and hM3d rats.

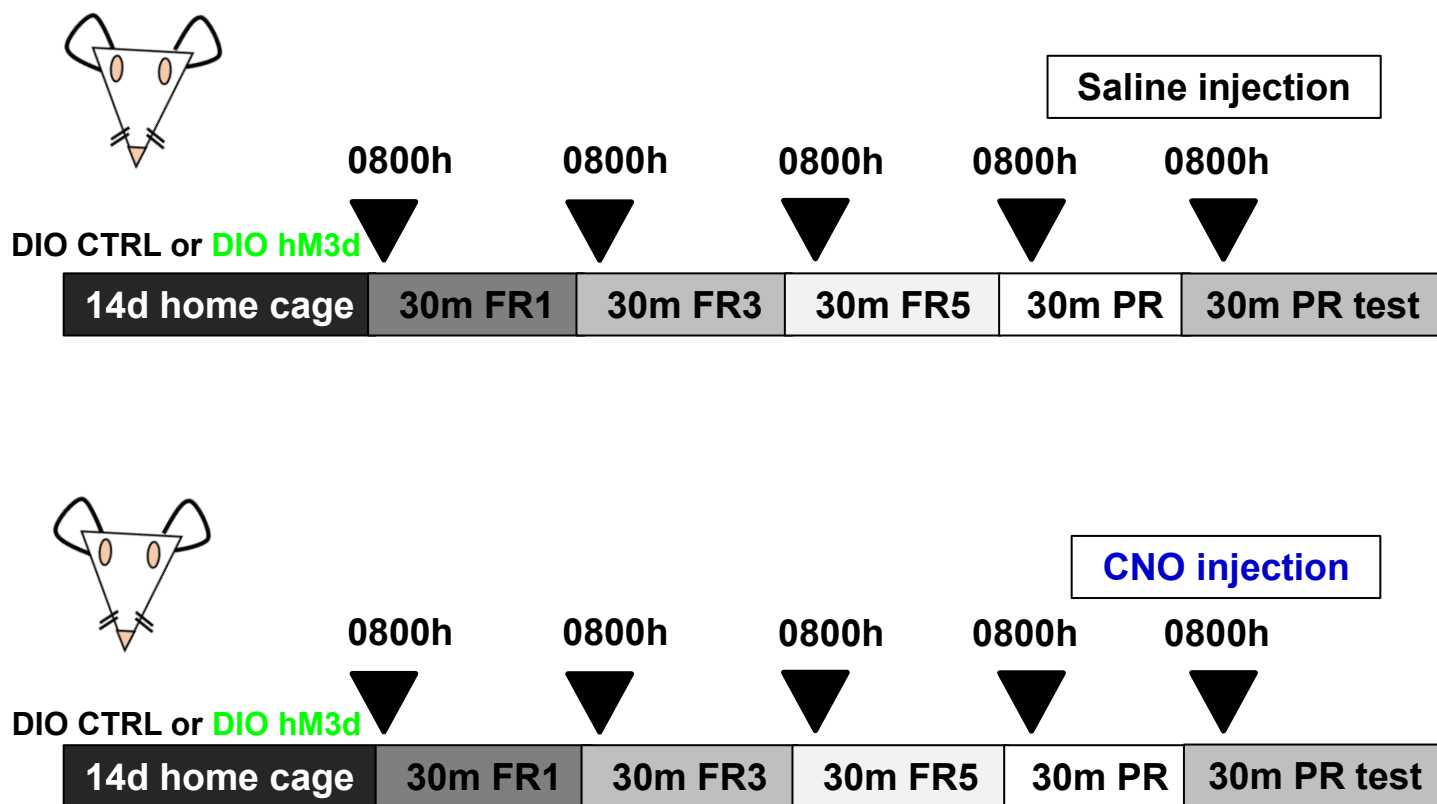


**Figure 5.8: Experimental timeline for operant conditioning: DIO CTRL/hM3d cohort.**

Rats expressing CTRL or hM3d virus recovered in their home cages for 14 days to allow for peak viral expression. Rats underwent operant conditioning, beginning with a fixed ratio 1 (FR1) schedule for 30 minutes. Once rats reached stability, they were advanced to a fixed ratio 3 (FR3) schedule, then to a fixed ratio 5 (FR5) schedule, and finally to a progressive ratio (PR) schedule for 30 minutes. On experimental day 1, CTRL and hM3d rats received intra-NAc aCSF or 1uM CNO prior to a 30-minute PR session. On the experimental day 2, CTRL and hM3d rats received intra-NAc aCSF (CNO on experimental day 1) or CNO (aCSF on experimental day 2). Active lever presses and reinforcements were quantified.



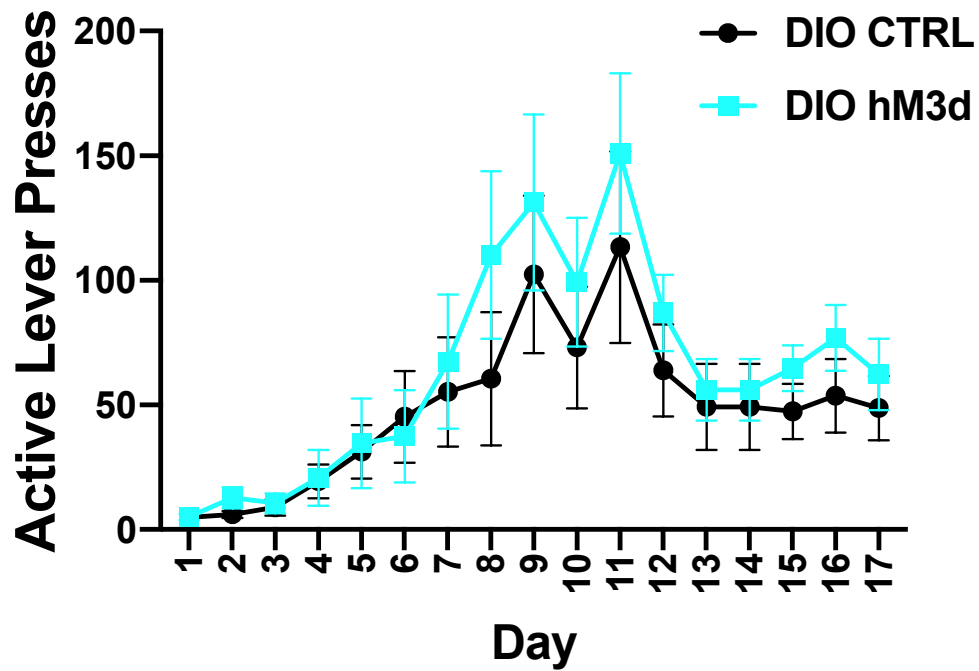


**Figure 5.9: Training acquisition for DIO CTRL/hM3d cohort.**

Rats expressing DIO CTRL or DIO hM3d virus were trained to lever press for a 45% fat/kcal food pellet on a fixed ratio 1 schedule of reinforcement. Upon acquisition, rats were advanced to a fixed ratio 3 schedule, fixed ratio 5 schedule, then finally a progressive ratio schedule (Day 12-17) where earning each successive high-fat food pellet requires more effort.

Once DIO CTRL and DIO hM3d rats reached stability on PR responding, saline or CNO was administered via I.P. injection immediately prior to a 30-minute PR session (**Figure 5.8**). Each rat received saline and CNO on different PR test days to control for potential CNO-related effects on active lever presses and reinforcers earned. No effect on active lever presses was observed in DIO CTRL+saline rats or DIO CTRL+CNO rats (**Figure 5.10a**). DIO hM3d+CNO rats significantly decreased active lever presses compared to DIO hM3d+saline rats via paired T-test, suggesting that hM3d-induced stimulation of PVN→NAc with a DIO viral vector approach decreases operant responding for high-fat food (**Figure 5.10b**).

During the 30-minute PR test, we also quantified high-fat food pellets or reinforcers earned. Reinforcers earned is a proxy for reinforcement efficacy-or how effective the reinforcer is at generating a behavioral response. No difference was identified in reinforcers earned in DIO CTRL+saline compared to DIO CTRL+CNO rats (**Figure 5.10c**). As seen with active lever presses, DIO hM3d+CNO rats had less reinforcers earned compared to DIO hM3d+saline rats, however this finding was not statistically significant (**Figure 5.10d**).

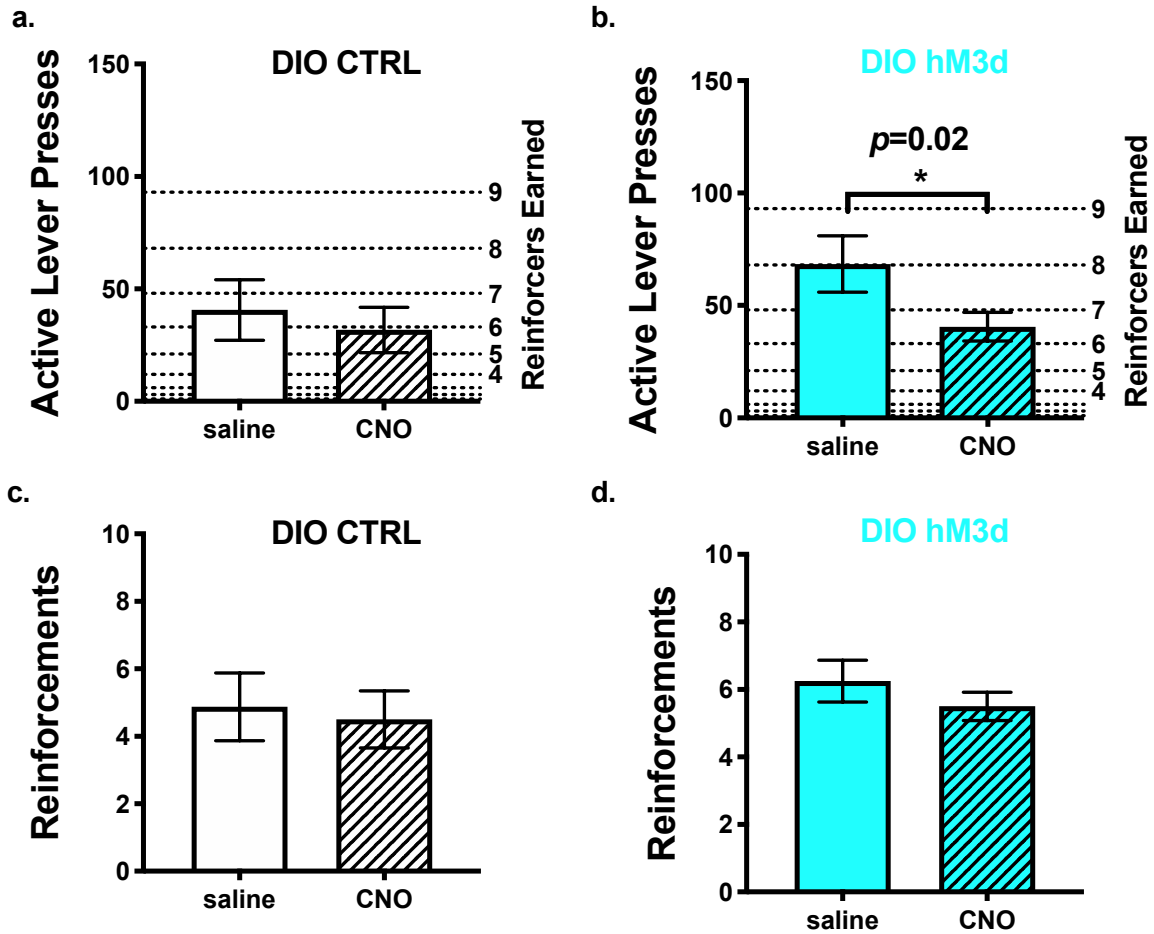


**Figure 5.10: hM3d-induced stimulation of PVN→NAc with a DIO viral vector approach decreases operant responding for high-fat food.**

a. Intraperitoneal administration of saline or CNO to DIO CTRL rats does not alter active lever presses for a high-fat food reinforcer.  $n=8$ . b. Intraperitoneal administration of CNO to DIO hM3d rats significantly decreases active lever presses for a high-fat food reinforcer.  $n=7$ ,  $*p=0.02$  by paired T-test. c. Intraperitoneal administration of saline or CNO does not alter high-fat reinforcements earned on a PR schedule of reinforcement in DIO CTRL rats.  $n=8$ . d. Intraperitoneal administration of saline or CNO does not alter high-fat reinforcements earned on a PR schedule of reinforcement in DIO hM3d rats.  $n=7$ .

***HM3D-INDUCED STIMULATION OF PVN→NAC WITH A DIO VIRAL VECTOR APPROACH DOES NOT ALTER LOCOMOTOR ACTIVITY***

To identify any effects on locomotor activity, we quantified central, peripheral and vertical locomotor activity during a 30-minute test session. DIO CTRL and DIO hM3d rats received IP injection of saline or CNO on different test days to control for CNO-specific effects. No changes in total horizontal activity were observed in DIO CTRL or DIO hM3d groups (**Figure 5.11a**). These findings show that any changes in food intake/active lever presses/reinforcers earned are not the result of changes in locomotor activity.

a.

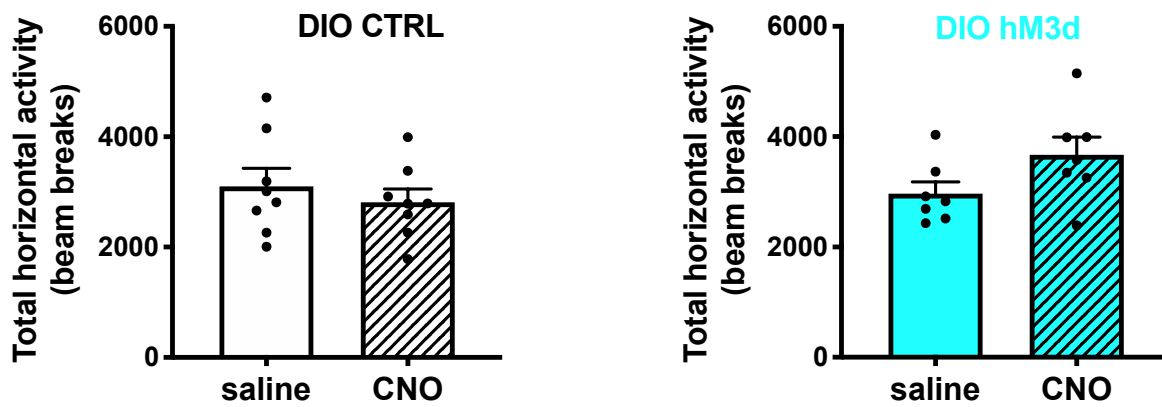


**Figure 5.11: hM3d-induced stimulation of PVN→NAc with a DIO viral vector approach does not alter locomotor activity.**

a. saline or CNO administration does not alter locomotor activity in DIO CTRL or DIO hM3d rats.

## DISCUSSION

### *GENERAL DISCUSSION*

Throughout this chapter, we investigated the effects of hM3d-induced stimulation on feeding behaviors using two different viral paradigms. Previously, we showed that a single virus with intra-NAc CNO administration facilitates presynaptic release of glutamate from PVN→NAc projections. Indeed, blockade of glutamate release into the NAc increases feeding. Specifically, intra-NAc infusion of non-N-methyl-D-aspartate receptor (non-NMDAR) glutamate antagonists into the medial NAc shell have been shown to evoke an immediate and sustained increase in food intake (Maldonado-Irizarry et al., 1995; Stratford et al., 1998). Additionally, intra-NAc administration of AMPA decreases food intake in food restricted rats (Stratford et al., 1998), emphasizing the relevance of accumbal glutamate as a regulator of feeding behavior.

We hypothesized that PVN→NAc regulates motivation for high-fat food through glutamate release. Although some PVN neurons are glutamatergic, the neurotransmitter(s) used in the PVN→NAc pathway was largely unknown until our microdialysis studies (Chapter 3) supporting that pharmacogenetic stimulation of PVN→NAc with the excitatory hM3d DREADD increases extracellular glutamate pre-synaptically in the NAc (Ziegler et al., 2002).

To directly probe the role of PVN→NAc glutamate release in driving feeding behaviors, we employed two different viral strategies utilizing the hM3d DREADD. Our first strategy directly mirrored the microdialysis approach- we administered an AAV2 containing hM3d in the PVN and implanted bilateral guide cannula in the

NAc for aCSF/CNO micro-infusion. In this paradigm, hM3d is expressed in all PVN projection neurons, including collaterals, in addition to PVN→NAc projections. To achieve PVN→NAc specific glutamate release, aCSF/CNO were micro-infused directly into the NAc. Presumably, administration of CNO facilitates presynaptic glutamate release from glutamate-containing vesicles of PVN→NAc neurons, but an action potential is not generated.

Our second strategy utilized a dual viral vector approach to attain selective stimulation of PVN→NAc. First, we administered a Cre-dependent AAV2 containing hM3d into the PVN, and an AAV6 containing Cre into the NAc. In this paradigm, only neurons that project from the PVN to the NAc and that are infected with both viruses express functional hM3d receptors throughout the neuron. IP administration of CNO depolarizes PVN→NAc neurons to generate an action potential, which releases glutamate, and potentially other neurotransmitters and neuropeptides.

While both paradigms achieve PVN→NAc selective glutamate release, the single virus approach allowed us to investigate the effects of presynaptic glutamate release on feeding behavior. The dual virus approach allowed us to investigate the effects of a PVN→NAc action potential on feeding behavior. Based on the initial hypothesis-that glutamate release decreases feeding behavior-we expected that the single virus approach would decrease intake of high-fat food, and decrease motivation for high-fat food. We expected a similar outcome with the dual virus approach but with a larger magnitude, meaning a greater decrease in intake of high-fat food, and a greater decrease in motivation for high-fat food.

With the single virus approach (CTRL and hM3d), the results demonstrated a significant suppression in intake of high-fat food in hM3d+CNO rats, with 9 out of 15 rats decreasing intake at 2-hours, and 10 out of 15 rats decreasing intake at 4-hours. There was no significant change in active lever presses or reinforcers earned in hM3d+CNO rats, suggesting that presynaptic release of glutamate from PVN→NAc is not sufficient to affect motivation for high-fat food.

With the dual viral approach (DIO CTRL and DIO hM3d), there was no significant change in intake of high-fat food in DIO hM3d+CNO rats, with only 2 out of 7 rats suppressing intake at 2-hours and at 4-hours. However, there was a significant decrease on active lever presses in hM3d+CNO vs hM3d+saline rats, indicating that stimulation of PVN→NAc projections decreases motivation for high-fat food.

The behavioral results were both unexpected and interesting. CTRL and hM3d rats exhibited higher baseline intake of high-fat food compared to DIO CTRL and DIO hM3d rats, but DIO hM3d rats increased intake of high-fat food at 2-hours and 4-hours post CNO administration. This would suggest an effect of IP CNO administration on intake, however DIO CTRL rats decreased intake of high-fat food at 2-hours and 4-hours post CNO administration. During the operant task, only DIO hM3d+CNO rats significantly decreased responding for a high-fat food pellet, but DIO CTRL and DIO hM3d rats exhibited higher baseline active lever presses/reinforcers earned compared to CTRL and hM3d. Taken together, these results underscore the differences in our hM3d DREADD approaches to stimulating PVN→NAc neurons.



Our microdialysis data suggest that intra-NAc CNO induces an immediate and sustained increase in extracellular glutamate pre-synaptically in the NAc for a duration of approximately 40-45 minutes. For operant sessions, rats received intra-NAc micro-infusions of CNO (4 min, followed by 2 min wait) and were immediately placed in chambers. The progressive ratio program lasted for 30 minutes total, unless the active lever remained untouched for 10 minutes (then the program timed out). Based on the duration of glutamate release from the microdialysis data, 30 minutes should have been long enough to observe a behavioral effect. Potential explanations for these differential findings are explored in the following sections.

#### ***VIRAL PROMOTER SPECIFICITY***

In our single virus paradigm, expression of both CTRL and hM3d viruses is driven by a calmodulin-dependent protein kinase II (CAMKII) promoter. The CAMKII promoter has been shown to drive viral expression in both excitatory and inhibitory neurons, but demonstrates a strong bias towards infection of excitatory neurons (Nathanson et al., 2009). Therefore, in the single virus rats, hM3d expression is likely biased towards excitatory projections, which primarily facilitates glutamate release in the NAc. While this bias limits our broader understanding of the neuromodulatory effects of PVN→NAc, it did allow us to determine glutamate-specific effects on feeding. In the dual virus paradigm, expression of hM3d is under the control of the human synapsin (hSyn) promoter. The hSyn promoter demonstrates considerably less bias than the CAMKII promoter, and consequently drives expression in both excitatory and inhibitory

neurons (Nathanson et al., 2009). Because hM3d expression is also Cre-dependent in this paradigm, only neurons projecting from the PVN to the NAc express hM3d. It is possible that there are other projections to the NAc not identified here that are inhibitory in nature, or have other neuromodulatory effects. Future microdialysis studies investigating this dual virus paradigm would clarify whether hM3d is expressed in inhibitory projections, and identify other neuromodulatory molecules (i.e. neuropeptides) that may be co-released from PVN→NAc projections.

### ***GLUTAMATE DYNAMICS***

Firstly, the rapid hM3d-induced increase in extracellular glutamate in the NAc may be high enough to cause post-synaptic ionotropic (AMPA) and metabotropic (mGluR) glutamate receptor desensitization and internalization. Based on the microdialysis data, hM3d+CNO rats demonstrated a 175% increase over CTRL+CNO rats, and an increase in extracellular glutamate concentration up to 14 $\mu$ M. Because glutamate receptors can be desensitized by only 0.5-5 $\mu$ M of glutamate, hM3d-induced glutamate release from PVN→NAc neurons may have exceeded behaviorally relevant post-synaptic glutamate concentrations in the NAc (Colquhoun et al., 1992; Featherstone and Shippey, 2008; Otis et al., 1996; Trussell and Fischbach, 1989). An interesting experiment would be to test whether intake of high-fat food stimulates glutamate release from PVN→NAc projections, but we did not measure this.

Another plausible but untested hypothesis is that presynaptic glutamate release from PVN→NAc projections is reinforcing in nature, and time dependent.

This could explain why we observed no effect on motivation for high-fat food in hM3d+CNO rats (as in the operant task), but did observe a decrease in intake of high-fat food. Based on the microdialysis data, presynaptic glutamate release lasts for 35-40 minutes, and therefore persists beyond the duration of the operant session (30 minutes). If presynaptic glutamate release from PVN→NAc projections was indeed reinforcing, hM3d+CNO rats would be less motivated to respond for high-fat food. A longer progressive ratio session, i.e. 1+ hours, would help elucidate this hypothesis-if active lever presses and reinforcers increase after the duration of glutamate release, this suggests that glutamate may, in part, mediate the reinforcing effects of high-fat food. Another way to test this would be to identify whether animals would respond for glutamate infusion (or infusion of a glutamate receptor agonist) into the NAc.

During the intake of high-fat food, we employed longer time points, 2-hours and 4-hours post micro-infusion. These longer time points are required to accurately quantify food intake due to the inherent variability associated with the initiation of spontaneous food intake in animals. In other words, the error associated with 30-minute spontaneous (non-stimulated) food intake is too high to identify significant effects. In this study, presynaptic glutamate was released from PVN→NAc neurons for 35-40 minutes, but rats had access to high-fat food beyond the duration of glutamate release. After presynaptic glutamate release subsided, hM3d+CNO rats consumed significantly less high-fat food than hM3d+aCSF rats, indicating that presynaptic release of glutamate decreases intake of high-fat food.

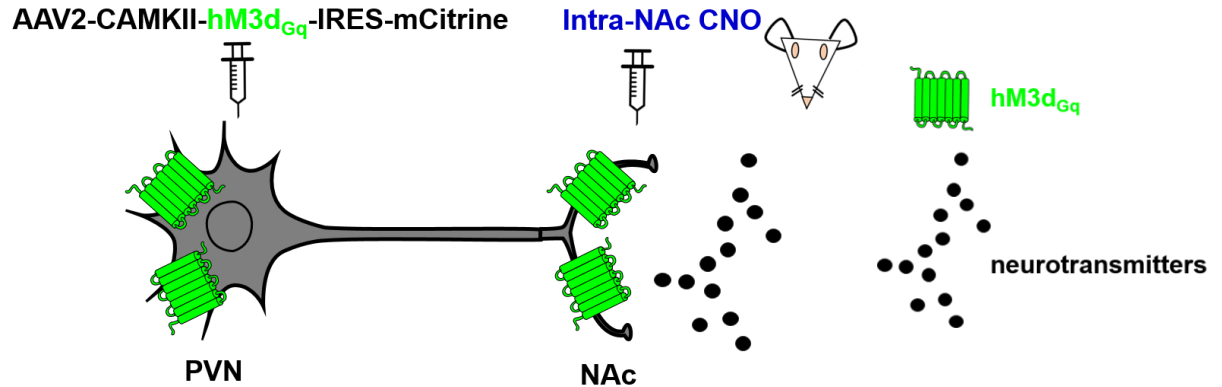
### ***HM3D-MEDIATED PRESYNAPTIC RELEASE VS. DIO HM3D-MEDIATED ACTION POTENTIAL***

The use of a single virus in combination with intra-NAc CNO administration allowed us to achieve selective pharmacogenetic stimulation of PVN→NAc neurons. The main advantage (and a limitation) of this approach is that intra-NAc CNO administration facilitates local release of glutamate from synaptic vesicles located pre-synaptically in the NAc (Campbell and Marchant, 2018). This effect is diagrammed in **Figure 5.12a**. Notably, an action potential is not generated from PVN→NAc neurons, which allowed us to disentangle the effect of presynaptic glutamate release alone on feeding behaviors (Campbell and Marchant, 2018). While this specificity is an advantage in identifying the role of glutamate in PVN→NAc mediated feeding behaviors, the lack of action potential generation in these neurons narrows our view of how PVN→NAc mediates these feeding behaviors.

We set out to further our understanding with a dual virus paradigm in combination with IP CNO administration to facilitate an action potential in PVN→NAc neurons. In addition to glutamate, an action potential would induce the release of other neurotransmitters and neuropeptides from PVN→NAc (Campbell and Marchant, 2018). This effect is diagrammed in **Figure 5.12b**. Neuropeptides are signaling molecules that are packaged in the cell bodies of neurons and transported to synapses where they are stored in dense core vesicles. Release of dense core vesicles occurs when an action potential is generated, but an action potential has a lower probability of releasing dense core vesicles versus clear core vesicles, and thus it takes longer for release compared to neurotransmitter release

(neurotransmitters are readily available for release at the synapse and have vesicular stores). Neuropeptides are well-known regulators of feeding, including oxytocin and enkephalin, both of which may be involved in PVN→NAc signaling (Dölen et al., 2013).

a.



b.

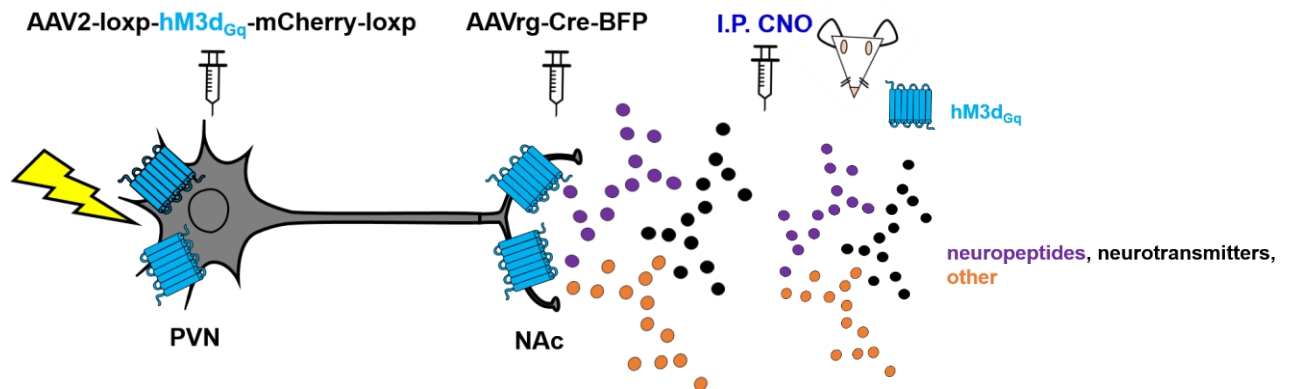


**Figure 5.12: Proposed mechanisms of hM3d DREADD approaches.**

Graphical representation of two PVN→Nac specific viral paradigms for expression of hM3d. a. An anterograde AAV2 virus was used to deliver hM3d into the PVN of rats. In PVN→Nac neurons, hM3d is expressed both pre- and post-synaptically, however administration of CNO directly into the NAc via guide cannula evokes pre-synaptic release of neurotransmitter stores specifically from these projections. b. An anterograde AAV2 virus was used to deliver hM3d into the PVN of rats, and a retrograde AAV expressing Cre was administered into the NAc. Recombination of the viruses in PVN→Nac neurons results in the expression of hM3d pre- and post-synaptically in PVN→Nac projections only. Intraperitoneal administration of CNO with this viral paradigm results in depolarization of PVN→Nac neurons and action potential firing that releases neurotransmitters, neuropeptides, and other molecules.

## ***DUAL TRANSMISSION NEURONS***

There is mounting evidence to suggest that neurons are capable of co-transmission or co-release of neurotransmitters and neuropeptides (Trudeau and El Mestikawy, 2018; Vaaga et al., 2014; Zimmermann et al., 2015). Co-transmission is defined as the release of multiple neuromodulators simultaneously, co-release is differentiated by the packaging of multiple neuromodulators within a single population of vesicles (Trudeau and El Mestikawy, 2018; Vaaga et al., 2014; Zimmermann et al., 2015). Currently, there are three models of co-transmission and co-release: two fast acting neurotransmitters, a fast acting neurotransmitter and monoamine, and a fast acting neurotransmitter and neuromodulator (Vaaga et al., 2014). Fast neurotransmitters include glutamate and GABA, monoamines include dopamine, serotonin and norepinephrine, and neuromodulators include neuropeptides among other signaling molecules (Trudeau and El Mestikawy, 2018).

While we did not observe co-localization of PVN→NAc neurons with GAD<sub>67</sub>, TH or TPH, we cannot rule out the possibility of dual transmission by PVN→NAc neurons, nor the co-release of neuropeptide(s) with glutamate. One approach to answer this question is to conduct microdialysis experiments tailored to the quantification of neuropeptides, especially oxytocin. Dolen and colleagues established that PVN→NAc neurons release oxytocin in the NAc to mediate social reinforcement- it's plausible that PVN→NAc neurons co-release glutamate and oxytocin in our studies examining feeding behaviors. Indeed, glutamate-oxytocin co-release could be a mechanism by which individuals develop powerful

relationships with specific foods, i.e. “comfort” foods.” Indeed, oxytocin release is known to decrease food intake, and an ongoing clinical trial is investigating the efficacy of intranasal oxytocin for hypothalamic obesity (Spetter et al., 2018).

As mentioned in Chapter 4, our microdialysis design was limited by an inability to detect uncharged neurotransmitters, such as acetylcholine, which has been implicated in feeding behaviors, especially in the NAc. Intra-NAc infusion of the muscarinic receptor antagonist scopolamine decreases intake of high-fat food (Perry et al., 2009). Additionally, chronic binge-intake is known to alter NAc acetylcholine levels and create an imbalance (Avena et al., 2008a). Based on this literature, we cannot rule out the possibility to glutamate and acetylcholine co-release from PVN→NAc neurons.

An additional strategy to determine whether glutamate is co-released is to virally transduce a short hairpin RNA directed against VGLUT1 to PVN→NAc neurons. This approach would theoretically inhibit PVN→NAc neurons from packaging and releasing glutamate. Interestingly, one group found that knockdown of the vesicular GABA transporter (VGAT) in VTA GABA neurons did not block GABA transmission from these neurons (Tritsch et al., 2012). Instead, their studies demonstrated that GABA is co-packaged and co-released with dopamine from vesicular monoamine transporter (VMAT) vesicles (Tritsch et al., 2012).



## Chapter 6 Summary and Conclusions

### GENERAL CONCLUSIONS

BED and obesity are major public health problems that are associated with psychosocial distress, impairments in daily function, and life-threatening comorbidities (2013; 2017; Berridge, 2009; Berridge et al., 2010; de Zwaan, 2001; Freeman et al., 2014; Guerdjikova et al., 2017; Hales et al., 2017; Javaras, 2017; Kessler et al., 2013; Moore et al., 2017; Rancourt and McCullough, 2015; Volkow et al., 2013b). Both diseases are driven by maladaptive feeding behaviors, namely pathological overconsumption of high-fat food (Javaras, 2017; Moore et al., 2017). Pathological overconsumption of high-fat food is potentiated by dysregulation in portion control (i.e. titration of caloric intake mediated by the PVN), and is exacerbated by the reinforcing properties of high-fat food (i.e. hedonic feeding mediated by the NAc and the VTA). Furthermore, dysfunction of homeostatic (PVN) and hedonic (NAc, VTA) feeding circuitry is hypothesized to underlie pathological overconsumption of high-fat food (Corwin et al., 2016; Davis and Carter, 2009; Dichter et al., 2012; Guerdjikova et al., 2017; Hommel et al., 2006; Satta et al., 2018; Volkow et al., 2013a, b; Volkow and Wise, 2005; Witt and Lowe, 2014). This dissertation aimed to elucidate the interconnected mechanisms of homeostatic and hedonic signaling that may underlie pathological overconsumption of high-fat food, and identified the neuropeptide receptor NMUR2 and the neurotransmitter glutamate as novel regulators of binge-type eating, intake of high-fat food, and motivation for high-fat food (**Figure 6.1**).

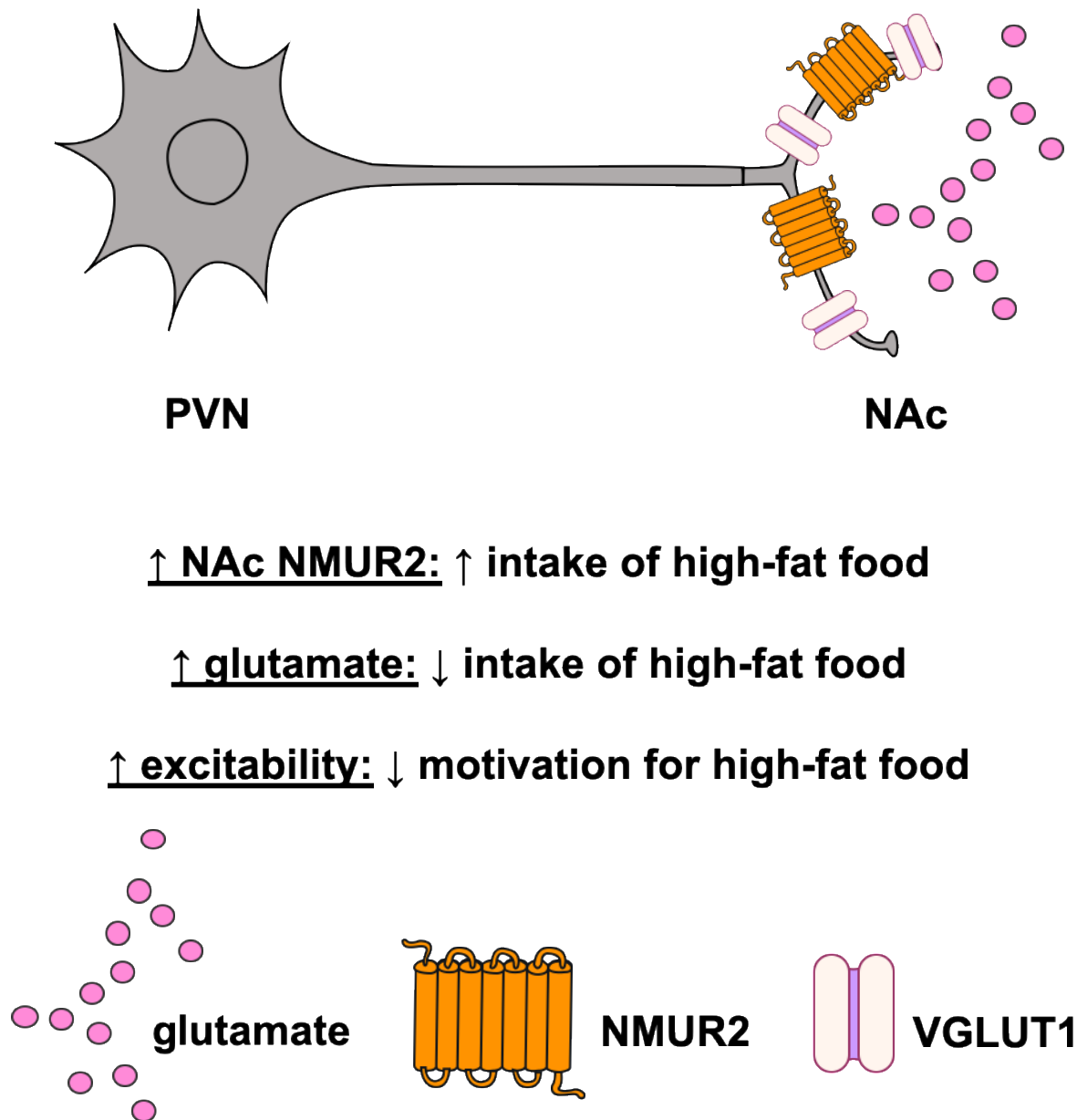


**Figure 6.1: Integration of homeostatic and hedonic brain centers in the regulation of feeding behaviors.**

Diagram and summary of findings about PVN→NAc regulation of feeding behaviors. In Chapter 3, we found that high NAc expression of NMUR2 drives binge-intake of preferred food. In Chapters 4 and 5 we found that presynaptic glutamate release from

PVN→NAc projections decreases intake of high-fat food, while increased excitability (depolarization) of PVN→NAc projections decreases motivation for high-fat food.

Oxytocin is an important neuropeptide involved in PVN→NAc signaling. Dolen *et al*/demonstrated that PVN→NAc neurons release oxytocin in the NAc and mediate social reward in an oxytocin dependent manner (Dölen et al., 2013). While this dissertation identified that PVN→NAc neurons release glutamate pre-synaptically in the NAc, it is likely that these projections co-release glutamate and oxytocin to mediate food reward. Accordingly, oxytocin is known to decrease intake of rewarding foods in humans (Spetter et al., 2018). Oxytocin signaling is a hypothesized link between social behavior and feeding behavior (Spetter and Hallschmid, 2017). With the knowledge that oxytocin mediates both social reward and food reward, it is conceivable that oxytocin release underlies the development of powerful relationships with food. In fact, human studies have shown that humans tend to consume larger meals in the presence of others, eat for a longer duration of time in the presence of others, and titrate the quantity of food consumed to other weight-matched subjects (Cruwys et al., 2015; De Castro, 1990; de Castro and de Castro, 1989; Robinson et al., 2014). In rodents, similar social cues have been demonstrated to modulate the effects of oxytocin on feeding, although more studies are needed to determine these effects in humans (Spetter and Hallschmid, 2017). Overall, intranasal oxytocin has demonstrated efficacy in the treatment of hypothalamic obesity, and may be a mechanism through which we observed decreased motivation for high-fat food (Arletti et al., 1989; Lawson, 2017; Ott et al., 2013; Spetter et al., 2018). While more studies are needed to pinpoint the exact mechanism by which PVN→NAc oxytocin regulates feeding, this work presented

in this dissertation identifies another regulatory role of PVN→NAc projections in coordinating homeostatic and hedonic control of feeding.

Enkephalin is another crucial neuropeptide involved in feeding behavior that may be involved in PVN→NAc signaling to regulate intake and motivation for high-fat food. Enkephalin is an endogenous opioid with high affinity for the mu opioid receptor, and is hypothesized to underlie “liking” (Berridge and Robinson, 1998; Pickel et al., 1980; Robinson and Berridge, 1993). Unpublished work from the Hommel Laboratory demonstrated that both the PVN and the NAc express enkephalin and that PVN→NAc projections co-express NMUR2 and enkephalin. Given that intra-NAc micro-infusion of DAMGO potently and selectively increases intake of high-fat food and motivation for high-fat food, enkephalin in PVN→NAc projections may oppose the actions of glutamate (Kelley et al., 1996; Zhang et al., 1998; Zhang and Kelley, 1997).

Glutamate signaling in PVN→NAc projections is a major focus of this dissertation, and a novel finding that extends our understanding of this circuit. Presynaptic glutamate release from PVN→NAc projections alters feeding behaviors, an effect which is presumably modulated by a variety of glutamate receptors within the NAc. Electrophysiology studies established that glutamate neurotransmission into the NAc is primarily mediated non-NMDA ionotropic glutamate receptors, namely AMPA receptors, and that mGluRs inhibit excessive glutamate signaling (Hu and White, 1996). Group II mGluRs, including mGluR2 and mGluR3, are primarily presynaptic, and have been implicated in feeding as well as substance use (Bossert et al., 2006; Windisch and Czachowski, 2018).

Specifically, mGluR2/3 agonist LY379268 decreases sucrose-seeking and ethanol-seeking (Windisch and Czachowski, 2018). Additionally, intra-NAc infusions of LY379268 also dose-dependently decrease opiate reinstatement (Bossert et al., 2006). These findings align with other literature and the data presented in this dissertation about the modulatory effects of glutamate on feeding.

Furthermore, this glutamatergic signaling from PVN→NAc projections may underlie synaptic plasticity in the NAc. It is established that exposure to a “junk food” diet upregulates calcium permeable AMPA receptors, and that chronic high-fat diet exposure induces alterations in plasticity within striatal sites, including the NAc (Matikainen-Ankney and Kravitz, 2018; Oginsky et al., 2016). These changes in synaptic function may contribute to decreased physical activity, deficits in motivational state, and altered reward processing, all of which perpetuate pathological overconsumption of high-fat food (Matikainen-Ankney and Kravitz, 2018). Our findings that glutamatergic transmission into the NAc decreases intake of high-fat food and motivation for high-fat food may have therapeutic relevance to targeting aberrant plasticity in the NAc resulting from chronic exposure to a high-fat diet, although future studies are needed to test this idea.

Our microdialysis approach allowed for the direct measurement of glutamate *in vivo*, and identified concentrations of glutamate within the synaptic space and extra-synaptic space (Moussawi et al., 2011). During basal conditions, the glutamate concentration in dialysate is mainly from non-synaptic, or extra-synaptic sources (van der Zeyden et al., 2008). However, under basal conditions, glutamate spill-over to extracellular fluid is extremely limited (van der Zeyden et

al., 2008). Because our microdialysis probe is too large to sample directly from the intracellular space within synapses, our robust and sustained increase in glutamate upon hM3d-induced stimulation of PVN→NAc is likely reflective of synaptic and extra-synaptic glutamate. Glial cells also utilize glutamate and provide glutamatergic tone, and quantification of glutamate in the extra-synaptic space may reflect these concentrations of glutamate in addition to our experimental concentrations of glutamate (Moussawi et al., 2011).

While this dissertation has mainly focused on PVN→NAc projections, the PVN has several efferents to other brain regions, including other regions known to regulate the rewarding properties of high-fat food. The VTA receives projections from the PVN that also release oxytocin to mediate social reward (Hung et al., 2017). Hung and colleagues also established that PVN→VTA oxytocinergic drive excites dopamine neurons downstream in the VTA (Hung et al., 2017). It is quite likely that PVN→VTA projections also encode the reinforcing properties of high-fat food via oxytocin and dopamine. In fact, dopaminergic signaling is widely implicated in the feeding literature, from mediating natural food reward, to the addictive dimensionality of obesity, and finally to dysfunction at the circuit-level resulting from chronic intake of both high-fat and high-sucrose diets (Avena et al., 2008a; Avena et al., 2008b, c, 2009; Bello et al., 2002; Volkow et al., 2007; Volkow et al., 2013a, b; Wang et al., 2011).

In this dissertation, we corroborate previous work identifying pre-synaptic NMUR2 in the NAc, and extend these findings through establishing both pre- and post-synaptic NMUR2 expression in the VTA. Other work from the Hommel Laboratory

identified NMUR2 expression in the PVN and in other hypothalamic regions (Benzon et al., 2014; Kasper et al., 2016; McCue et al., 2017). Hypothalamic knockdown of NMUR2 increases intake of high-fat food, and conversely intra-PVN administration of NMU decreases intake of high-fat food and motivation for high-fat food (Benzon et al., 2014; McCue et al., 2017). Through a combination of electrophysiological and molecular techniques, Qui and colleagues established that administration of NMU in the PVN increases neuronal excitability of PVN neurons (Qiu et al., 2005). The work presented here corroborates this finding: PVN→NAc neurons demonstrate increased excitability via hM3d-induced stimulation and release glutamate. Collectively, NMUR2 signaling increases excitability of PVN→NAc projections to decrease intake of high-fat food, presumably through modulation of glutamate release in the NAc.

### **CHAPTER 3 CONCLUSIONS**

The neurobiological basis of pathological overconsumption observed in BED and obesity is poorly understood, and demands a more mechanistic appreciation of the neurobiological underpinnings of feeding behavior. NMUR2 facilitates binge-type eating in rats through promoting binge intake of “lower” fat diets via the NAc while simultaneously suppressing intake of “extreme” higher fat diets via the VTA, thus decreasing total fat intake during a binge session. Therefore, NMUR2 represents a promising druggable target to treat BED and obesity, and has already been shown to successfully alter feeding behavior (Kaisho et al., 2017; Kanematsu-Yamaki et al., 2017; Sampson et al., 2018). The work presented here demonstrates key relationships between NMUR2 expression

in hedonic brain centers and binge-type behavior that will contextualize the interpretation of future research determining the therapeutic potential of NMUR2 to regulate pathological overconsumption.

Overall, our findings in Chapter 3 demonstrate key relationships between synaptosomal NMUR2 expression in the NAc and the VTA and binge-type eating in rats. We observed both brain region-specific differences in synaptosomal NMUR2 protein expression, as well as individual differences in NMUR2 expression. Binge-type eating changes based on fat content and NMUR2 expression varies not only across animals, but across brain regions. Thus, endogenous NMUR2 may be a driver of individual differences in binge-type eating, especially binge-type eating of high-fat food. Specifically, a genome wide association study revealed decreased NMUergic signaling in the hypothalamus of mice maintained on a high-fat diet, which suggests that NMUergic signaling may become dysregulated in recurring instances of pathological overconsumption of high-fat food (Hu et al., 2018). Additionally, a single nucleotide polymorphism in NMU was identified in children with obesity, further supporting a role for NMUergic signaling in regulating intake of high-fat food (Hainerová et al., 2006). While the high degree of inter-animal variability and inter-brain region variability in NMUR2 protein expression is somewhat limiting, it does suggest that NMUR2 may contribute to individual differences observed in humans with BED.

The clinical implications of our findings establish NMUR2 as a novel regulator of binge-type eating, and therefore as a future druggable target for pathological overconsumption observed in BED and obesity. Recently, we showed



that small-molecule NMUR2 agonists successfully decrease high-fat food intake in rats, which supports NMUR2 as a viable drug target (Sampson et al., 2018). Future studies will continue to investigate the contribution of NMUR2 in the NAc and the VTA at molecular, neural, and pharmacological levels, including investigating the effects of these small-molecule NMUR2 agonists on binge-type eating in rats.

#### **CHAPTER 4 CONCLUSIONS**

Homeostatic (PVN) and hedonic (NAc) brain regions are integrated through PVN→NAc projections, which were largely uncharacterized until this work. We established the neuroanatomical properties of PVN→NAc, and identified glutamate as the major neurotransmitter involved in PVN→NAc signaling (Figure 6.1). PVN projections to the NAc are broadly distributed throughout the parvocellular PVN, a region implicated in intake of high-fat food (Jhanwar-Uniyal et al., 1993). Additionally, we determined that PVN→NAc projections co-localize with VGLUT1, and that hM3d-induced stimulation results in glutamate release (Figure 6.1). These findings extend previous findings beyond PVN→NAc oxytocin release to glutamate release (Dölen et al., 2013). Pharmacological manipulations of NAc glutamate illustrated the importance of glutamate in stimulating and suppressing feeding behavior (Baldo and Kelley, 2007; Maldonado-Irizarry and Kelley, 1995b; Maldonado-Irizarry et al., 1995; Stratford et al., 1998). Indeed, it is likely that PVN→NAc is the endogenous circuit that regulates feeding and underlies these previous pharmacological studies.

#### **CHAPTER 5 CONCLUSIONS**

While homeostatic (PVN) and hedonic (NAc) brain regions are independently linked to feeding behaviors, we elucidated PVN→NAc connectivity in regulating intake of high-fat food and motivation for high-fat food. Through glutamatergic inputs to the NAc, the PVN decreases intake of high-fat food, and motivation for high-fat food. Our identification of glutamate as a regulator of intake of high-fat food combined with existing literature on the robust effects of pharmacological manipulations of glutamate on feeding behaviors warrant further investigation into glutamate as a potential therapeutic target for the treatment of pathological overconsumption of high-fat food (Kreitzer and Malenka, 2007; Loweth et al., 2013; Sidorov et al., 2013).

Our findings from Chapter 3 indicate that NMUR2 is expressed pre-synaptically in the NAc and the VTA, and we suspect that NMUR2 is involved in the individual differences observed in binge-type eating, especially palatability. In the NAc, NMUR2 co-localizes with projections from the dorsal raphe nucleus, but it is not known whether presynaptic NMUR2 in the NAc also co-localizes with PVN→NAc projections (Kasper et al., 2016). However, knockdown of NMUR2 in the PVN increases intake of high-fat food, and intra-PVN administration of NMU decreases intake of high-fat food and motivation for high-fat food (Benzon et al., 2014; McCue et al., 2017). The work presented in this dissertation aligns with these previous NMUR2 findings in that PVN→NAc selective stimulation using the hM3d DREADD decreases intake of high-fat food and motivation for high-fat food (Figure 6.1). The two viral strategies we utilized are important for understanding PVN→NAc selective stimulation in the context of feeding. First, we utilized a

single virus strategy in combination with intra-NAc administration of aCSF/CNO. Intra-NAc administration of aCSF/CNO allowed for PVN→NAc selective presynaptic release of glutamate, despite hM3d expression in other collaterals and projections.

The second strategy utilized a dual virus approach to selectively express hM3d in PVN→NAc projections in combination with I.P. administration of saline/CNO. This viral paradigm depolarizes only PVN→NAc projections expressing hM3d and generates an action potential. This dual virus hM3d DREADD strategy is more optimal because it more closely resembles PVN→NAc function in vivo. Because NMUR2 is expressed on PVN cell bodies, the action potential firing in PVN→NAc projections resulting from the dual virus strategy likely incorporates NMUR2ergic input.

## **SUMMARY AND FUTURE DIRECTIONS**

In summary, this dissertation has investigated the interconnectedness of homeostatic and hedonic circuitry that underlies pathological overconsumption of high-fat food. We identified the neuropeptide receptor NMUR2 and the neurotransmitter glutamate as novel regulators of feeding behaviors. Overall, NMUR2 demonstrates inter-brain region variability, inter-animal variability, and regulates binge-type eating in rats. We believe that the variability we observed in NMUR2 expression may underlie individual differences in the pathology of BED. We also demonstrated that glutamatergic signaling between homeostatic (PVN) and hedonic (NAc) brain regions decreases intake and motivation for high-fat food.

Dysfunction in glutamatergic signaling may also potentiate pathological overconsumption of high-fat food.

Future directions of the current work include experiments to further probe the role of glutamate in suppressing feeding, and to better understand the mechanisms that underlie PVN→NAc signaling (i.e. involvement of NMUR2 in PVN→NAc signaling), and to identify upstream and downstream regulators of PVN→NAc.

Future studies can test the hypotheses that (a) blockade of presynaptic PVN→NAc glutamate release increases motivation for high-fat food, and (b) intra-NAcSh administration of the non-NMDAR antagonist 6, 7-dinitroquinoxaline-2, 3-dione (DNQX) increases motivation for high-fat food. Our data suggest that stimulation of PVN→NAc elicits glutamate release and decreases intake of high-fat food and motivation for high-fat food. To extend these findings, future studies can employ viral-mediated delivery of short hairpin RNA against VGLUT1 to attenuate glutamate release from PVN→NAc neurons and quantify motivation for high-fat food. Additionally, administration of the non-NMDA antagonist DNQX directly to the NAc may increase motivation for high-fat food. Together, these experiments would determine whether PVN→NAc glutamate is necessary and sufficient to drive motivated behavior for high-fat food, and would emphasize the value of glutamate as a pharmacotherapeutic target in the treatment of pathological overconsumption of high-fat food.

Previous work from the Hommel Laboratory demonstrated that NMUR2 is expressed on cell bodies in the PVN, and knockdown of NMUR2 in the PVN results

in binge-type intake of high-fat food and greater preference for high-fat food (Benzon et al., 2014). We confirmed that NMUR2 is expressed pre-synaptically in the NAc, and that PVN→NAc projections release glutamate (Benzon et al., 2014; Kasper et al., 2016). An important future experiment is to knockdown NMUR2 expression in PVN→NAc and quantify neurotransmitter and neuropeptide release via microdialysis to determine whether NMUR2 regulates presynaptic release of glutamate, oxytocin, and/or neuromedin U, the endogenous neuropeptide ligand for NMU (in addition to other neurotransmitters and neuropeptides).

Future studies can also conduct microdialysis during intake of high-fat food to identify neurotransmitter and neuropeptide release from PVN→NAc. Another interesting question to pursue would be to determine whether chronic exposure to a high-fat diet contributes to aberrant glutamatergic signaling, and if these changes are reversed by alterations in food choices.

Further neuroanatomical studies are needed to identify the upstream and downstream targets of PVN→NAc. Ongoing experiments are utilizing trans-synaptic tracing to determine brain regions upstream (i.e. arcuate nucleus, lateral hypothalamus) and downstream (i.e. VTA, ventral pallidum, amygdala, prefrontal cortex) of PVN→NAc.

Our results indicate that hM3d-induced stimulation of PVN→NAc projections excites downstream neurons in the NAc. In addition to identifying what downstream targets PVN→NAc projections are synapsing with (described above), it is important to characterize what types of neurons are downstream, including what receptors are expressed post-synaptically. The most likely targets of

PVN→NAc glutamate release are post-synaptic AMPA receptors and metabotropic glutamate receptors.

This work is the foundation of future research investigating glutamate receptors as a potential therapeutic target for the treatment of pathological overconsumption of high-fat food. Existing literature supports the efficacy of metabotropic glutamate receptor agonists to decrease maladaptive behaviors that potentiate substance use disorder (Guo et al., 2009; Loweth et al., 2014a; Loweth et al., 2013, 2014b; Schwendt et al., 2012). Because substance use disorder shares neural circuitry with feeding neural circuitry, metabotropic glutamate receptors might present a reasonable target for pathological overconsumption of high-fat food.

Currently, lisdexamfetamine is the only approved pharmacotherapy for the treatment of BED (McElroy et al., 2016; McElroy et al., 2015). While the mechanism of action of lisdexamfetamine is unknown, it is an amphetamine derivative that functions as both a stimulant and an appetite suppressant (McElroy et al., 2016; McElroy et al., 2015). Selective-serotonin reuptake inhibitors (SSRIs) have demonstrated efficacy in BED, but this is likely due to the high comorbidity of BED with other mental illnesses, especially anxiety, depression, and substance use disorder (Kessler et al., 2013; Kessler et al., 2016). Because lisdexamfetamine cannot be administered in combination with SSRIs, effective treatment for BED is lacking. Coincidentally, safe and efficacious treatment for obesity is also limited. The work presented in this dissertation identifies PVN→NAc as a critical neural circuit underlying the pathological overconsumption of high-fat food, and

establishes the mechanism of PVN→NAc signaling. Altogether, this work provides a solid foundation for future discovery of pharmacotherapies to adequately address the neurobiological dysfunctions in BED and obesity.

## References

(2013). Managing Overweight and Obesity in Adults, Systematic Evidence Review from the Obesity Expert Panel. (National Institutes of Health, National Heart, Lung, and Blood Institute), pp. 1-501.

(2017). Eating Disorders and Obesity A Comprehensive Handbook, Third edn (New York, NY: The Guilford Press).

Anastasio, N.C., Stutz, S.J., Fink, L.H., Swinford-Jackson, S.E., Sears, R.M., DiLeone, R.J., Rice, K.C., Moeller, F.G., and Cunningham, K.A. (2015). Serotonin (5-HT) 5-HT<sub>2A</sub> Receptor (5-HT<sub>2AR</sub>):5-HT<sub>2CR</sub> Imbalance in Medial Prefrontal Cortex Associates with Motor Impulsivity. ACS Chem Neurosci 6, 1248-1258.

Anastasio, N.C., Stutz, S.J., Price, A.E., Davis-Reyes, B.D., Sholler, D.J., Ferguson, S.M., Neumaier, J.F., Moeller, F.G., Hommel, J.D., and Cunningham, K.A. (2019). Convergent neural connectivity in motor impulsivity and high-fat food binge-like eating in male Sprague-Dawley rats. Neuropsychopharmacology.

Arletti, R., Benelli, A., and Bertolini, A. (1989). Influence of oxytocin on feeding behavior in the rat. Peptides 10, 89-93.

Association, A.P. (2013a). Diagnostic and Statistical Manual of Mental Disorders (Washington, D.C.).

Association, A.P. (2013b). *Feeding and Eating Disorders* (Washington, D.C.).



Avena, N.M., Bocarsly, M.E., Rada, P., Kim, A., and Hoebel, B.G. (2008a). After daily bingeing on a sucrose solution, food deprivation induces anxiety and accumbens dopamine/acetylcholine imbalance. *Physiol Behav* 94, 309-315.

Avena, N.M., Rada, P., and Hoebel, B.G. (2008b). Evidence for sugar addiction: behavioral and neurochemical effects of intermittent, excessive sugar intake. *Neurosci Biobehav Rev* 32, 20-39.

Avena, N.M., Rada, P., and Hoebel, B.G. (2008c). Underweight rats have enhanced dopamine release and blunted acetylcholine response in the nucleus accumbens while bingeing on sucrose. *Neuroscience* 156, 865-871.

Avena, N.M., Rada, P., and Hoebel, B.G. (2009). Sugar and fat bingeing have notable differences in addictive-like behavior. *J Nutr* 139, 623-628.

Babbs, R.K., Wojnicki, F.H., and Corwin, R.L. (2012). Assessing binge eating. An analysis of data previously collected in bingeing rats. *Appetite* 59, 478-482.

Baldo, B.A., and Kelley, A.E. (2007). Discrete neurochemical coding of distinguishable motivational processes: insights from nucleus accumbens control of feeding. *Psychopharmacology (Berl)* 191, 439-459.

Baldo, B.A., Sadeghian, K., Basso, A.M., and Kelley, A.E. (2002). Effects of selective dopamine D1 or D2 receptor blockade within nucleus accumbens subregions on ingestive behavior and associated motor activity. *Behav Brain Res* 137, 165-177.

Basso, A.M., and Kelley, A.E. (1999). Feeding induced by GABA(A) receptor stimulation within the nucleus accumbens shell: regional mapping and characterization of macronutrient and taste preference. *Behav Neurosci* 113, 324-336.

Bello, N.T., Lucas, L.R., and Hajnal, A. (2002). Repeated sucrose access influences dopamine D2 receptor density in the striatum. *Neuroreport* 13, 1575-1578.

Benzon, C.R., Johnson, S.B., McCue, D.L., Li, D., Green, T.A., and Hommel, J.D. (2014). Neuromedin U receptor 2 knockdown in the paraventricular nucleus modifies behavioral responses to obesogenic high-fat food and leads to increased body weight. *Neuroscience* 258, 270-279.

Berridge, K.C. (1996). Food reward: brain substrates of wanting and liking. *Neurosci Biobehav Rev* 20, 1-25.

Berridge, K.C. (2009). 'Liking' and 'wanting' food rewards: brain substrates and roles in eating disorders. *Physiol Behav* 97, 537-550.

Berridge, K.C., Ho, C.Y., Richard, J.M., and DiFeliceantonio, A.G. (2010). The tempted brain eats: pleasure and desire circuits in obesity and eating disorders. *Brain Res* 1350, 43-64.

Berridge, K.C., and Robinson, T.E. (1998). What is the role of dopamine in reward: hedonic impact, reward learning, or incentive salience? *Brain Res Brain Res Rev* 28, 309-369.

Berthoud, H.R. (2011). Metabolic and hedonic drives in the neural control of appetite: who is the boss? *Curr Opin Neurobiol* 21, 888-896.

Berthoud, H.R., Lenard, N.R., and Shin, A.C. (2011). Food reward, hyperphagia, and obesity. *Am J Physiol Regul Integr Comp Physiol* 300, R1266-1277.

Bossert, J.M., Gray, S.M., Lu, L., and Shaham, Y. (2006). Activation of group II metabotropic glutamate receptors in the nucleus accumbens shell attenuates context-induced relapse to heroin seeking. *Neuropsychopharmacology* 31, 2197-2209.

Bowser, M.T., and Kennedy, R.T. (2001). In vivo monitoring of amine neurotransmitters using microdialysis with on-line capillary electrophoresis. *Electrophoresis* 22, 3668-3676.

Breukel, A.I., Besselsen, E., and Ghijsen, W.E. (1997). Synaptosomes. A model system to study release of multiple classes of neurotransmitters. *Methods Mol Biol* 72, 33-47.

Brighton, P.J., Szekeres, P.G., and Willars, G.B. (2004). Neuromedin U and its receptors: structure, function, and physiological roles. *Pharmacol Rev* 56, 231-248.

Campbell, E.J., and Marchant, N.J. (2018). The use of chemogenetics in behavioural neuroscience: receptor variants, targeting approaches and caveats. *Br J Pharmacol* 175, 994-1003.

Carlezon, W.A., and Thomas, M.J. (2009). Biological substrates of reward and aversion: a nucleus accumbens activity hypothesis. *Neuropharmacology* 56 *Suppl* 1, 122-132.

Carstairs, S.A., Caton, S.J., Blundell-Birtill, P., Rolls, B.J., Hetherington, M.M., and Cecil, J.E. (2018). Can Reduced Intake Associated with Downsizing a High Energy Dense Meal Item be Offset by Increased Vegetable Variety in 3-5-year-old Children? *Nutrients* 10.

Colquhoun, D., Jonas, P., and Sakmann, B. (1992). Action of brief pulses of glutamate on AMPA/kainate receptors in patches from different neurones of rat hippocampal slices. *J Physiol* 458, 261-287.

Corwin, R.L., Avena, N.M., and Boggiano, M.M. (2011). Feeding and reward: perspectives from three rat models of binge eating. *Physiol Behav* 104, 87-97.

Corwin, R.L., and Babbs, R.K. (2012). Rodent models of binge eating: are they models of addiction? *ILAR J* 53, 23-34.

Corwin, R.L., and Wojnicki, F.H. (2006). Binge eating in rats with limited access to vegetable shortening. *Curr Protoc Neurosci Chapter 9*, Unit9.23B.

Corwin, R.L., Wojnicki, F.H., Zimmer, D.J., Babbs, R.K., McGrath, L.E., Olivos, D.R., Mietlicki-Baase, E.G., and Hayes, M.R. (2016). Binge-type eating disrupts dopaminergic and GABAergic signaling in the prefrontal cortex and ventral tegmental area. *Obesity (Silver Spring)* 24, 2118-2125.

Cruwys, T., Bevelander, K.E., and Hermans, R.C. (2015). Social modeling of eating: a review of when and why social influence affects food intake and choice. *Appetite* 86, 3-18.

Davis, C., and Carter, J.C. (2009). Compulsive overeating as an addiction disorder. A review of theory and evidence. *Appetite* 53, 1-8.

Dayan, P., and Balleine, B.W. (2002). Reward, motivation, and reinforcement learning. *Neuron* 36, 285-298.

De Castro, J.M. (1990). Social facilitation of duration and size but not rate of the spontaneous meal intake of humans. *Physiol Behav* 47, 1129-1135.

de Castro, J.M., and de Castro, E.S. (1989). Spontaneous meal patterns of humans: influence of the presence of other people. *Am J Clin Nutr* 50, 237-247.

De Souza, C.T., Araujo, E.P., Bordin, S., Ashimine, R., Zollner, R.L., Boschero, A.C., Saad, M.J., and Velloso, L.A. (2005). Consumption of a fat-rich diet activates a proinflammatory response and induces insulin resistance in the hypothalamus. *Endocrinology* 146, 4192-4199.

de Zwaan, M. (2001). Binge eating disorder and obesity. *Int J Obes Relat Metab Disord* 25 Suppl 1, S51-55.

Dichter, G.S., Damiano, C.A., and Allen, J.A. (2012). Reward circuitry dysfunction in psychiatric and neurodevelopmental disorders and genetic syndromes: animal models and clinical findings. *J Neurodev Disord* 4, 19.

Drewnowski, A. (1997). Taste preferences and food intake. *Annu Rev Nutr* 17, 237-253.

Drewnowski, A., and Almiron-Roig, E. (2010). Human Perceptions and Preferences for Fat-Rich Foods. In *Fat Detection: Taste, Texture, and Post Ingestive Effects*, J. Montmayeur, and J. le Coutre, eds. (Boca Raton, FL: CRC Press/Taylor & Francis).

Drewnowski, A., and Greenwood, M.R. (1983). Cream and sugar: human preferences for high-fat foods. *Physiol Behav* 30, 629-633.

Drewnowski, A., Grinker, J.A., and Hirsch, J. (1982). Obesity and flavor perception: multidimensional scaling of soft drinks. *Appetite* 3, 361-368.

Dölen, G., Darvishzadeh, A., Huang, K.W., and Malenka, R.C. (2013). Social reward requires coordinated activity of nucleus accumbens oxytocin and serotonin. *Nature* 501, 179-184.

Egecioglu, E., Ploj, K., Xu, X., Bjursell, M., Salomé, N., Andersson, N., Ohlsson, C., Taube, M., Hansson, C., Bohlooly-Y, M., *et al.* (2009). Central NMU signaling in body weight and energy balance regulation: evidence from NMUR2 deletion and chronic central NMU treatment in mice. *Am J Physiol Endocrinol Metab* 297, E708-716.

El Mestikawy, S., Wallén-Mackenzie, A., Fortin, G.M., Descarries, L., and Trudeau, L.E. (2011). From glutamate co-release to vesicular synergy: vesicular glutamate transporters. *Nat Rev Neurosci* 12, 204-216.

Elmquist, J.K., Elias, C.F., and Saper, C.B. (1999). From lesions to leptin: hypothalamic control of food intake and body weight. *Neuron* 22, 221-232.

Evans, K.R., and Vaccarino, F.J. (1986). Intra-nucleus accumbens amphetamine: dose-dependent effects on food intake. *Pharmacol Biochem Behav* 25, 1149-1151.

Featherstone, D.E., and Shippey, S.A. (2008). Regulation of synaptic transmission by ambient extracellular glutamate. *Neuroscientist* 14, 171-181.

Ferrario, C.R., Labouèbe, G., Liu, S., Nieh, E.H., Routh, V.H., Xu, S., and O'Connor, E.C. (2016). Homeostasis Meets Motivation in the Battle to Control Food Intake. *J Neurosci* 36, 11469-11481.

Fink, L.H., Anastasio, N.C., Fox, R.G., Rice, K.C., Moeller, F.G., and Cunningham, K.A. (2015). Individual Differences in Impulsive Action Reflect Variation in the Cortical Serotonin 5-HT<sub>2A</sub> Receptor System. *Neuropsychopharmacology* 40, 1957-1968.

Finkelstein, E.A., Trogon, J.G., Cohen, J.W., and Dietz, W. (2009). Annual medical spending attributable to obesity: payer-and service-specific estimates. *Health Aff (Millwood)* 28, w822-831.

Freeman, L.R., Haley-Zitlin, V., Rosenberger, D.S., and Granholm, A.C. (2014). Damaging effects of a high-fat diet to the brain and cognition: a review of proposed mechanisms. *Nutr Neurosci* 17, 241-251.

Gartlon, J., Szekeres, P., Pullen, M., Sarau, H.M., Aiyar, N., Shabon, U., Michalovich, D., Steplewski, K., Ellis, C., Elshourbagy, N., *et al.* (2004). Localisation of NMU1R and NMU2R in human and rat central nervous system and effects of neuromedin-U following central administration in rats. *Psychopharmacology (Berl)* 177, 1-14.

Guerdjikova, A.I., Mori, N., Casuto, L.S., and McElroy, S.L. (2017). Binge Eating Disorder. *Psychiatr Clin North Am* 40, 255-266.

Guo, Y., Wang, H.L., Xiang, X.H., and Zhao, Y. (2009). The role of glutamate and its receptors in mesocorticolimbic dopaminergic regions in opioid addiction. *Neurosci Biobehav Rev* 33, 864-873.

Hainerová, I., Torekov, S.S., Ek, J., Finková, M., Borch-Johnsen, K., Jørgensen, T., Madsen, O.D., Lebl, J., Hansen, T., and Pedersen, O. (2006). Association between neuromedin U gene variants and overweight and obesity. *J Clin Endocrinol Metab* 91, 5057-5063.

Hajnal, A., Mark, G.P., Rada, P.V., Lénárd, L., and Hoebel, B.G. (1997). Norepinephrine microinjections in the hypothalamic paraventricular nucleus increase extracellular dopamine and decrease acetylcholine in the nucleus accumbens: relevance to feeding reinforcement. *J Neurochem* 68, 667-674.

Hales, C.M., M.D., Carroll, M.D., M.S.P.H., Fryar, C.D., M.S.P.H., and Ogden, C.L., Ph.D. (2017). Prevalence of Obesity Among Adults And Youth: United States, 2015-2016. NCHS data brief, no. 288



Hyattsville, MD: National Center for Health Statistics. 2017.

Heffner, T.G., Zigmond, M.J., and Stricker, E.M. (1977). Effects of dopaminergic agonists and antagonists of feeding in intact and 6-hydroxydopamine-treated rats. *J Pharmacol Exp Ther* 201, 386-399.

Hommel, J.D., Trinko, R., Sears, R.M., Georgescu, D., Liu, Z.W., Gao, X.B., Thurmon, J.J., Marinelli, M., and DiLeone, R.J. (2006). Leptin receptor signaling in midbrain dopamine neurons regulates feeding. *Neuron* 51, 801-810.

Hosoya, M., Moriya, T., Kawamata, Y., Ohkubo, S., Fujii, R., Matsui, H., Shintani, Y., Fukusumi, S., Habata, Y., Hinuma, S., *et al.* (2000). Identification and functional characterization of a novel subtype of neuromedin U receptor. *J Biol Chem* 275, 29528-29532.

Howard, A.D., Wang, R., Pong, S.S., Mellin, T.N., Strack, A., Guan, X.M., Zeng, Z., Williams, D.L., Feighner, S.D., Nunes, C.N., *et al.* (2000). Identification of receptors for neuromedin U and its role in feeding. *Nature* 406, 70-74.

Hu, S., Wang, L., Yang, D., Li, L., Togo, J., Wu, Y., Liu, Q., Li, B., Li, M., Wang, G., *et al.* (2018). Dietary Fat, but Not Protein or Carbohydrate, Regulates Energy Intake and Causes Adiposity in Mice. *Cell Metab* 28, 415-431.e414.

Hu, X.T., and White, F.J. (1996). Glutamate receptor regulation of rat nucleus accumbens neurons in vivo. *Synapse* 23, 208-218.

Hung, L.W., Neuner, S., Polepalli, J.S., Beier, K.T., Wright, M., Walsh, J.J., Lewis, E.M., Luo, L., Deisseroth, K., Dölen, G., *et al.* (2017). Gating of social reward by oxytocin in the ventral tegmental area. *Science* 357, 1406-1411.

Javaras, K.N. (2017). Will Viewing Overeating as Compulsive Lead to Novel Pharmacological Interventions? *Neuropsychopharmacology* 42, 1373-1374.

Jhanwar-Uniyal, M., Beck, B., Jhanwar, Y.S., Burlet, C., and Leibowitz, S.F. (1993). Neuropeptide Y projection from arcuate nucleus to parvocellular division of paraventricular nucleus: specific relation to the ingestion of carbohydrate. *Brain Res* 631, 97-106.

Kaisho, T., Nagai, H., Asakawa, T., Suzuki, N., Fujita, H., Matsumiya, K., Nishizawa, N., Kanematsu-Yamaki, Y., Dote, K., Sakamoto, J.I., *et al.* (2017). Effects of peripheral administration of a Neuromedin U receptor 2-selective agonist on food intake and body weight in obese mice. *Int J Obes (Lond)* 41, 1790-1797.

Kanematsu-Yamaki, Y., Nishizawa, N., Kaisho, T., Nagai, H., Mochida, T., Asakawa, T., Inooka, H., Dote, K., Fujita, H., Matsumiya, K., *et al.* (2017). Potent Body Weight-Lowering Effect of a Neuromedin U Receptor 2-selective PEGylated Peptide. *J Med Chem* 60, 6089-6097.

Kasper, J., Smith, A., and Hommel, J. (2018). Cocaine-Evoked Locomotor Activity Correlates With The Expression of Neuromedin-U Receptor 2 In The Nucleus Accumbens. *Frontiers in Behavioral Neuroscience*, In press.

Kasper, J.M., Booth, R.G., and Peris, J. (2015). Serotonin-2C receptor agonists decrease potassium-stimulated GABA release in the nucleus accumbens. *Synapse* 69, 78-85.

Kasper, J.M., Johnson, S.B., and Hommel, J.D. (2014). Fat Preference: a novel model of eating behavior in rats. *J Vis Exp*, e51575.

Kasper, J.M., McCue, D.L., Milton, A.J., Szwed, A., Sampson, C.M., Huang, M., Carlton, S., Meltzer, H.Y., Cunningham, K.A., and Hommel, J.D. (2016). Gamma-Aminobutyric Acidergic Projections From the Dorsal Raphe to the Nucleus Accumbens Are Regulated by Neuromedin U. *Biol Psychiatry* 80, 878-887.

Kasper, J.M., Milton, A.J., Smith, A.E., Laezza, F., Taglialatela, G., Hommel, J.D., and Abate, N. (2017). Cognitive deficits associated with a high-fat diet and insulin resistance are potentiated by overexpression of ecto-nucleotide pyrophosphatase phosphodiesterase-1. *Int J Dev Neurosci*.

Kelley, A.E., Bakshi, V.P., Haber, S.N., Steininger, T.L., Will, M.J., and Zhang, M. (2002). Opioid modulation of taste hedonics within the ventral striatum. *Physiol Behav* 76, 365-377.

Kelley, A.E., Baldo, B.A., Pratt, W.E., and Will, M.J. (2005). Corticostriatal-hypothalamic circuitry and food motivation: integration of energy, action and reward. *Physiol Behav* 86, 773-795.

Kelley, A.E., and Berridge, K.C. (2002). The neuroscience of natural rewards: relevance to addictive drugs. *J Neurosci* 22, 3306-3311.

Kelley, A.E., Bless, E.P., and Swanson, C.J. (1996). Investigation of the effects of opiate antagonists infused into the nucleus accumbens on feeding and sucrose drinking in rats. *J Pharmacol Exp Ther* 278, 1499-1507.

Kessler, R.C., Berglund, P.A., Chiu, W.T., Deitz, A.C., Hudson, J.I., Shahly, V., Aguilar-Gaxiola, S., Alonso, J., Angermeyer, M.C., Benjet, C., *et al.* (2013). The prevalence and correlates of binge eating disorder in the World Health Organization World Mental Health Surveys. *Biol Psychiatry* 73, 904-914.

Kessler, R.M., Hutson, P.H., Herman, B.K., and Potenza, M.N. (2016). The neurobiological basis of binge-eating disorder. *Neurosci Biobehav Rev* 63, 223-238.

Kreitzer, A.C., and Malenka, R.C. (2007). Endocannabinoid-mediated rescue of striatal LTD and motor deficits in Parkinson's disease models. *Nature* 445, 643-647.

Lawson, E.A. (2017). The effects of oxytocin on eating behaviour and metabolism in humans. *Nat Rev Endocrinol* 13, 700-709.

Le Merrer, J., Becker, J.A., Befort, K., and Kieffer, B.L. (2009). Reward processing by the opioid system in the brain. *Physiol Rev* 89, 1379-1412.

Leibowitz, S.F., Hammer, N.J., and Chang, K. (1981). Hypothalamic paraventricular nucleus lesions produce overeating and obesity in the rat. *Physiol Behav* 27, 1031-1040.

Li, Z., Zharikova, A., Bastian, J., Esperon, L., Hebert, N., Mathes, C., Rowland, N.E., and Peris, J. (2008). High temporal resolution of amino acid levels in rat nucleus accumbens during operant ethanol self-administration: involvement of elevated glycine in anticipation. *J Neurochem* 106, 170-181.

Liguz-Leczna, M., and Skangiel-Kramska, J. (2007). Vesicular glutamate transporters (VGLUTs): the three musketeers of glutamatergic system. *Acta Neurobiol Exp (Wars)* 67, 207-218.

Lizarbe, B., Soares, A.F., Larsson, S., and Duarte, J.M.N. (2018). Neurochemical Modifications in the Hippocampus, Cortex and Hypothalamus of Mice Exposed to Long-Term High-Fat Diet. *Front Neurosci* 12, 985.

Loweth, J.A., Scheyer, A.F., Milovanovic, M., LaCrosse, A.L., Flores-Barrera, E., Werner, C.T., Li, X., Ford, K.A., Le, T., Olive, M.F., *et al.* (2014a). Synaptic depression via mGluR1 positive allosteric modulation suppresses cue-induced cocaine craving. *Nat Neurosci* 17, 73-80.

Loweth, J.A., Tseng, K.Y., and Wolf, M.E. (2013). Using metabotropic glutamate receptors to modulate cocaine's synaptic and behavioral effects: mGluR1 finds a niche. *Curr Opin Neurobiol* 23, 500-506.

Loweth, J.A., Tseng, K.Y., and Wolf, M.E. (2014b). Adaptations in AMPA receptor transmission in the nucleus accumbens contributing to incubation of cocaine craving. *Neuropharmacology* 76 Pt B, 287-300.

Lyons, J., Walton, J., and Flynn, A. (2018). Larger Food Portion Sizes Are Associated with Both Positive and Negative Markers of Dietary Quality in Irish Adults. *Nutrients* 10.

Maldonado-Irizarry, C.S., and Kelley, A.E. (1995a). Excitatory amino acid receptors within nucleus accumbens subregions differentially mediate spatial learning in the rat. *Behav Pharmacol* 6, 527-539.

Maldonado-Irizarry, C.S., and Kelley, A.E. (1995b). Excitotoxic lesions of the core and shell subregions of the nucleus accumbens differentially disrupt body weight regulation and motor activity in rat. *Brain Res Bull* 38, 551-559.

Maldonado-Irizarry, C.S., Swanson, C.J., and Kelley, A.E. (1995). Glutamate receptors in the nucleus accumbens shell control feeding behavior via the lateral hypothalamus. *J Neurosci* 15, 6779-6788.

Matikainen-Ankney, B.A., and Kravitz, A.V. (2018). Persistent effects of obesity: a neuroplasticity hypothesis. *Ann N Y Acad Sci* 1428, 221-239.

McCue, D.L., Kasper, J.M., and Hommel, J.D. (2017). Regulation of motivation for food by neuromedin U in the paraventricular nucleus and the dorsal raphe nucleus. *Int J Obes (Lond)* 41, 120-128.

McElroy, S.L., Hudson, J., Ferreira-Cornwell, M.C., Radewonuk, J., Whitaker, T., and Gasior, M. (2016). Lisdexamfetamine Dimesylate for Adults with Moderate to Severe Binge Eating Disorder: Results of Two Pivotal Phase 3 Randomized Controlled Trials. *Neuropsychopharmacology* 41, 1251-1260.

McElroy, S.L., Hudson, J.I., Mitchell, J.E., Wilfley, D., Ferreira-Cornwell, M.C., Gao, J., Wang, J., Whitaker, T., Jonas, J., and Gasior, M. (2015). Efficacy and safety of lisdexamfetamine for treatment of adults with moderate to severe binge-eating disorder: a randomized clinical trial. *JAMA Psychiatry* 72, 235-246.

Meredith, G.E., Pennartz, C.M., and Groenewegen, H.J. (1993). The cellular framework for chemical signalling in the nucleus accumbens. *Prog Brain Res* 99, 3-24.

Mimee, A., Smith, P.M., and Ferguson, A.V. (2013). Circumventricular organs: targets for integration of circulating fluid and energy balance signals? *Physiol Behav* 121, 96-102.

Moore, C.F., Sabino, V., Koob, G.F., and Cottone, P. (2017). Pathological Overeating: Emerging Evidence for a Compulsivity Construct. *Neuropsychopharmacology* 42, 1375-1389.

Morton, G.J., Cummings, D.E., Baskin, D.G., Barsh, G.S., and Schwartz, M.W. (2006). Central nervous system control of food intake and body weight. *Nature* 443, 289-295.

Moussawi, K., Riegel, A., Nair, S., and Kalivas, P.W. (2011). Extracellular glutamate: functional compartments operate in different concentration ranges. *Front Syst Neurosci* 5, 94.

Mucha, R.F., and Iversen, S.D. (1986). Increased food intake after opioid microinjections into nucleus accumbens and ventral tegmental area of rat. *Brain Res* 397, 214-224.

Nathanson, J.L., Yanagawa, Y., Obata, K., and Callaway, E.M. (2009). Preferential labeling of inhibitory and excitatory cortical neurons by endogenous tropism of adeno-associated virus and lentivirus vectors. *Neuroscience* 161, 441-450.

Oginsky, M.F., Goforth, P.B., Nobile, C.W., Lopez-Santiago, L.F., and Ferrario, C.R. (2016). Eating 'Junk-Food' Produces Rapid and Long-Lasting Increases in NAc CP-AMPA Receptors: Implications for Enhanced Cue-Induced Motivation and Food Addiction. *Neuropsychopharmacology* 41, 2977-2986.

Otis, T., Zhang, S., and Trussell, L.O. (1996). Direct measurement of AMPA receptor desensitization induced by glutamatergic synaptic transmission. *J Neurosci* 16, 7496-7504.

Ott, V., Finlayson, G., Lehnert, H., Heitmann, B., Heinrichs, M., Born, J., and Hallschmid, M. (2013). Oxytocin reduces reward-driven food intake in humans. *Diabetes* 62, 3418-3425.

Ozcan, L., Ergin, A.S., Lu, A., Chung, J., Sarkar, S., Nie, D., Myers, M.G., and Ozcan, U. (2009). Endoplasmic reticulum stress plays a central role in development of leptin resistance. *Cell Metab* 9, 35-51.

Paxinos, G., and Watson, C. (2007). *The Rat Brain in Stereotaxic Coordinates*. (Academic Press, Cambridge, MA).



Perry, M.L., Baldo, B.A., Andrzejewski, M.E., and Kelley, A.E. (2009). Muscarinic receptor antagonism causes a functional alteration in nucleus accumbens mu-opiate-mediated feeding behavior. *Behav Brain Res* 197, 225-229.

Pi-Sunyer, X., Astrup, A., Fujioka, K., Greenway, F., Halpern, A., Krempf, M., Lau, D.C., le Roux, C.W., Violante Ortiz, R., Jensen, C.B., *et al.* (2015). A Randomized, Controlled Trial of 3.0 mg of Liraglutide in Weight Management. *N Engl J Med* 373, 11-22.

Pickel, V.M., Sumal, K.K., Beckley, S.C., Miller, R.J., and Reis, D.J. (1980). Immunocytochemical localization of enkephalin in the neostriatum of rat brain: a light and electron microscopic study. *J Comp Neurol* 189, 721-740.

Price, A.E., Anastasio, N.C., Stutz, S.J., Hommel, J.D., and Cunningham, K.A. (2018a). Serotonin 5-HT. *Front Pharmacol* 9, 821.

Price, A.E., Anastasio, N.C., Stutz, S.J., Hommel, J.D., and Cunningham, K.A. (2018b). Serotonin 5-HT<sub>2C</sub> Receptor Activation Suppresses Binge Intake and the Reinforcing and Motivational Properties of High-Fat Food. *Front Pharmacol* 9, 821.

Price, A.E., Stutz, S.J., Hommel, J.D., Anastasio, N.C., and Cunningham, K.A. (2018c). Anterior insula activity regulates the associated behaviors of high fat food binge intake and cue reactivity in male rats. *Appetite* 133, 231-239.

Qiu, D.L., Chu, C.P., Tsukino, H., Shirasaka, T., Nakao, H., Kato, K., Kunitake, T., Katoh, T., and Kannan, H. (2005). Neuromedin U receptor-2 mRNA and HCN

channels mRNA expression in NMU-sensitive neurons in rat hypothalamic paraventricular nucleus. *Neurosci Lett* 374, 69-72.

Raddatz, R., Wilson, A.E., Artymyshyn, R., Bonini, J.A., Borowsky, B., Boteju, L.W., Zhou, S., Kouranova, E.V., Nagorny, R., Guevarra, M.S., *et al.* (2000). Identification and characterization of two neuromedin U receptors differentially expressed in peripheral tissues and the central nervous system. *J Biol Chem* 275, 32452-32459.

Rancourt, D., and McCullough, M.B. (2015). Overlap in Eating Disorders and Obesity in Adolescence. *Curr Diab Rep* 15, 78.

Reale, S., Kearney, C.M., Hetherington, M.M., Croden, F., Cecil, J.E., Carstairs, S.A., Rolls, B.J., and Caton, S.J. (2018). The Feasibility and Acceptability of Two Methods of Snack Portion Control in United Kingdom (UK) Preschool Children: Reduction and Replacement. *Nutrients* 10.

Rippin, H.L., Hutchinson, J., Jewell, J., Breda, J.J., and Cade, J.E. (2018). Portion Size of Energy-Dense Foods among French and UK Adults by BMI Status. *Nutrients* 11.

Robinson, E., Thomas, J., Aveyard, P., and Higgs, S. (2014). What everyone else is eating: a systematic review and meta-analysis of the effect of informational eating norms on eating behavior. *J Acad Nutr Diet* 114, 414-429.

Robinson, T.E., and Berridge, K.C. (1993). The neural basis of drug craving: an incentive-sensitization theory of addiction. *Brain Res Brain Res Rev* 18, 247-291.

Rossi, M.A., and Stuber, G.D. (2018). Overlapping Brain Circuits for Homeostatic and Hedonic Feeding. *Cell Metab* 27, 42-56.

Salamone, J.D., Zigmond, M.J., and Stricker, E.M. (1990). Characterization of the impaired feeding behavior in rats given haloperidol or dopamine-depleting brain lesions. *Neuroscience* 39, 17-24.

Sampson, C.M., Kasper, J.M., Felsing, D.E., Raval, S.R., Ye, N., Wang, P., Patrikeev, I., Rytting, E., Zhou, J., Allen, J.A., *et al.* (2018). Small-Molecule Neuromedin U Receptor 2 Agonists Suppress Food Intake and Decrease Visceral Fat in Animal Models. *Pharmacol Res Perspect* 6, e00425.

Saper, C.B., Chou, T.C., and Elmquist, J.K. (2002). The need to feed: homeostatic and hedonic control of eating. *Neuron* 36, 199-211.

Satta, V., Scherma, M., Piscitelli, F., Usai, P., Castelli, M.P., Bisogno, T., Fratta, W., and Fadda, P. (2018). Limited Access to a High Fat Diet Alters Endocannabinoid Tone in Female Rats. *Front Neurosci* 12, 40.

Schebendach, J., Broft, A., Foltin, R.W., and Walsh, B.T. (2013). Can the reinforcing value of food be measured in bulimia nervosa? *Appetite* 62, 70-75.

Schwendt, M., Reichel, C.M., and See, R.E. (2012). Extinction-dependent alterations in corticostriatal mGluR2/3 and mGluR7 receptors following chronic methamphetamine self-administration in rats. *PLoS One* 7, e34299.

Shan, L., Qiao, X., Crona, J.H., Behan, J., Wang, S., Laz, T., Bayne, M., Gustafson, E.L., Monsma, F.J., and Hedrick, J.A. (2000). Identification of a novel neuromedin U receptor subtype expressed in the central nervous system. *J Biol Chem* 275, 39482-39486.

Sharma, S., Fernandes, M.F., and Fulton, S. (2013). Adaptations in brain reward circuitry underlie palatable food cravings and anxiety induced by high-fat diet withdrawal. *Int J Obes (Lond)* 37, 1183-1191.

Sidorov, M.S., Auerbach, B.D., and Bear, M.F. (2013). Fragile X mental retardation protein and synaptic plasticity. *Mol Brain* 6, 15.

Smith, A.E., Kasper, J.M., Anastasio, N.C., Hommel, J.D., and 13, A. (2019). Binge-Type Eating in Rats is Facilitated by Neuromedin U Receptor 2 in the Nucleus Accumbens and Ventral Tegmental Area. *Nutrients* 11.

Spetter, M.S., Feld, G.B., Thienel, M., Preissl, H., Hege, M.A., and Hallschmid, M. (2018). Oxytocin curbs calorie intake via food-specific increases in the activity of brain areas that process reward and establish cognitive control. *Sci Rep* 8, 2736.

Spetter, M.S., and Hallschmid, M. (2017). Current findings on the role of oxytocin in the regulation of food intake. *Physiol Behav* 176, 31-39.

Stachniak, T.J., Ghosh, A., and Sternson, S.M. (2014). Chemogenetic synaptic silencing of neural circuits localizes a hypothalamus→midbrain pathway for feeding behavior. *Neuron* 82, 797-808.

Stratford, T.R., Kelley, A.E., and Simansky, K.J. (1999). Blockade of GABAA receptors in the medial ventral pallidum elicits feeding in satiated rats. *Brain Res* 825, 199-203.

Stratford, T.R., Swanson, C.J., and Kelley, A. (1998). Specific changes in food intake elicited by blockade or activation of glutamate receptors in the nucleus accumbens shell. *Behav Brain Res* 93, 43-50.

Swanson, L. (1989). The neural basis of motivated behavior. In *Acta morphologica neerlandoscandinavica*, pp. 165-176.

Swanson, L.W. (2000). Cerebral hemisphere regulation of motivated behavior. *Brain Res* 886, 113-164.

Tritsch, N.X., Ding, J.B., and Sabatini, B.L. (2012). Dopaminergic neurons inhibit striatal output through non-canonical release of GABA. *Nature* 490, 262-266.

Trojniar, W., Plucińska, K., Ignatowska-Jankowska, B., and Jankowski, M. (2007). Damage to the nucleus accumbens shell but not core impairs ventral tegmental area stimulation-induced feeding. *J Physiol Pharmacol* 58 Suppl 3, 63-71.

Trudeau, L.E., and El Mestikawy, S. (2018). Glutamate Cotransmission in Cholinergic, GABAergic and Monoamine Systems: Contrasts and Commonalities. *Front Neural Circuits* 12, 113.

Trussell, L.O., and Fischbach, G.D. (1989). Glutamate receptor desensitization and its role in synaptic transmission. *Neuron* 3, 209-218.

Vaaga, C.E., Borisovska, M., and Westbrook, G.L. (2014). Dual-transmitter neurons: functional implications of co-release and co-transmission. *Curr Opin Neurobiol* 29, 25-32.

van der Zeyden, M., Oldenziel, W.H., Rea, K., Cremers, T.I., and Westerink, B.H. (2008). Microdialysis of GABA and glutamate: analysis, interpretation and comparison with microsensors. *Pharmacol Biochem Behav* 90, 135-147.

Volkow, N.D., Fowler, J.S., Wang, G.J., Swanson, J.M., and Telang, F. (2007). Dopamine in drug abuse and addiction: results of imaging studies and treatment implications. *Arch Neurol* 64, 1575-1579.

Volkow, N.D., Wang, G.J., Tomasi, D., and Baler, R.D. (2013a). Obesity and addiction: neurobiological overlaps. *Obes Rev* 14, 2-18.

Volkow, N.D., Wang, G.J., Tomasi, D., and Baler, R.D. (2013b). The addictive dimensionality of obesity. *Biol Psychiatry* 73, 811-818.

Volkow, N.D., and Wise, R.A. (2005). How can drug addiction help us understand obesity? *Nat Neurosci* 8, 555-560.

Wang, G.J., Geliebter, A., Volkow, N.D., Telang, F.W., Logan, J., Jayne, M.C., Galanti, K., Selig, P.A., Han, H., Zhu, W., *et al.* (2011). Enhanced striatal dopamine release during food stimulation in binge eating disorder. *Obesity (Silver Spring)* 19, 1601-1608.

White, N.M. (2011). Reward: What Is It? How Can It Be Inferred from Behavior? In *Neurobiology of Sensation and Reward*, J. Gottfried, ed. (Boca Raton, FL: CRC Press/Taylor & Francis).

Williams, G., Bing, C., Cai, X.J., Harrold, J.A., King, P.J., and Liu, X.H. (2001). The hypothalamus and the control of energy homeostasis: different circuits, different purposes. *Physiol Behav* 74, 683-701.

Windisch, K.A., and Czachowski, C.L. (2018). Effects of group II metabotropic glutamate receptor modulation on ethanol- and sucrose-seeking and consumption in the rat. *Alcohol* 66, 77-85.

Witt, A.A., and Lowe, M.R. (2014). Hedonic hunger and binge eating among women with eating disorders. *Int J Eat Disord* 47, 273-280.

Wojnicki, F.H., Babbs, R.K., and Corwin, R.L. (2010). Reinforcing efficacy of fat, as assessed by progressive ratio responding, depends upon availability not amount consumed. *Physiol Behav* 100, 316-321.

Yanovski, S.Z., Leet, M., Yanovski, J.A., Flood, M., Gold, P.W., Kissileff, H.R., and Walsh, B.T. (1992). Food selection and intake of obese women with binge-eating disorder. *Am J Clin Nutr* 56, 975-980.

Zander, M.E., and De Young, K.P. (2014). Individual differences in negative affect and weekly variability in binge eating frequency. *Int J Eat Disord* 47, 296-301.

Zhang, M., Balmadrid, C., and Kelley, A.E. (2003). Nucleus accumbens opioid, GABAergic, and dopaminergic modulation of palatable food motivation: contrasting effects revealed by a progressive ratio study in the rat. *Behav Neurosci* 117, 202-211.

Zhang, M., Gosnell, B.A., and Kelley, A.E. (1998). Intake of high-fat food is selectively enhanced by mu opioid receptor stimulation within the nucleus accumbens. *J Pharmacol Exp Ther* 285, 908-914.

Zhang, M., and Kelley, A.E. (1997). Opiate agonists microinjected into the nucleus accumbens enhance sucrose drinking in rats. *Psychopharmacology (Berl)* 132, 350-360.

Zhang, M., and Kelley, A.E. (2000). Enhanced intake of high-fat food following striatal mu-opioid stimulation: microinjection mapping and fos expression. *Neuroscience* 99, 267-277.

Zhi, J., Melia, A.T., Guercioli, R., Chung, J., Kinberg, J., Hauptman, J.B., and Patel, I.H. (1994). Retrospective population-based analysis of the dose-response (fecal fat excretion) relationship of orlistat in normal and obese volunteers. *Clin Pharmacol Ther* 56, 82-85.

Zhu, X., Ottenheimer, D., and DiLeone, R.J. (2016). Activity of D1/2 Receptor Expressing Neurons in the Nucleus Accumbens Regulates Running, Locomotion, and Food Intake. *Front Behav Neurosci* 10, 66.



Ziegler, D.R., Cullinan, W.E., and Herman, J.P. (2002). Distribution of vesicular glutamate transporter mRNA in rat hypothalamus. *J Comp Neurol* *448*, 217-229.

Zimmermann, J., Herman, M.A., and Rosenmund, C. (2015). Co-release of glutamate and GABA from single vesicles in GABAergic neurons exogenously expressing VGLUT3. *Front Synaptic Neurosci* *7*, 16.

## **Vita**

Ashley Elizabeth Smith was born on November 20, 1987 in Allentown, Pennsylvania to parents Edward and Cindy Smith. She graduated from Hutchinson High School, in Hutchinson, Minnesota. Subsequently, she attend the University of Minnesota in Minneapolis, Minnesota where she earned her B.S. in Genetics, Cell Biology and Development. During her time at the University of Minnesota, Ms. Smith participated in a work-study program where she conducted undergraduate research in the laboratory of Vivian Bardwell, Ph.D. Ms. Smith was also awarded a small grant from the University of Minnesota's Undergraduate Research Opportunity Program (UROP) to support her research project. After graduation, Ms. Smith worked in both academic and industry laboratory settings to gain more scientific expertise. In Fall 2015, Ms. Smith joined the Cell Biology Graduate Program at the University of Texas Medical Branch in Galveston, Texas. She subsequently joined the laboratory of Jonathan D. Hommel, Ph.D., where she conducted her dissertation work. In Fall 2017, Ms. Smith was awarded a predoctoral position on National Institute on Drug Abuse T32 training grant within the Center for Addiction Research. She has presented her research at local and national conferences and has authored/co-authored several publications in peer-reviewed journals.

### Awards:

1. James E. Beall II Memorial Award, Graduate School of Biomedical Sciences, University of Texas Medical Branch (12/2019)
2. Research Technology Award, Center for Addiction Research, University of Texas Medical Branch (06/2018)
3. Travel Award, Behavior, Biology and Chemistry: Translation Research in Addiction Meeting (03/2018)
4. Outstanding Service Award, 4<sup>th</sup> Annual Cell Biology Student Symposium, Cell Biology Graduate Program, University of Texas Medical Branch (05/2017)
5. Outstanding Service Award, 3<sup>rd</sup> Annual Cell Biology Student Symposium, Cell Biology Graduate Program, University of Texas Medical Branch (05/2016)

### Peer-reviewed publications:

1. **Smith, A.E.**, Ogunseye, K.O., McCue, D.M., DeBenedictis, J.N., Peris, J., Kasper, J.M., Hommel, J.D. Glutamatergic projections from homeostatic to hedonic brain nuclei regulate intake of highly palatable food. *Submitted*.
2. **Smith, A.E.**, Kasper, J.M., Ara 13, Anastasio, N.C., Hommel, J.D. Binge-type eating in rats is facilitated by neuromedin U receptor 2 in the nucleus accumbens and ventral tegmental area. *Nutrients*. 2019. [PMID 30717427](#)
3. Kasper, J.M., **Smith, A.E.**, Hommel, J.D. Cocaine-evoked locomotor activity negatively correlates with the expression of neuromedin U receptor 2 in the nucleus accumbens. *Frontiers in Behavioral Neuroscience*. 2018. [PMID 30483076](#)
4. Scala, F., Nenov, M.N., Crofton, E., Singh, A.K., Folorunso, O., Zhang, Y., Chesson, B.C., Wildburger, N.C., James, T.F., Alshammari, M.A., Alshammari, T.K., Elfrink, H., Grassi, C., Kasper, J.M., **Smith, A.E.**, Hommel, J.D. Lichti, C.F., Rudra, J.S., D'Ascenzo, M., Green, T.A., & Laezza, F. Environmental enrichment and social isolation mediate neuroplasticity of medium spiny neurons through GSK3 pathway. *Cell Reports*. 2018. [PMID29642012](#)
5. Kasper, J.M., Milton, A.J., **Smith, A.E.**, Laezza, F., Taglialatela, G., Hommel, J.D., Abate, N. Cognitive deficits associated with a high-fat diet and insulin resistance are potentiated by overexpression of ecto-nucleotide

pyrophosphatase phosphodiesterase-1. *International Journal of Developmental Neuroscience*. 2017. PMID28373023

Permanent address: 1225 Lawrence Rd Apt 225, Kemah, TX, 77565

This dissertation was typed by Ashley E. Smith.